RSC Advances

REVIEW

View Article Online
View Journal | View Issue

Cite this: *RSC Adv.*, 2024, **14**, 29693

A comprehensive review of enhanced CO_2 capture using activated carbon derived from biomass feedstock

Shreyase Kundu,†[a] Tasmina Khandaker,†[b] Md Al-Amin Mia Anik,†[a] Md. Kamrul Hasan,[a] Palash Kumar Dhar,[a] Sagar Kumar Dutta,[a] M. Abdul Latif[c] and Muhammad Sarwar Hossain*[a]

The increasing level of atmospheric CO_2 requires the urgent development of effective capture technologies. This comprehensive review thoroughly examines various methods for the synthesis of carbon materials, modification techniques for converting biomass feedstock into carbon materials and pivotal factors impacting their properties. The novel aspect of this review is its in-depth comparison of how these modifications specifically affect the pore structure and surface area together with the exploration of the mechanism underlying the enhancement of CO_2 adsorption performance. Additionally, this review addresses research gaps and provides recommendations for future studies concerning the advantages and drawbacks of CO_2 adsorbents and their prospects for commercialization and economic feasibility. This article revealed that among the various strategies, template carbonization offers a viable option for providing control of the material pore diameter and structure without additional modification treatments. Optimizing the pore structure of activated carbons, particularly those activated with agents such as KOH and $ZnCl_2$, together with synthesizing hybrid activated carbons using multiple activating agents, is crucial for enhancing their CO_2 capture performance. Cost-benefit analysis suggests that biomass-derived activated carbons can significantly meet the escalating demand for CO_2 capture materials, offering economic advantages and supporting sustainable waste management.

Received 21st June 2024
Accepted 2nd September 2024

DOI: 10.1039/d4ra04537h

rsc.li/rsc-advances

1. Introduction

In the last 20 years, the amount of atmospheric carbon dioxide (CO_2), a potent greenhouse gas, has exhibited a steady increase, as documented by Goel (2021).[1] This increase can be attributed to multiple factors, including the repercussions of the industrial revolution, characterized by an annual increment of 0.17 °C, and burning of fossil fuels. Industries such as those involved in energy production from coal, oil, and natural gases; cement manufacturing; chemical synthesis; metal production; and refineries significantly contribute to CO_2 emissions. Consequently, the atmospheric CO_2 concentration reached 423 parts per million (ppm) in 2023, surpassing the anticipated level of around 400 ppm or 0.04% of CO_2 in the air by volume.[2] This surge represents an approximately 50% increase since the pre-industrial era and an additional 13% since the turn of the millennium. The escalating rate of CO_2 emissions raises concerns on various fronts, primarily because of its pivotal role in climate change and its adverse impact on human health. Manifestations of these impacts include respiratory complications, elevated blood pressure, and accelerated heart rates among individuals. Thus, to lower CO_2 emissions, several carbon capture systems have been developed. Numerous initiatives focus on mitigating climate change by capturing and separating CO_2, particularly from large power plants and the atmosphere, using different technologies such as membranes, absorption, microbial methods, cryogenics, and chemical looping. However, these technologies often face challenges such as high operational costs and substantial energy consumption. Fortunately, physical processes such as adsorption offer a cost-effective solution and have been widely used to capture various contaminants, including CO_2.[3] Despite the initial skepticism, the need to develop green technologies has become increasingly evident, given the incontrovertible link between CO_2 emissions, climate change, and the resulting health risks. Therefore, the development and adoption of effective and socially acceptable solutions are imperative. Addressing the challenge of CO_2 emissions necessitates innovative approaches and concerted efforts to safeguard both the environment and human well-being.

Accordingly, adsorption has emerged as a viable and cost-effective approach for the sequestration and storage of

[a]*Chemistry Discipline, Khulna University, Khulna-9208, Bangladesh. E-mail: sarwar@chem.ku.ac.bd*

[b]*Department of Chemistry, Bangladesh Army University of Engineering & Technology (BAUET), Qadirabad Cantonment, Natore-6431, Bangladesh*

[c]*Department of Chemistry, Begum Rokeya University, Rangpur-5404, Bangladesh*

† These authors contributed equally to this work.

carbon. Among the many absorbents used, those that stand out include polymers, carbon compounds, metal oxides, amine-based materials, zeolites, alumina, silica, and metal–organic frameworks (MOFs). In this case, zeolites exhibit sensitivity to moisture, adsorption temperature, and pressure, whereas carbon materials offer notable advantages. Carbon materials, including hydrocarbons, charcoal, carbon nanotubes, graphite, graphene, fullerene, and activated carbon, are simple to prepare and control. Efficient CO_2 capture is possible due to their well-developed pore architectures and high specific surface area. Unlike MOFs, carbon materials are not moisture sensitive, making them more reliable for industrial applications.[4] Therefore, it is necessary to develop carbon materials with remarkable capabilities for capturing CO_2, given their abundant and economical sources. The process for the preparation of carbon materials is straightforward and easily manageable. Their substantial specific surface area and well-formed pore structures significantly enhance their capacity for capturing CO_2 effectively. Furthermore, carbon materials exhibit resistance to moisture, unlike their alternatives. Additionally, activated carbon demonstrates the ability to function across a broad temperature range.

Activated carbons (AC) have emerged as incredibly encouraging adsorbents for CO_2 capture due to their significantly enhanced physiochemical, mechanical, thermal, and chemical stability, as depicted in Fig. 1. Although numerous porous carbon-based materials exist, porous carbonaceous materials derived from biomass hold particular appeal as CO_2 adsorbents. The preference for biomass as a material is driven by its excellent textural characteristics, high CO_2 adsorption capacity, and ease of synthesis, combined with its cost-effectiveness and the renewable nature of biomass resources.[5] Biomass, which is derived from both plant and animal origins, captures solar energy through photosynthesis, making it a sustainable energy source that can be used for heating or transformed into liquid and gaseous fuels using various methods. Among the diverse biomass sources, traditional options such as bagasse, algae, municipal waste, wet waste, forestry residues, agricultural crop residues, and wood processing by-products stand out due to their potential to reduce costs. Pyrolysis stands out as the predominant thermochemical technology for biomass conversion, wherein biomass undergoes decomposition into biochar, tar, and gas. Traditionally, biomass is subjected to pyrolysis, a thermal treatment conducted at moderate temperatures without oxygen, resulting in the production of biochar.[6] Pyrolysis methods include different approaches such as slow or fast pyrolysis, low or high-temperature conditions, and dry or wet pyrolysis.[7] A variety of biomass sources, including wood, non-wood materials, and agricultural or fruit residues, has been utilized for the production of charcoal. The creation of activated porous carbons, similar to biochar, involves the addition of an activating agent either before or after the biochar is produced. An efficient technique for producing activated porous carbon has been developed using *Arundo donax* biomass, which was activated in a single step with KOH.[8] This innovative approach simplifies the conventional two-step activation process, thereby reducing the time constraints. Various activating agents, whether physical or chemical, are utilized in the production of these carbons, including steam, CO_2, KOH, $ZnCl_2$, H_3PO_4, HNO_3, and H_2O_2.[9] Changes in the pyrolysis conditions affect the yield, specific surface area, and surface chemistry of biochar. For instance, Ighalo *et al.* conducted pyrolysis at temperatures ranging from 250 °C to 650 °C, demonstrating an increase in specific surface area of the biochar with an increase in temperature, together with a decrease in its yield, as evidenced by BET data.[10] The composition and quantity of functional groups on the surface of carbon materials are influenced by their preparation techniques and the characteristics of the employed biomass sources. Fig. 2 illustrates the formation of carbon fibers, activated porous carbons, and other byproducts that arise from the combustion of various biomass types, together with their potential applications across different industries.[11]

Several studies have shown that unmodified biochar has limited effectiveness in absorbing contaminants, leading to the investigation of various modification techniques, including reactions with steam, acid or alkaline treatments, and doping with heteroatoms.[12] To significantly improve the

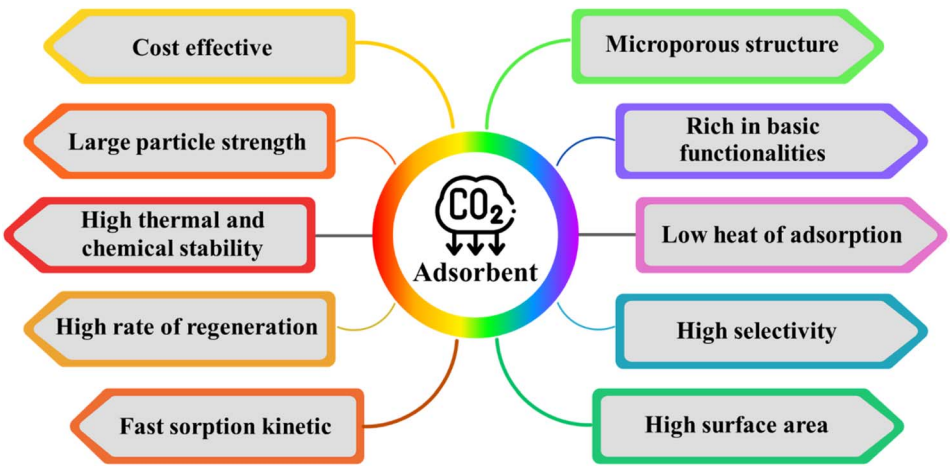

Fig. 1 Properties of activated carbon for carbon dioxide capture.

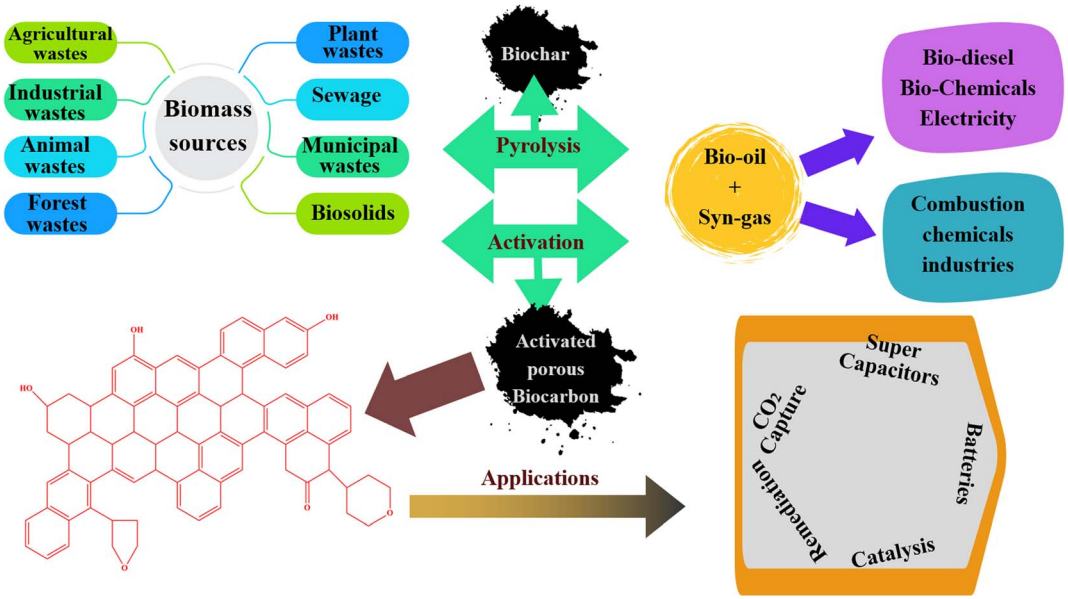

Fig. 2 Illustration of the process of producing biochar and activated carbons from biomass together with their potential applications across different industries. Reproduced from ref. 11.

ability of carbon sorbents to capture CO_2, it is essential to introduce basic sites and increase the porosity of the material. Nitrogen doping, a prevalent modification technique, involves the incorporation of nitrogen-containing chemicals such as polyethyleneimide (PEI) and triethylenephosphoramide (TEPA) into carbon materials, resulting in the introduction of pyridinic N or pyrrolic N groups, which both play pivotal roles in CO_2 capture.[13,14] For example, incorporating chitosan into carbonized materials has been shown to significantly improve their CO_2 adsorption capacity, achieving 5.83 mmol g^{-1} at 0 °C.[15] Additionally, metal oxides or salts are used to modify carbon materials, allowing the introduction of alkaline metal oxides or hydroxides. This modification increases the alkalinity of carbon materials, thereby enhancing their ability to adsorb acidic CO_2. Research has demonstrated that biochar derived from walnut shells and impregnated with metal nitrates, particularly magnesium–biochar combinations, exhibits superior CO_2 adsorption capabilities compared to other metal–biochar composites (such as that with aluminum, iron, nickel, calcium, or sodium).[1,16] However, despite the progress in modification techniques and their application in CO_2 capture, there is still a lack of comprehensive reviews on the methods for the preparation and modification of biomass-based carbon materials. Thus, this review provides a critical analysis of the preparation technologies and conversion conditions that influence the properties of carbon materials derived from biomass. Also, the emerging techniques for modifying these carbon materials, their applications in CO_2 capture, and the underlying capture mechanisms are explored. Finally, the potential future directions and challenges for research in this field are highlighted.

2. Navigating thermochemical conversion technologies for biomass

A wide range of thermochemical conversion methods designed for utilizing biomass has been investigated, including pyrolysis, gasification, and hydrothermal processes. This study assesses their effectiveness in converting biomass into valuable energy resources, with a focus on environmental sustainability and resource optimization.

2.1 Conventional pyrolysis

Pyrolysis, a thermochemical process devoid of oxygen, is instrumental in converting biomass into valuable products such as char, oil, and syngas through high-temperature heating.[17] This process is highly versatile, encompassing variations such as fast, flash, and slow pyrolysis, which are categorized based on the temperature and heating rate. Typically, natural biomass derived from plants primarily consists of three key biopolymers, *i.e.*, cellulose (making up 35–50% of the biomass), hemicellulose (comprising 25–30%), and lignin (constituting 10–30%), with a small fraction of mineralized inorganic components.[18,19] These components differ in their chemical structures and undergo distinct, complex reactions during pyrolysis. Among the various pyrolytic conditions, temperature is regarded as the most critical factor, given that it greatly impacts the final textural properties and surface functionalities of biochar. Fig. 3 depicts the thermal decomposition behavior of these components over a wide temperature range, highlighting the specific temperature intervals at which each component undergoes thermal breakdown. The intricate mechanism of pyrolysis involves sequential decomposition stages of biomass constituents. Initially, water evaporation occurs, followed by the degradation of hemicellulose at around

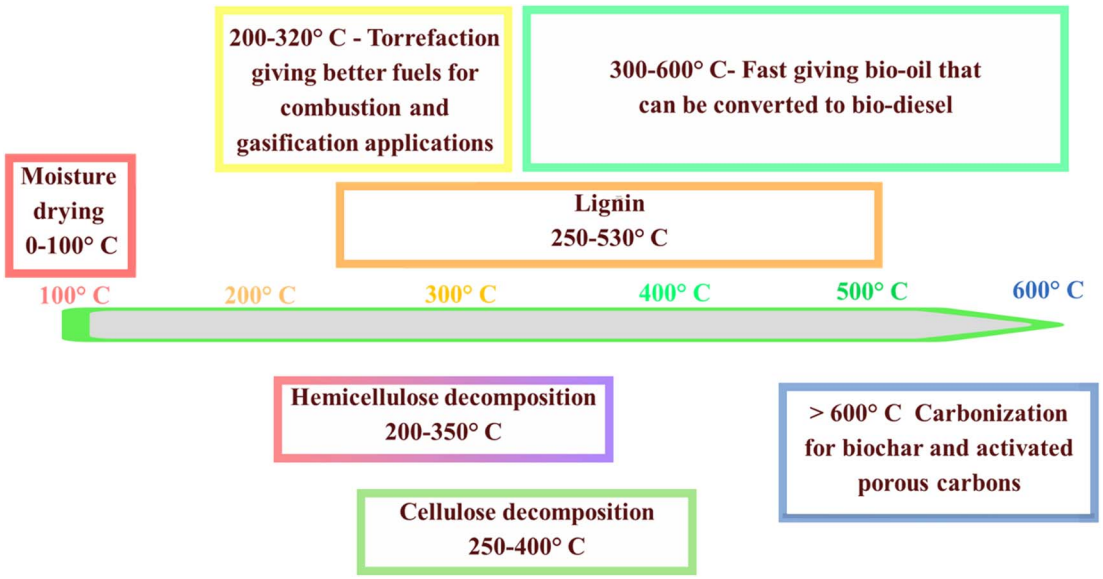

Fig. 3 Decomposition temperatures for lignin, cellulose, and hemicellulose in biomass during thermal processing.

200–350 °C. Subsequently, cellulose undergoes decomposition with an increase in temperature, while lignin is decomposed at temperatures exceeding 400 °C. These temperature-dependent reactions are pivotal in determining the final properties and functionalities of the resulting biochar. Among the pyrolytic conditions, temperature stands out as a critical parameter influencing the texture and surface characteristics of biochar. Slow pyrolysis, which operates at temperatures between 300–600 °C and with low heating rates of 0.1–1 °C s^{-1}, primarily produces biochar, with the typical yields in the range of 30–50%.[20] In contrast, fast and flash pyrolysis methods are designed to efficiently produce bio-oil. These methods are characterized by extremely high heating rates, such as 1000 °C s^{-1}, and very short residence times.[21] The pyrolysis cycle can be comprehensively understood through four distinct stages, as elucidated by the thermogravimetric analysis (TGA) of biomass. These stages involve moisture removal, hemicellulose degradation, cellulose decomposition, and lignin degradation, occurring in specific temperature ranges. Thus, a comprehensive understanding of these stages is crucial for optimizing the properties of biochar and activated porous carbons. This knowledge allows better control of the product selectivity, particularly in balancing the production of char, bio-oil, and syngas.[22]

The initial phase of pyrolysis involves removing moisture entirely at temperatures up to 220 °C, followed by the disintegration of hemicellulose in the temperature range of 220–315 °C. Subsequently, cellulose decomposes in the range of 315–400 °C, and lignin degradation occurs beyond 400 °C.[23] Understanding the transformations these biopolymers undergo during pyrolysis is crucial for gaining deep insight into the overall mechanism. This deep understanding not only enables an improvement in the inherent properties of biochar and precise control of the selectivity for products such as char, bio-oil, and syngas, as well as activated porous carbons, but it also aids in selecting the most suitable biomass sources from a diverse range of naturally occurring feedstocks.[24] Fig. 4 illustrates the quantities of biochar, syngas, and bio-oil produced under various pyrolysis conditions. Fast and flash pyrolysis techniques yield significantly more bio-oil than slow pyrolysis, mainly because the shorter residence time minimizes secondary cracking reactions, thereby increasing the bio-oil yield. Maintaining the optimal pyrolysis temperature is crucial for maximizing bio-oil production, given that higher temperatures typically favor its generation. However, conventional pyrolysis methods have inherent drawbacks, such as low heat transfer efficiency and prolonged heating times, resulting in high costs. In contrast, microwave pyrolysis offers rapid heating rates and shorter reaction times, thereby enhancing the productivity and reducing expenses. Additionally, water, a strong absorber of microwaves, enables the direct microwave-pyrolysis of high-moisture biomass without pretreatment. Comparative studies indicate that microwave pyrolysis results in biochar with a greater specific surface area and higher

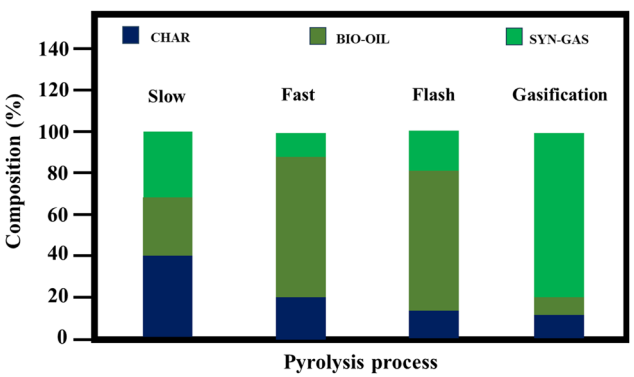

Fig. 4 Proportional breakdown of char, bio-oil, and syngas produced through various pyrolysis methods.

Table 1 Influence of pyrolysis parameters on the generation of biochar, bio-oil, and syngas

Classification of pyrolysis	Biochar/bio-oil/syngas%	Temperature range (°C)	Heating rate (°C min^{-1})	Holding time (s)
Flash	~10/65–70/20–25	<650	~1000	<1
Fast	~10–12/70–75/13–20	400–600	>10	0.5–5
Slow	~35/30/35	300–800	<10	min–h
Gasification	~10/5/85	700–1500	~1000	s

porosity compared to conventional pyrolysis under similar temperature conditions. However, conventional pyrolysis tends to produce a higher yield of char. This is because conventional methods often lead to reduced yields of biochar and bio-oil due to the increased occurrence of biomass cracking and gas formation.

Table 1 shows the influence of the pyrolysis parameters on the generation of biochar, bio-oil, and syngas. Additionally, these insights will aid in identifying suitable biomass sources from the diverse array of naturally occurring biomass feedstocks. In summary, elucidating the mechanism of pyrolysis and its intricate stages not only improves the understanding of biochar production but also facilitates the development of efficient thermochemical conversion processes for the utilization of biomass, contributing to sustainable resource management and energy production.

2.2 Microwave pyrolysis

Microwave pyrolysis has emerged as a promising strategy for carbonizing raw materials, offering solutions to the challenges associated with conventional pyrolysis methods. Analogous to commercial microwave applications in daily life, this approach transfers electromagnetic energy to the precursor material, effecting rapid and targeted heating. Microwave pyrolysis offers distinct advantages compared to traditional furnaces, primarily due to its capability for precise and rapid heating, which results in a highly energy-efficient system. Additionally, carbon-based compounds with high microwave absorbance enable the selective absorption of microwave radiation, allowing the targeted heating of the reactants and promoting specific chemical reactions. Consequently, microwave pyrolysis is expected to result in higher char yields and maintain a more stable temperature profile.[25] These attributes contribute to enhanced production rates and optimal production costs, underscoring the potential of microwave pyrolysis as a transformative approach in biomass conversion processes. Table 2 summarizes the key differences between conventional and microwave pyrolysis based on insights gathered from studies conducted by various research groups.[26,27] The key advantage of microwave pyrolysis is its unique heating mechanism. Unlike traditional methods, which rely on convection and conduction through heated coils to transfer heat to materials, often facing limitations due to the thermal properties and surface temperature of materials, microwave pyrolysis uses the interaction between microwave energy and the dipoles in the target material to generate heat internally. This internal heating process makes the system more efficient than traditional surface heating, given that it facilitates uniform heat distribution and consistent heating throughout the material. Consequently, microwave pyrolysis is recognized for its energy efficiency, rapid processing, and time-saving procedures, facilitating high heating rates and temperatures.[28] These advantages contribute to the superior reputation of microwave pyrolysis compared to traditional pyrolysis methods.

Pecan nutshells were used as precursors for producing activated carbon through a one-step process. The nutshells were treated and mixed with two different chemical agents, potassium carbonate and potassium hydroxide, in a 1 : 1 ratio. Subsequently, this mixture was subjected to microwave pyrolysis at power levels of 300 W and 400 W for periods ranging from 2 to 6 min. Notably, microwave pyrolysis significantly improved the formation of microporous structures, especially

Table 2 Comparative analysis of conventional *versus* microwave pyrolysis methods

Physical parameters	Conventional pyrolysis	Microwave pyrolysis
Heating procedure	Inconsistent surface heating	Internal and bulk heating
Physical activation temperature (°C)	750–1000	600–900
Chemical activation temperature (°C)	400–700	300–650
Physical activation time (min)	30–300	15–210
Chemical activation time (min)	30–120	5–20
Process flexibility	Less flexible	Flexible
Heat control	Not as exact	Accurate and regulated heating
Char yield	15–20%	20–35%
Gas yield	10–15%	30–60%
Bio-oil yield	65–75%	30–60%
Capital plant expenses, USD	~16 300	~20 000
Complexity	Low	High

in the samples activated with potassium hydroxide. For example, the samples pyrolyzed at 300 W for 6 min exhibited more than 73% ultra-microporosity. Additionally, these samples demonstrated an excellent CO_2 adsorption performance, achieving 5.3 mmol g^{-1} at 1 bar and 0 °C. This level of performance was comparable to that of the activated carbon synthesized through conventional methods reported in the literature, underscoring the significant potential of microwave pyrolysis for future application in the production of activated carbon. Vairaja *et al.* investigated the performance disparities between conventional and microwave pyrolysis in producing AC.[29] Both methods were employed to fabricate carbon activated from the husk of sunflower seeds. Following washing and drying, the precursor material was impregnated with varying concentrations of $ZnCl_2$ and subjected to microwave carbonization at power levels ranging from 200 to 1000 W for durations spanning 5 to 40 min. Subsequently, the samples underwent conventional treatment. The results indicated that the highest the activated carbon surface area was achieved at 600 W microwave power. In a separate study, Ali and Idris examined the influence of activation processes on the characteristics of synthesized activated carbon.[30] Pistachio shells were combined with different concentrations of K_2CO_3, KOH, $ZnCl_2$, and H_2SO_4, and the impact of the microwave power level in the range of 450 to 800 W was assessed. The optimal yields were obtained using a microwave power of 600 W with 15 min of irradiation when K_2CO_3 was used as the activation agent. Additionally, the surface area of the activated carbon increased by nearly 600% when the power was increased from 450 W to 600 W. However, this increase was followed by a decline of 27% and 58% in surface area as the power was further increased to 700 W and 800 W, respectively. Microwave pyrolysis shows promising results in biochar production due to its high yield, reduced energy requirements, and shorter activation times. Despite these advantages, the use of microwave technology for the synthesis of activated carbon is still limited to laboratory-scale applications, largely due to the technical challenges associated with scaling up to industrial levels.

2.3 Mechanism of pyrolysis

In elucidating the mechanism of pyrolysis, it is crucial to delineate the sequential transformations that three key biopolymers undergo throughout the pyrolysis cycle. Understanding the intricate processes involved not only sheds light on the fundamental principles governing pyrolysis but also aids in identifying the optimal biomass sources for extraction. By comprehending the underlying mechanisms, researchers can discern the most suitable biomass substrates from the vast array of naturally occurring sources, thereby facilitating the efficient conversion of biomass into valuable products. This elucidation of the pyrolysis mechanisms not only enhances our understanding of bioenergy production but also contributes to sustainable resource utilization.

2.3.1 Cellulose. Cellulose is a polymer formed through the linking of D-glucose units through β-(1–4) glycosidic bonds, creating a continuous network of chains that can range from several hundred to thousands of units. The formation of intramolecular and intermolecular hydrogen bonds between the –OH groups results in linear, parallel, and crystalline structures known as microfibrils. These microfibrils are aligned longitudinally within the cell walls of biomass materials, providing rigidity and strength to their cellular structures. Thus, understanding the pyrolysis mechanism of cellulose into biochar is crucial for leveraging this thermochemical process for the effective conversion of biomass. During pyrolysis, cellulose undergoes a sequence of intricate thermal decomposition reactions, ultimately yielding biochar as the primary product. Initially, cellulose undergoes dehydration, liberating water vapor as it disintegrates into smaller molecular fragments. Subsequently, these fragments undergo depolymerization and cross-linking reactions, leading to the generation of a complex mixture of volatile compounds, including gases and organic vapors, together with solid char residues. The pyrolysis process is initiated with the slow pyrolysis of cellulose at temperatures below 250 °C, accompanied by a reduction in the polymerization degree and the release of H_2O, CO_2, and CO. Above 250 °C, cellulose transforms into tar, which is predominantly comprised of organic compounds, while leaving behind a charred black residue. Mechanistically, the process begins with solid cellulose depolymerizing through the breaking of the glucosidic bond, resulting in the formation of a bicyclic compound, levoglucosan (LGA).[31] Subsequent dehydration and isomerization of LGA produce levoglucosenone (LGO), as well as 1,4:3,6-dianhydro-β-D-glucopyranose (DGP) and 1,6-anhydro-β-D-glucofuranose (AGF).[32] Both DGP and AGF undergo conversion to LGO through a dehydration reaction. LGA undergoes successive dehydration and rearrangement reactions, resulting in the generation of furan derivatives such as 5-methylfurfural, 2,3-butanedione, furfural, hydroxymethylfurfural, glycolaldehyde, and glyceraldehyde.[33] Further rearrangements, including aromatization, condensation, and polymerization, lead to the formation of a network of carbon matrix commonly known as biochar. Accordingly, understanding these intricate mechanisms sheds light on optimizing the production of biochar and its potential applications in various fields.

The presence of hydroxyl groups (–OH) plays a pivotal role in the formation of biochar, particularly influencing its hydrophilic surface properties, which are crucial for facilitating the dispersion of metal species. This investigation specifically addresses the relationship between the functionalities of biochar and its polarities by subjecting cellulose to pyrolysis at temperatures in the range of 200 °C to 700 °C, and subsequently characterizing the resulting biochar. The findings revealed that –OH, rather than the carbon–oxygen (C=O) and carbon–oxygen–carbon (C–O–C) functionalities, significantly contribute to the formation of biochar with a hydrophilic surface. Furthermore, this study identified the temperature of 440 °C as crucial, marking the peak abundance of hydroxyl groups (–OH) and aliphatic carbon–hydrogen (C–H) bonds. Beyond this temperature threshold in the range of 460 °C to 700 °C, a notable transition from oxygen-rich functionalities to carbon-rich functionalities occurs, with the dominant aromatization process leading to a substantial increase in the hydrophobicity of the biochar. The hydrophilic

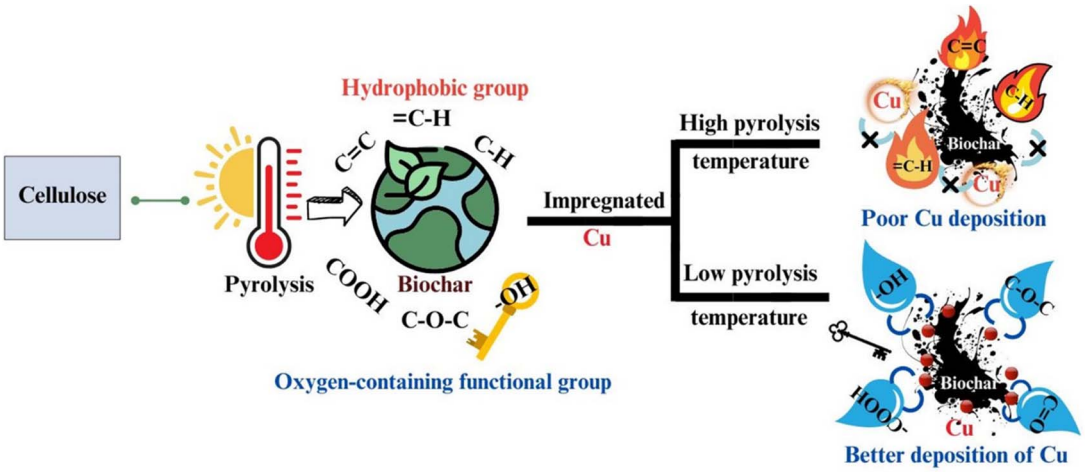

Fig. 5 Schematic showing the relationship between hydrophilicity and functional development of biochar. Reproduced from ref. 34.

nature of the biochar surface is vital in its utility as a support material for enhancing the dispersion of metals, such as copper (Cu), as demonstrated by the creation of bonding sites conducive to chelating with Cu^{2+} (Fig. 5).[34]

2.3.2 Hemicellulose. Hemicellulose, the second most abundant component in biomass-based materials, is crucial for maintaining the structural integrity of cell walls. It consists of a variety of heteropolymerized saccharides, including xylan, glucoxylan, glucomannans, and glucuronoxylan. Its diverse composition arises from monomer units such as xylose, glucose, galactose, mannose, and arabinose.[35] This heterogeneity gives rise to the amorphous nature of hemicellulose, providing essential support to cellulose. Upon pyrolysis, the decomposition of hemicellulose is initiated through depolymerization, yielding oligosaccharides similar to cellulose. Glucomannans and xylan, for instance, breakdown into various intermediates, including levoglucosenone, 1,6-anhydro-α-D-galactopyranose, levomannosan, 1,6-anhydro-β-D-mannopyranose, and 1,4-anhydro-D-xylopyranose.[36] These intermediates undergo additional changes into syngas and bio-oil products or directly participate in chemical reactions, leading to the formation of biochar networks. Aromatization, dehydration, and decarboxylation reactions dominate the conversion process, facilitating the formation of stable biochar structures (Fig. 6). Understanding the intricate mechanism of hemicellulose pyrolysis is crucial for optimizing the biomass conversion processes and harnessing biochar as a sustainable resource for various applications. Moreover, elucidating the pathways involved in the decomposition of hemicellulose sheds light on the fundamental principles governing biomass pyrolysis, paving the way for advancements in bioenergy production and environmental sustainability.

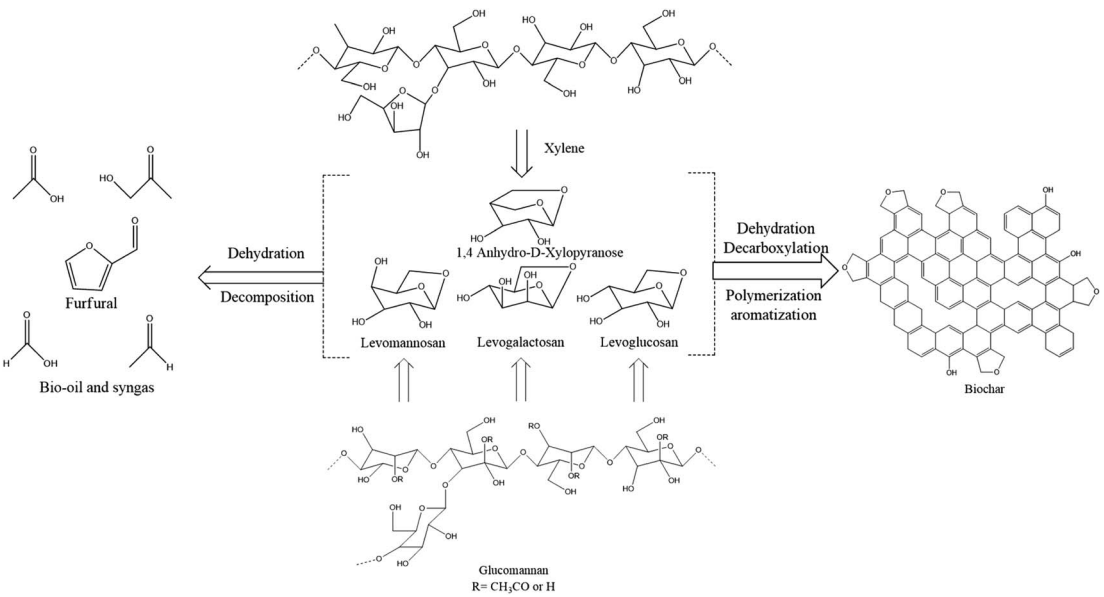

Fig. 6 Illustration of the breakdown mechanism of hemicellulose during pyrolysis and subsequent biochar formation.

2.3.3 Lignin. Lignin is an intricate organic polymer composed of *p*-hydroxyphenol, syringyl, and guaiacyl units, exhibiting a highly variable three-dimensional amorphous structure due to the differences in relative proportions and crosslinkages through –O– and C–C linkages.[37] Functional groups such as $-OCH_3$, OH, COOH, and C=O confer high polarity to lignin molecules. The pyrolysis of lignin is a complex process occurring over a wide temperature range owing to its diverse structure. The majority of interconnections in lignin involve β-O-4 linkages, constituting about 60% of its structure.[38] Upon pyrolysis, these linkages undergo cleavage, generating free radical species. Subsequent radical reactions lead to chain polymerization, ultimately leading to the production of a biochar network.[39] Moreover, methane gas is released during pyrolysis when the methoxy groups are broken. The intricate nature of biomass, combined with the distinct behavior of its constituent biopolymers at varying temperatures during pyrolysis, poses a significant challenge in elucidating the precise mechanism of the entire process. Furthermore, understanding the process by which activated porous carbons are derived from biomass presents an even greater challenge. Despite these complexities, previous review articles have attempted to describe the pyrolysis process, highlighting the ongoing efforts to unravel the intricate mechanisms underlying biomass conversion and biochar formation.[36]

2.4 Hydrothermal carbonization

Hydrothermal carbonization (HTC), recognized as hydrous pyrolysis, stands out as cost-effective and sustainable thermochemical conversion technology. It operates through exothermic reactions, primarily involving dehydration and decarboxylation reactions aimed at reducing the oxygen (O) and hydrogen (H) content in biomass. In a sealed reactor system using water as the reaction solvent, biomass undergoes a sequence of chemical transformations, including hydrolysis, dehydration, decarboxylation, polymerization, and aromatization. HTC is executed in the temperature range of 180 °C to 260 °C, under pressures of approximately 2–6 MPa, and for durations spanning 5–240 min.[40] This process encompasses two main techniques, *i.e.*, hydrothermal vaporization and liquefaction, which occur at temperatures exceeding 260 °C, leading to the substitution of gaseous and liquid fuel generation for solid fuel.[41] A distinctive advantage of HTC lies in its ability to process high moisture content feedstock and wet biomasses, eliminating the need for pre-drying as required in traditional pyrolysis methods. This not only streamlines the process but also significantly reduces the energy consumption, thereby enhancing the overall efficiency.[42] The resulting products from HTC include hydrochar (solid carbon matter), bio-oil (liquid), and small amounts of gases, with their properties and percentage distribution influenced by the process conditions.[43]

Table 3 Various biomass types utilized under different pyrolysis conditions

	Conditions				
Material	Temperature (°C)	Residence time (h)	Activation	Product yield (%)	Ref.
Apple pomace	300	0.5	Air	40.5	47
Prosopis juliflora	300–700	1–4	KOH	62	47
Yerba mate twig (YMT)	400–600	—	H_3PO_4	63	48
Date palm waste	500	2	—	75.4	49
Cassava peel	500	0.5	—	55	50
Palm kernel shell	450	1.5	KOH/carbon = 2 at 750 °C	57	51
Rambutan peel	600	3	KOH/HC = 2 at 850 °C	122	52
Corn stover	250	10	KOH	88	53
Bamboo waste	700	3.0	Alkali metal salt	70	54
Cellulose	450	1	Alkali metal salt	28	55
Bamboo waste	400–600	2–3	Steam	40	56
Sugarcane bagasse	450–600	1–3	KOH	55	57
Plastic waste	300	—	KOH	17	58
Birch bark	750	2	KOH	57	59
Wood chips	500	2	—	25	60
Loblolly pine	240	—	—	48.54	61
Tobacco stalk	180	2	—	80	62
Rice husk	400–700	1–2	CO_2	60	63
Eucalyptus bark	220	2	—	46.4	64
Sweet potato waste	180	1	—	63.18	65
Lignocellulose	200	—	—	50	66
Holocellulose	220	4	—	66.7	67
Lignin	300–390	—	KOH/carbon = 2, 600 °C	35.6	68
Lignin	300–390	—	KOH/carbon = 2, 700 °C	27.0	68
D-Glucose with urea	180	12	KOH/carbon = 1–3, 600–700 °C	—	69
Food waste	200	1	—	7	70

Hydrocar has emerged as a crucial product due to its versatile applications, displaying properties such as hydrophobicity and low ash content, which improve the mass, energy density, and combustion performance compared to the original feedstock.[44] Alternatively, biochar offers advantages in terms of porosity and surface area, making it suitable for applications such as adsorption and soil conditioning. HTC involves hydrothermal carbonization at both high and low temperatures (>220 °C, HHTC and ≤220 °C, LHTC, respectively). Although HHTC produces materials similar to coal under natural formation processes, LHTC, conducted under milder conditions, is more commonly employed in laboratories.[45] Notably, current LHTC technology has been employed for the production of useful carbon compounds in a variety of shapes, including honeycomb and fibrous structures.[46] HTC has significant utility in treating high-water-content biomass, similar to that seen in municipal sludge, resulting in considerable energy savings and positioning HTC as technology for green thermochemical conversion.

The primary byproducts of HTC treatment are gas, bio-oil, and hydrochar, which exhibit distinct characteristics. Hydrochar is comprised of matrix and coke microparticles, with the matrix formed through condensation, dehydration, and decarboxylation of unhydrolyzed biomass. In contrast, the coke microparticles originate from the aggregation of organic molecules and are rich in functional groups such as –OH, C=O, and –COOH, facilitating their reactivity with organic molecules in the liquid phase. Overall, HTC represents a promising avenue for biomass conversion, offering a range of valuable products with diverse applications and demonstrating potential for both laboratory-scale research and industrial implementation (Table 3).[71]

3. Key factors impacting the characteristics of carbon materials

Considering that pyrolysis stands out as the dominant method for biomass conversion, this section delves deeply into the diverse array of factors that influence the initiation and characteristics of carbon materials during pyrolysis. Besides the inherent qualities of biomass itself, significant emphasis is placed on manipulating the variables involved in the reaction. Parameters such as pyrolysis temperature, duration of residence, rate of heating, and ambient conditions all play pivotal roles in determining the outcomes of carbon materials. These variables not only govern the yield of char but also intricately mold its properties, encompassing aspects such as surface area and pH levels. Given the profound interplay between adsorption capacity and the attributes of sorbents, it is essential to meticulously scrutinize the full spectrum of factors that impact carbon materials.

3.1 Biomass-derived feedstocks for the production of carbon materials

Exploring the diverse array of biomass-derived feedstocks for the production of carbon materials reveals a promising avenue for sustainable resource utilization. The categorization of feedstock for AC production plays a pivotal role in evaluating the nutrient content and determining appropriate conversion techniques. Carbon-rich biomass, derived from both plant and animal sources, stands as the primary feedstock for AC production, with the objective of maximizing the carbon content in solid form.[72] Activated carbon encompasses carbon materials with a robust carbon framework and a highly developed internal pore structure and surface area. The properties of activated carbon are influenced by the structural polymers found in biomass, including cellulose, hemicelluloses, and lignin. A higher cellulose and hemicellulose content contributes to increased volatile vapor production, while lignin serves as the principal precursor for the synthesis of AC.[73] The characteristics of biomass, including mineral matter content, significantly impact the pyrolysis properties and resultant product yield.[74] Classification based on moisture content delineates between wet (above 30%) and dry (below 30%) biomass, aiding in the selection of suitable conversion methods.[75] Biomass can be further categorized as 'purpose-grown' and 'waste biomass'. Purpose-grown biomass, cultivated specifically for AC production, exhibits a low moisture content (<5%), high yield, and energy density, finding applications in the energy and biofuel sectors. Conversely, waste biomass, lacking economic value, serves as an alternative feedstock for char production, often undergoing hydrothermal carbonization due to its elevated moisture content.[76] Biomass sources encompass a wide range, including animal sources (such as pig dung, pigskin, wool, and fishbone), plant sources (such as straw, rapeseed, sawdust, and peanut shell), and municipal waste (such as sludge).[77] The main elements in biomass are carbon, hydrogen, and oxygen, with minor amounts of nitrogen and sulfur. The appropriate treatment of biomass enables its conversion into carbon materials with commendable adsorption capabilities. However, certain types of biomass, such as rice husk, which contains high levels of silicon, are commonly used in the production of silicon carbide (SiC).[78] Thus, the selection of suitable biomass constitutes the initial step in preparing high-quality carbon-based adsorbents. This chapter primarily reviews the biomass thermochemical conversion technologies, including pyrolysis, gasification, and hydrothermal carbonization, together with the factors influencing the properties of carbon materials such as the feedstock, temperature, residence time, and heating.

3.2 Pressure

In the domain of carbon material science, the influence of pressure stands as a pivotal yet often underestimated determinant. Pressure serves as a dynamic force that profoundly impacts the synthesis, structure, and properties of carbon materials across various manufacturing processes. Whether in the realm of crafting carbon nanomaterials or producing activated carbons, the application of varying pressure levels plays a central role in shaping the final product. Under high-pressure conditions, structural transformations are induced, porosity is altered, and mechanical properties are enhanced, thereby offering avenues for precise material tailoring. Conversely, low-pressure environments may foster the formation of specific carbon allotropes or facilitate unique chemical transformations, adding to the

intricacy of material design. The significance of pressure is particularly notable in the production of biochar and hydrochar. The reactions occurring within the reaction chamber adhere to Le Chatelier's principle, highlighting the critical role of pressure modulation. Increasing the pressure within the chamber, either through the introduction of non-reactive gases or elevating reaction temperatures, leads to notable enhancements in the yield and quality of both hydrochar and biochar.[45] This improvement is attributed to the accelerated decomposition of biomass, resulting in a superior end-product. In processes such as HTC, surpassing the critical pressure threshold enhances both the hydrolysis process and biomass decomposition, underscoring the multifaceted impact of pressure.[79] Although the physical structure of hydrochar remains relatively unchanged under increasing pressure, finer and more uniformly distributed particles emerge, accentuating the role of pressure in morphology control. Similarly, in pyrolysis, an increase in pressure prolongs the residence time, facilitating the formation of secondary carbon and augmenting the char quality. Moreover, pressure exerts a tangible influence on the carbon content and energy density of biochar, with high-pressure pyrolysis yielding superior outcomes in these aspects.[80] Understanding the subtle interplay between pressure and carbon materials is paramount for optimizing their performance across an extensive array of applications, spanning from energy conversion and storage to environmental remediation and beyond.

3.3 Temperature

Temperature stands as a pivotal determinant in shaping the characteristics of carbon materials, exerting a profound influence on their synthesis, structure, and intrinsic properties. Varied temperature regimes dictate the ultimate outcomes of carbon materials, exerting notable effects on parameters such as porosity, surface area, and chemical reactivity. In addition to feedstock considerations, the significance of operating conditions cannot be overstated. Among these factors, the synthesis temperature holds particular prominence. As the pyrolysis temperature increases, discernible trends emerge, where the specific surface area and pH levels tend to increase, while the char yield experiences a decline. For instance, investigations by Singh *et al.* illustrated a notable reduction in biochar yield together with an increase in pH and surface area across the temperature range of 250 °C to 650 °C during the pyrolysis of rice husk.[11] However, excessive temperatures can lead to detrimental effects, such as the destruction of surface and pore structures due to melting and collapse. This phenomenon can be ascribed to the high temperature-induced disintegration and reorganization of the biomass components. Moreover, pH levels exhibit a positive correlation with temperature due to the enrichment of alkaline minerals such as sodium and potassium under high-temperature pyrolysis conditions. Elevated pyrolysis temperatures also facilitate the expulsion of volatile substances, thereby contributing to the formation of more developed pore structures. The research by Lahijani *et al.* underscored the impact of pyrolysis temperature on the CO_2 capture efficiency, revealing that the biochar produced at higher temperatures exhibited enhanced CO_2 adsorption capabilities.[81] This enhancement can be attributed to the fragmentation of the carbon particles, reduction in average pore size, and formation of micropores induced by increasing the carbonization temperatures. The presence of a microporous structure significantly augments the adsorption of CO_2, underscoring the critical role of temperature in tailoring carbon materials for diverse applications, including environmental remediation and carbon capture technologies.

3.4 Residence time

Residence time, which denotes the duration in which the feedstock undergoes thermal decomposition in a reactor at a predefined temperature, has emerged as a critical parameter influencing the characteristics of carbon materials. Particularly in pyrolysis processes, the residence time exerts a substantial influence on both the yield and physicochemical attributes of biochar, primarily by fostering pore formation and structural refinement.[82] Prolonged reaction durations often yield positive outcomes, enhancing the energy density and facilitating the production of secondary hydrochar, distinguished by its polyaromatic structure. Conversely, shorter residence times tend to yield a higher hydrochar content, a phenomenon notably observed in HTC processes.[83] Manipulation of the residence time induces the release of volatile compounds, consequently affecting the composition of the resulting materials, with a lower soil product content observed under increased residence times.[84] Additionally, the residence time significantly impacts the texture of hydrochar, modulating processes such as polymerization and hydrolysis, and influencing the micropore diameter. Co-pyrolysis experiments involving agricultural residues and sewage sludge further elucidated the role played by the residence time, demonstrating a pronounced decrease in biochar yield with extended durations, suggesting the completion of organic compound degradation within 150 min.[85] Correspondingly, surface area exhibits a notable increase with longer residence times, which is attributed to the enhanced thermal decomposition and subsequent porous structure development, potentially augmenting the CO_2 adsorption capacity.[86] However, a further increase beyond 150 min resulted in a decline in surface area due to structural collapse. These insights underscore the intricate relationship between residence time and properties of carbon materials, emphasizing the need for meticulous control and optimization to tailor the characteristics of materials for diverse applications, including carbon sequestration and environmental remediation.

3.5 Heating rate

The rate at which heating occurs plays a crucial role in shaping the characteristics of carbon materials, influencing parameters such as carbonization efficiency, surface morphology, and chemical composition. Typically, accelerated heating rates result in higher carbonization temperatures, fostering rapid pyrolysis and potentially inducing structural alterations, whereas slower rates afford a more controlled decomposition process, yielding materials with distinctive surface functionalities. This aspect of the heating rate significantly impacts the

pyrolysis carbonization mechanism and the characteristics of the resultant biochar. Notably, an increase in heating rate is often correlated with enhanced biomass weight loss. For instance, the research conducted by Li *et al.* scrutinized the pyrolysis of lignin at varying heating rates, revealing a decrease in biochar yield from 55.5% to 50.1% as the heating rate increased from 5 to 20 °C min^{-1}, together with a concomitant rise in gas yield from 18.2% to 22.2%.[87] Moreover, increased heating rates facilitate the cracking of organic constituents and volatiles within biochar, expediting the generation of gas. Despite the prevailing assumptions that higher heating rates uniformly augment the specific surface area of biochar, contradictory findings have been documented. Hu *et al.* observed a decrease in specific surface area from 362 to 146 m^2 g^{-1} with an increase in the heating rate from 2 to 15 °C min^{-1}, followed by an increase to 327 m^2 g^{-1} at 25 °C min^{-1}.[88] This phenomenon is attributed to the intense decomposition and volatile diffusion occurring at steep heating rates, underscoring the interplay between the heating rate and biochar characteristics.

4. Activated carbon

Activated carbon, commonly known as AC, encompasses carbonaceous materials featuring a sturdy carbon framework together with a fully developed surface area and interior pore structure. Various organic materials possess the potential for conversion into activated carbon, with petroleum coke, peat, and wood being the common precursors utilized in its development.[89] Therefore, comprehending the composition and structure of the precursor material is imperative in determining the most suitable activating agent for AC production. The constituent structural polymers within biomass, including cellulose, hemicelluloses, and lignin, significantly influence the characteristics of the resulting AC. Typically, biomass is comprised of approximately 40% cellulose, 30% hemicellulose, and 30% lignin, with lignin requiring higher temperatures for complete decomposition compared to cellulose.[90] Consequently, materials rich in lignin content tend to yield AC with a lower surface area at lower activation temperatures.[91] Additionally, non-structural components such as proteins, ash, waxes, pectin, tannins, and chlorophylls contribute to the raw material composition.[92] Micropores, among the various pore structures present, play a pivotal role in adsorption due to their small void space, facilitating the trapping of organic molecules. The micropores formed during the activation of carbon are crucial for the adsorption of carbon dioxide, given that they allow localized van der Waals forces to overlap, promoting strong electrostatic attraction and physisorption.[93] A pore size of less than 1.0 nm is deemed effective for CO_2 capture due to the small molecular size of CO_2.[94] The adsorption process exhibits low activation energy, enabling reversible adsorption and the potential for multiple-layer CO_2 adsorption on AC, thereby enhancing the adsorption capacity. Thus, optimizing the synthesis process is paramount for producing AC with a high surface area, which is conducive to efficient CO_2 adsorption. However, despite its stability and superior surface area, activated carbon faces challenges regarding economic and environmental viability.[95] Recent advancements highlight the equivalent CO_2 adsorption capabilities of activated carbon derived from various waste material precursors compared to their commercial counterparts, offering promising avenues for the sustainable production of AC.[96]

4.1 Carbon material modification techniques

In the field of carbon materials, investigating techniques for their modification is a crucial area of study driving research and innovation forward. This review offers a comprehensive examination of the various methodologies intended to customize the properties and functions of carbon materials, elucidating a wide array of modification techniques and their applications across different fields. Carbon materials derived from biomass in their original state exhibit inherent limitations in chemical composition and pore structure, restricting their ability to adsorb CO_2 effectively. Therefore, modifying carbon materials becomes exceedingly significant, particularly in the realm of CO_2 capture.

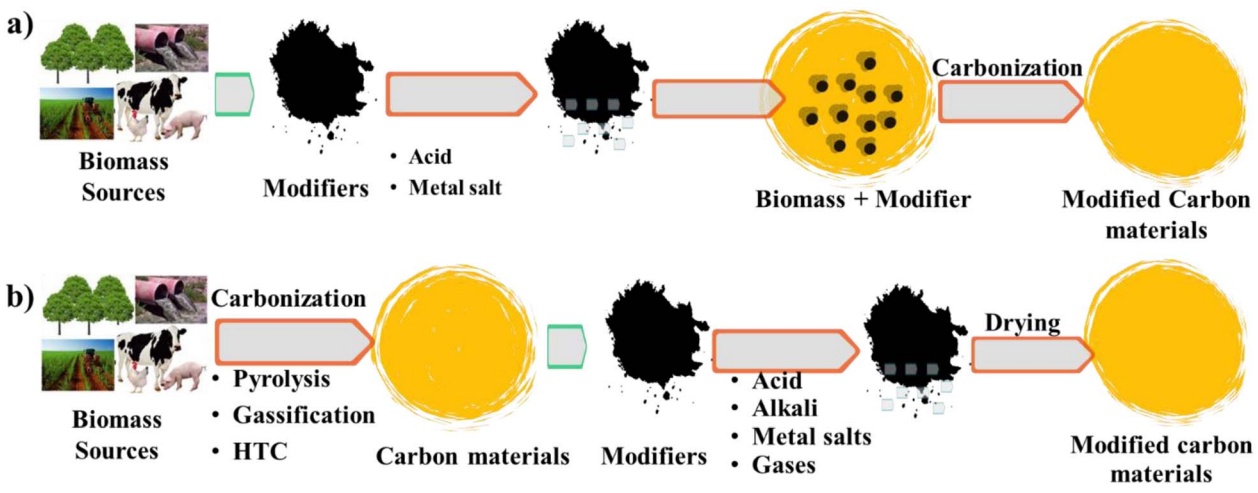

Fig. 7 Schematic illustrating the two primary approaches for modifying carbon materials: (a) pre-treatment and (b) post-treatment methods.

The two primary approaches for modifying carbon materials are outlined, as illustrated in Fig. 7, *i.e.*, pre-treatment, which involves directly mixing raw biomass with acids or metal salts before carbonization, and post-treatment, modifying carbonized biomass through activation with substances such as acids, bases, metal salts, and gases. Notably, it is imperative to treat raw biomass with diluted acid prior to its modification to remove its ash content, thus averting pore blockage during the carbonization process. This review thoroughly explores the modification methods, which are classified into three main categories of physical methods (steam/air/CO_2 activation), chemical processes (acid/alkaline activation, metal or metal oxide impregnation, and heteroatom doping), and supplementary techniques (ball milling, microwave, ultrasound, and plasma treatment). Through a detailed analysis of these techniques, this review seeks to offer valuable insights into the latest advancements and future trajectories in the modification of carbon materials, aiming to enhance their performance and widen their range of applications.

4.1.1 Physical treatment. Physical activation presents an eco-friendly, cost-efficient, and straightforward method compared to chemical activation approaches. By employing gases as templates, precise control of the textural characteristics of activated carbon is achievable. During pyrolysis in the temperature range of 300–1100 °C, diverse degradation by-products including CO_2, CO, CH_4, NO, H_2O, and NH_3 are produced, depending on the source of the precursor material. Moreover, external medium sources such as CO_2, NH_3, steam, He, Ar, air, and gas mixtures can be utilized to activate the surface of carbon. Extensive endeavors have been devoted to enhancing the pore volume and surface area of carbon materials through physical activation methodologies.

4.1.1.1 Steam activating methods. Steam activation is a significant technique for improving the textural characteristics of carbon materials by facilitating the creation of additional pores.[97] This process involves the diffusion of steam into the carbon material, which promotes the formation of pores. The underlying mechanisms of steam activation encompass various reactions, including the interaction between carbon and water vapor to generate carbon monoxide and hydrogen, together with the production of methane and other gases.

$$C + H_2O \rightarrow C(O) + H_2 \quad (1)$$

$$C(O) \rightarrow CO + C \quad (2)$$

$$CO + H_2O \rightarrow CO_2 + H_2 \quad (3)$$

$$C + 2H_2O \rightarrow CO_2 + 2H_2 \quad (4)$$

$$C + CO_2 \rightarrow 2CO \quad (5)$$

$$C + 2H_2 \rightarrow CH_4 \quad (6)$$

$$CH_4 + H_2O \rightarrow CO + 3H_2 \quad (7)$$

Observations demonstrate a notable enhancement in specific surface area and pore volume of biochar following its steam activation. For instance, Xie *et al.* employed steam activation to modify biochar derived from tea waste, resulting in a significant increase in specific surface area from 342 to 576 m^2 g^{-1} and enhancement in pore volume from 0.022 to 0.109 cm^3 g^{-1}.[98] The enhancement in pore structure resulting from steam activation can be attributed to the elimination of pore-clogging tar, the creation of new micropores, and the enlargement of existing pores. Different steam activation conditions, such as temperature and reaction time, have varying effects on the activation results. Other studies using cellulose fibers as a raw material revealed that steam activation facilitated the formation of new pores and influenced the expansion of the pore sizes, leading to a remarkable CO_2 adsorption capacity of 3.78 mmol g^{-1}.[99] Furthermore, the steam activation of carbon derived from cellulose fibers resulted in the expansion of existing ultra-micropores and the generation of additional ultra-micropores (Fig. 8).[100] This activation process disrupted the graphitic structure, resulting in pore sizes exceeding 2 nm and a significant increases in specific surface area and pore volume. Additionally, Chen *et al.* demonstrated that steam activation of biochar produced from pine sawdust not only enhanced its textural properties but also enriched its surface functional groups.[101] The specific surface area increased from 316 to 582 m^2 g^{-1}, and the pore volume increased from 0.17 to 0.25 cm^3 g^{-1}. XPS analysis indicated an increase in the oxygen content of biochar from 9.16% to 11.05% following steam activation, which was attributed to the increase in the content of C–O, C–OH, and O–C=O functional groups. These findings underscore the efficacy of steam activation in improving the textural properties and surface chemistry of carbon materials, thereby expanding their potential applications across various fields.

4.1.1.2 Air activating methods. Air activation has emerged as a notable strategy for altering carbon materials, offering an environmentally friendly alternative compared to chemical activation techniques. This method involves utilizing air as the activating agent, eliminating the need for additional chemicals. Oxygen, known for its potent oxidizing properties, plays a crucial role in the activation process. However, due to the prohibitive cost of pure oxygen, air is commonly utilized for activation purposes. The underlying mechanism for air activation can be understood through various reactions,[102] as follows:

$$2C + O_2\,(g) \rightarrow 2CO \quad (8)$$

$$C + O_2\,(g) \rightarrow CO_2 \quad (9)$$

$$C(O) + O_2\,(g) \rightarrow CO\,(g) + CO_2 \quad (10)$$

Air oxidation has the potential to introduce new functional groups into biochar. However, this oxidation process may lead to a slight decrease in surface area due to the new functional groups obstructing the pores. Kim *et al.* observed that air oxidation enriched the micropores of biochar and introduced O-groups, albeit resulting in reduced specific surface area.[103] Furthermore, carbon materials produced at lower temperatures are more susceptible to oxidation, leading to the introduction of additional –COOH and C=O groups. In comparison with steam

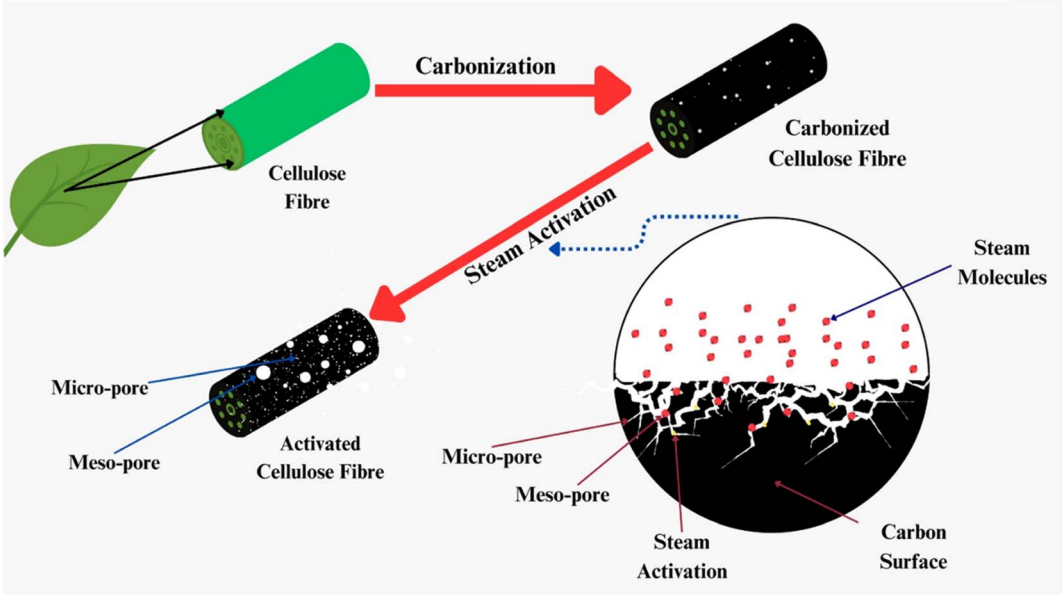

Fig. 8 Diagram illustrating the process of activating the surface of carbon with steam.

activation, air oxidation tends to introduce O-containing groups more readily. Another research group reported differing outcomes between steam activation and air oxidation, with steam activation resulting in an increased surface area but decreased functional group concentration, while air oxidation led to a higher functional group concentration in biochar.[104] Lee *et al.* conducted air activation on biochar at various temperatures and noted a significant enhancement in surface groups such as –OH, C=O, and C–O.[105] This enhancement is attributed to the reactions between O_2 and the lignocellulosic components or aromatic substances within the biochar. Additionally, they examined the impact of activation time on the process, observing an initial increase in the micropores within the first 15 min, followed by an increase in the content of mesopores. However, a prolonged activation time could potentially lead to micropore destruction, highlighting the importance of selecting an appropriate activation duration. For carbon materials intended for CO_2 capture applications, determining the optimal oxygen activation treatment time is essential to maximize their efficacy.

4.1.1.3 CO_2 activating methods. CO_2 activation has emerged as a significant technique for modifying carbon materials, providing an eco-friendly avenue to enhance their properties. This method involves employing CO_2 as the activating agent, leading to tailored advancements in the pore structures and surface functionalities within carbon materials. Its adoption is gaining recognition due to its environmentally benign nature and the abundance of CO_2 as a readily accessible resource. CO_2 activation can be carried out either simultaneously with biomass pyrolysis or as post-pyrolysis treatment. Studies suggest that pyrolysis conducted in a CO_2 atmosphere is advantageous for preserving C and N in biomass. Moreover, this activation approach significantly improves the porosity and specific surface area of carbon materials. For instance, Tomin *et al.* illustrated that CO_2 activation predominantly yields micropores in porous carbon fibers, resulting in a specific surface area of up to 1012 $m^2 g^{-1}$.[106] However, the development of mesoporous structures may be observed in certain carbon materials following CO_2 activation, which is influenced by factors such as the type of pristine materials and activation conditions. Activation of various biochars with CO_2, including wheat straw, softwood, and peach stones, resulted in a more pronounced development of mesoporous structure in wheat straw and softwood biochar, while peach stone biochar exhibited some enhancement in microporosity.[107] CO_2 activation involves the Boudouard reaction, an endothermic process, and thus higher temperatures favor CO_2 activation. For instance, CO_2 activation of biochar conducted at temperatures in the range of 800 °C to 950 °C showed an escalation in pore improvement with an increase in the activation temperature.[108] Specifically, the specific surface area of biochar increased from 392 $m^2 g^{-1}$ to 506, 854, 1059, and 2186 $m^2 g^{-1}$, respectively, with micropores less than 2 nm dominating the pore structures for all the samples. These findings underscore the efficacy of CO_2 activation in enhancing the porosity and specific surface area of carbon materials, offering promising avenues for their utilization in various applications.

4.1.2 Chemical treatment

4.1.2.1 Alkaline activating methods. Alkaline activation is a crucial method for modifying carbon materials, offering a flexible approach to customize their properties. This process involves the use of alkaline agents such as KOH and NaOH to activate the carbon precursors, leading to the formation of tailored pore structures and surface functionalities. This method is particularly advantageous for enhancing the CO_2 adsorption capacity by promoting pore development and incorporating alkaline groups. The common alkaline activators include KOH, NaOH, and amino ($–NH_2$) groups. Among them, KOH is widely recognized for its effectiveness as a metal

hydroxide in activating carbon materials. Typically, the activation process begins by thoroughly mixing KOH with the carbon precursor. The redox reaction between KOH and the carbon precursor starts at around 400 °C, producing K_2CO_3. As the temperature increases to about 600 °C, KOH is fully converted into K_2CO_3. At temperatures above 700 °C, K_2CO_3 begins to decompose into CO_2 and potassium oxide (K_2O). Additionally, at even higher temperatures, both K_2CO_3 and K_2O can be reduced to potassium (K), which infiltrates the carbon lattice in vapor form, assisting the formation of micropores and enhancing the porous structure.

The reaction sequence for KOH activation is outlined as follows:[108]

$$2C + 6KOH \rightarrow 2K + 2K_2CO_3 + 3H_2 \quad (11)$$

$$K_2CO_3 \rightarrow K_2O + CO_2 \quad (12)$$

$$C + CO_2 \rightarrow 2CO \quad (13)$$

$$2C + K_2CO_3 \rightarrow 2K + 3CO \quad (14)$$

$$C + K_2O \rightarrow 2K + CO \quad (15)$$

KOH activation enhances the surface functionality of carbon materials by introducing various groups such as –OH, C=O, C–C, and = C–H. However, as the synthesis temperature increases, the O-containing groups on the surface of the carbon material decompose, resulting in the production of CO and CO_2.[109] Due to the acidic nature of carbon dioxide, incorporating Lewis bases on the surface of carbon materials has been proven to be advantageous for CO_2 capture. An investigation into biochar derived from a mixture of food and wood waste demonstrated that although KOH activation led to superior microporous structures and enhanced CO_2 adsorption capacity, activation with KOH–CO_2 did not yield further improvements.[110] Researchers explored the impact of KOH activation on the production of porous carbon from biomass for supercapacitors, noting the significant influence of KOH on the microstructure of the resulting char. The optimized carbon materials exhibited a specific surface area of up to 2790 $m^2 g^{-1}$, with a graded pore structure enhancing the rate performance and achieving a maximum specific capacitance of 327 F g^{-1}.

Alternatively, NaOH activation offers stronger oxidizing properties and is more environmentally friendly. Studies indicate that the redox reaction between NaOH and carbon contributes to forming both micropores and mesopores in carbon materials. During activation, NaOH interacts with carbon materials through reactions as follows:[111]

$$2C + 6NaOH \rightarrow 2Na + 2Na_2CO_3 + 3H_2 \quad (16)$$

$$2C + Na_2CO_3 \rightarrow 2Na + 3CO \quad (17)$$

$$2Na + CO_2 \rightarrow Na_2O + CO \quad (18)$$

Sodium hydroxide (NaOH) activation of carbon generates active intermediates such as CO, CO_2, and H_2, simultaneously facilitating the infiltration of Na and Na_2CO_3 into the carbon layer, which expands its atomic structure and enhances the specific surface area and pore diameter of the resulting carbon materials. However, excessive NaOH concentrations can intensify gasification reactions, ultimately reducing the effective area. Elevated NaOH concentrations may also induce a series of reactions (*e.g.*, C–NaOH, C–Na_2CO_3, C–Na_2O, C–Na, C–CO_2, and C–CO), leading to the rupture of the C–C and C–O–C bonds and diminishing the yield of carbon materials.[112] Studies by Shin *et al.* demonstrated the synthesis of carbon materials from macroalgae using NaOH activation, yielding materials with a significant surface area of 1238 $m^2 g^{-1}$. Another investigation highlighted the enhancement of aromatic properties in biochar through NaOH activation, promoting π–π interactions during pollutant adsorption.[113]

Incorporating amino groups into carbon materials also significantly enhances their CO_2 capture capacity. NH_3 treatment, typically performed at high temperatures, introduces basic functional groups and removes acidic groups from the surface of carbon. This treatment results in the formation of amides, lactams, imides, and heterocyclic compounds such as pyrrole and pyridine.[114] Additionally, NH_3 activation moderately improves the pore size and specific surface area. Studies by Wu *et al.* demonstrated an increase in the specific surface area of biochar from coconut fiber from 4, 7, and 541 $m^2 g^{-1}$ to 9, 24, and 553 $m^2 g^{-1}$, respectively, after $NH_3 \cdot H_2O$ modification.[115] Liu *et al.* synthesized microporous N-doped carbon materials using NH_3 as the activator, highlighting the synergistic effects of pores and N-groups in determining high CO_2 capture capacity and selectivity over N_2.[116]

4.1.2.2 Acid activating methods. Acid activation serves as a crucial technique for tailoring the characteristics of carbon materials, significantly enhancing their surface area, pore structure, and functional groups, thereby improving their adsorption capabilities. Typically, this process involves treating carbonaceous materials, such as activated carbon, biochar, and carbon fibers, with strong acids such as H_3PO_4, H_2SO_4, and HNO_3. The acid activation process not only creates new pores but also widens the existing pores, leading to a well-developed pore structure, which is essential for various adsorption applications.

H_3PO_4 has emerged as the predominant acid activator in the production of activated carbon for carbon capture applications, undergoing transformation into polyphosphate during the activation process.[117]

$$2P_2O_5 + 5C \rightarrow P_4 + 5CO_2 \quad (19)$$

$$2H_2P_2O_7^{2-} \rightarrow P_4 + 6O_2 + 2H_2O \quad (20)$$

Activation with H_3PO_4 not only stimulates the development of pores but also introduces novel functional groups into the structure of carbon. For instance, the immersion of *Lantana camara* biomass in 85 wt% H_3PO_4 solution led to a significant increase in the specific surface area of the activated biochar from 117 to 1177 $m^2 g^{-1}$ and a 20-fold increase in pore volume compared to the untreated biochar.[118] Furthermore, the oxygen

content of the biochar increased, with the XPS analysis confirming the presence of surface groups such as C–PO_3, C–P_2O_6, and C–P_2O_5. Similarly, Bonga *et al.* observed surface groups such as C–O–PO_3 and C–PO_3 in biochar produced through phosphoric acid activation in the temperature range of 400–600 °C.[119] However, it is notable that the acidic P_xO_y groups resulting from H_3PO_4 activation have been found to hinder CO_2 chemisorption in carbon materials. In this case, fine-tuning of the surface chemistry and porous structures of carbon materials can be achieved by adjusting the concentration of H_3PO_4 and the treatment temperature.[120] Although a porous structure plays a crucial role in CO_2 capture at lower temperatures, surface chemistry, including the presence of functional groups, becomes increasingly influential at higher temperatures during adsorption. Thus, meticulous attention is warranted in both the preparation and application of H_3PO_4-activated carbon.

Sulfuric acid is an extremely reactive substance, which can interact with organic compounds, such as carbohydrates, to extract water and break down organic precursors into carbon, according to the following reaction:[121]

$$C_nH_{2n}O_n + H_2SO_4 \rightarrow nC + H_2SO_4 \cdot nH_2O \quad (21)$$

Additionally, sulfuric acid reacts with the mineral content in lignocellulosic materials, serving as an effective cleaning and de-ashing agent in the preparation of activated carbon. This makes H_2SO_4 a cost-effective option for carbonization processes, offering both economic and functional advantages.[121] Furthermore, the activation process using sulfuric acid is known to enhance the porous structure of the resulting activated carbon. Notably, the porous carbon treated with H_2SO_4 exhibited a commendable CO_2 adsorption capacity of 3.60 mmol g^{-1}, marking a 39.5% improvement compared to the untreated sample.[122] The acid penetrates the material, creating a surface with a combination of large and medium-sized pores, which is beneficial for a variety of applications.[121,123]

Additionally, nitric acid activation is primarily used to introduce a variety of oxygen-containing functional groups, such as carboxyl, hydroxyl, and carbonyl groups, on the surface of carbon. This treatment is usually conducted at room temperature to 100 °C. Nitric acid oxidizes the surface of carbon, creating defects and functional groups, which enhance the adsorption capacity for polar molecules, including heavy metals and organic pollutants. The reaction mechanism is as follows:[124]

$$HNO_3 \rightarrow NO_2 + O_2 + H_2O \quad (22)$$

$$2NO_2 + C \rightarrow C(O) + 2NO \quad (23)$$

$$C(O) + H_2O \rightarrow COOH \quad (24)$$

$$C + HNO_3 \rightarrow C\text{–}OH + 2NO_2 \quad (25)$$

$$C + O_2 \rightarrow C{=}O \quad (26)$$

The oxidation process increases the surface acidity and introduces active sites, which improve the interaction of carbon materials with the adsorbate, enhancing their performance in various applications.

4.1.2.3 Salt activating method. Salt activation is a crucial method for tailoring the properties of carbon materials, offering a versatile approach to enhance their surface area, pore structure, and adsorption capabilities. This technique employs various salts, such as potassium carbonate (K_2CO_3), sodium carbonate (Na_2CO_3), zinc chloride ($ZnCl_2$), and ferric chloride ($FeCl_3$), to activate the carbonaceous precursors through thermal treatment. Unlike traditional alkaline activators such as KOH and NaOH, which are strong bases, salts such as K_2CO_3 and Na_2CO_3 also contribute to activation by providing different chemical environments. These salts activate the carbonaceous precursors through thermal treatment, promoting the development of porous structures *via* specific reaction mechanisms.[125]

K_2CO_3 is a common activating agent, which upon heating typically between 700 °C and 900 °C, decomposes to release CO_2 and K_2O. The CO_2 generated in this reaction acts as a gasifying agent, creating pores within the carbon matrix. Additionally, K_2O can further react with the carbon structure to form metallic potassium, which intercalates into the carbon lattice, enhancing its porosity, as follows:

$$K_2CO_3 \rightarrow K_2O + CO_2 \quad (27)$$

$$K_2O + C \rightarrow 2K + CO \quad (28)$$

This process leads to a significant increase in surface area and pore volume, making K_2CO_3-activated carbons highly effective for adsorption applications.[126]

Na_2CO_3 follows a similar activation pathway to K_2CO_3. During thermal treatment, Na_2CO_3 decomposes into sodium oxide (Na_2O) and (CO_2). CO_2 aids in the development of a porous structure by gasifying the carbon material. Na_2O further reacts with carbon to produce elemental sodium, which intercalates into the carbon structure, enhancing the formation of pores, as follows:[127]

$$Na_2CO_3 \rightarrow Na_2O + CO_2 \quad (29)$$

$$Na_2O + C \rightarrow 2Na + CO \quad (30)$$

Carbon materials activated by Na_2CO_3 exhibit a high surface area and improved adsorption properties, making them suitable for various environmental applications, including pollutant capture and energy storage.

$ZnCl_2$ is widely recognized as an effective activation agent, particularly due to its strong dehydrating properties. The activation process with $ZnCl_2$ typically involves three stages during pyrolysis. Initially, biomass decomposes into small particles and volatiles as the temperature increases. In the subsequent stage, $ZnCl_2$ interacts with these particles, producing char, tar, and volatiles through the following reaction:[128]

$$ZnCl_2 + C \rightarrow Zn + Cl_2 + CO \quad (31)$$

In the final stage, the char undergoes further reaction with $ZnCl_2$, leading to significant pore development. Carbon

materials activated with $ZnCl_2$ are noted for their increased prevalence of mesopores and macropores, which is attributed to the deep penetration of molten $ZnCl_2$ into the carbon lattice, which expands the pore structure. Co-activation with CO_2 further enhances the specific surface area, total pore volume, and even generates ultra-fine pores.[129,130] Conversely, activation with ferric chloride ($FeCl_3$) is more effective in promoting micropore formation, as demonstrated by Elewa *et al.*, who achieved a micropore volume of 0.468 $cm^3\ g^{-1}$ using $FeCl_3$.[131] However, the environmental implications of $ZnCl_2$ activation warrant attention. During this process, some $ZnCl_2$ can be converted to ZnO, which may adsorb on the activated carbon, posing the risk of soil and groundwater contamination. Considering these concerns, the EU proposed restrictions on high concentrations of ZnO since 2017, with similar measures initiated by China in 2018.[132]

$FeCl_3$ is another effective activating agent, particularly favoring micropore formation. In the activation process, $FeCl_3$ acts as a catalyst, promoting the removal of volatile compounds and facilitating the development of a highly porous structure, as follows:

$$2FeCl_3 + 3C \rightarrow 2Fe + 3Cl_2 + 3CO \quad (32)$$

This reaction results in carbon materials with a high micropore volume, which is beneficial for applications such as gas storage and separation.[133]

4.1.2.4 Metal doping. The impregnation of biomass-derived carbon materials with metals such as sodium, calcium, magnesium, aluminum, nickel, and iron has attracted significant attention as a strategy to enhance their CO_2 capture capabilities. Biomass-derived carbon materials, including biochar and activated carbon, are attractive due to their sustainable and eco-friendly nature, offering a renewable alternative by recycling agricultural and forestry waste. These materials naturally possess high surface areas and porous structures, making them highly effective for gas adsorption. Furthermore, the introduction of metal species into these carbon matrices can enhance their CO_2 adsorption capacities and selectivity, making them more efficient and versatile for carbon capture applications.[134]

Sodium and calcium, both alkaline metals, have been shown to significantly enhance CO_2 capture through chemisorption mechanisms. When impregnated into biomass-derived carbon materials, these metals form stable carbonates, such as Na_2CO_3 and $CaCO_3$, respectively, which effectively bind CO_2 molecules. This chemisorptive process not only increases the efficiency of CO_2 capture but also reduces the likelihood of desorption, making these materials more reliable for long-term CO_2 storage.[135] The stability of these carbonates ensures that the captured CO_2 remains securely bound, reducing the risk of its release back into the atmosphere. Magnesium, another alkaline earth metal, also enhances the capture of CO_2 when incorporated into biomass-derived carbon materials. The formation of $MgCO_3$ within the carbon matrix, combined with the high surface area of the material, creates an effective platform for CO_2 adsorption. The presence of $MgCO_3$ not only increases the affinity of the material for CO_2 but also contributes to the overall stability of the adsorbed CO_2.[136] Aluminum impregnation introduces Lewis acid sites on the surface of carbon through the formation of alumina (Al_2O_3). These acid sites interact strongly with CO_2 molecules, significantly enhancing both the adsorption capacity and selectivity of the material.[13] The strong interaction between CO_2 and the aluminum-impregnated carbon material increases the efficiency of CO_2 capture, making it particularly suitable for selective CO_2 adsorption in mixed-gas streams.

Transition metals such as iron and nickel play crucial roles in improving CO_2 capture. Iron, forms iron oxides, such as Fe_2O_3 and Fe_3O_4, on the surface of carbon. These oxides facilitate both physisorption and chemisorption mechanisms, significantly enhancing the overall CO_2 capture efficiency.[137] Alternatively, Ni doping is a promising strategy to enhance their properties for various applications, particularly in CO_2 adsorption and electrochemical energy storage. Nickel doping involves impregnating carbon materials derived from biomass with a nickel precursor such as nickel nitrate ($Ni(NO_3)_2$) or nickel chloride ($NiCl_2$). This process begins with the pyrolysis of biomass to produce a porous carbon framework. Subsequently, this carbon material is impregnated with a nickel salt solution, allowing nickel ions to diffuse and become uniformly distributed within the carbon matrix. After impregnation, the material undergoes thermal activation, typically at temperatures in the range of 300 °C to 900 °C in an inert atmosphere. This thermal treatment reduces the nickel salts to metallic nickel, which is embedded within the carbon structure, forming nickel oxides and carbonates, serving as active sites for CO_2 interaction.[138]

The incorporation of nickel into biomass-derived carbons significantly enhances their CO_2 adsorption capacity and selectivity. Nickel carbonates and oxides provide additional active sites, which promote stronger interactions with CO_2 molecules, thereby increasing the amount of CO_2 that can be adsorbed. This is particularly advantageous for applications requiring selective adsorption, such as carbon capture and storage.[102] The presence of nickel also improves the selectivity of materials for CO_2 over other gases, making it more efficient in separating CO_2 from gas mixtures. This enhanced selectivity is due to the specific interactions between CO_2 molecules and the nickel-based active sites, which are less favorable for other gases. In addition to gas adsorption, nickel doping significantly improves the electrochemical properties of biomass-derived carbons. In applications such as fuel cells, batteries, and supercapacitors, nickel acts as a catalyst, which enhances the electrocatalytic activity and stability of the carbon material. Also, the presence of nickel increases the electrical conductivity and facilitates efficient charge transfer, which are crucial for high-performance energy storage and conversion devices.[139]

4.1.2.5 Heteroatom doping. Heteroatom doping provides a promising pathway for tailoring the characteristics of carbon materials by deliberately introducing elements such as nitrogen, sulfur, and boron into the carbon framework. This approach alters the electronic structure and surface chemistry of carbon, thereby improving its conductivity, catalytic activity, and ability to adsorb various substances. Nitrogen doping has

attracted considerable interest due to its capacity to create active sites and enhance the electrochemical performance of carbon-based materials. Similarly, sulfur and boron doping have been explored for their potential to augment the adsorption capacity and stability of carbon materials across diverse applications. Although micropores play a pivotal role in carbon dioxide capture, surface functional groups also significantly contribute to the adsorption process, accounting for about 38%. Surface alkalinity plays a crucial role in CO_2 adsorption, and heteroatom doping has been demonstrated to enhance the surface alkalinity, thereby improving the CO_2 uptake.[140] Nitrogen doping, being the most extensively researched method, not only regulates the pore structure of carbon materials but also enriches them with various forms of N-containing groups such as pyridone, cyanide, pyrrole, pyridine, amine, quaternary, and pyridine-*N*-oxide. Compounds such as PEI, TEPA, and DETA have been shown to be effective as nitrogen dopants for CO_2 capture.[129] However, the additional cost associated with nitrogen doping underscores the importance of identifying nitrogen-rich biomass sources for the synthesis of carbon materials. However, although biomass with a high nitrogen content tends to yield nitrogenous biochar, not all nitrogen in biomass can be converted to N in carbon materials, given that some may be transformed into NH_3 or other gases during the process. Beyond single nitrogen doping, other elements such as sulfur and co-doping have been proven to be effective. For instance, researchers synthesized sulfur-doped porous carbon with a CO_2 adsorption capacity of 4.5 mmol g^{-1}, surpassing similar materials doped with nitrogen, which is possibly due to the higher binding energy of CO_2–S compared to CO_2–N, resulting in more stable adsorption and higher capacity.[141] Guo *et al.* utilized poplar sawdust as a raw material and sulfur-containing wastewater as a modifier to co-load nitrogen, sulfur, and oxygen on activated carbon, yielding porous carbon with a CO_2 adsorption capacity of 5.61 mmol g^{-1} at 0 °C.[142]

4.1.2.6 Other modification methods. Besides the primary modification methods discussed previously, supplementary approaches such as ball milling, microwave irradiation, ultrasound treatment, and plasma modification show potential for further improving carbon materials. Ball-milling modification utilizes the kinetic energy produced during the movement of balls in machinery to diminish the particle size of materials or disrupt their chemical bonds, thereby modifying their pore structures. An examination of crayfish shell biochar pre- and post-ball milling unveiled notable enhancements in its specific surface area and micropore volume, escalating from 128 to 290 $m^2 g^{-1}$ and 0.028 to 0.061 $cm^3 g^{-1}$, respectively.[143] Additionally, the comparison among pristine biochar, ball-milled biochar, and ball-milled-N-doped biochar demonstrated superior pore structures in the modified biochar, coupled with increased CO_2 adsorption capacities.[144] Microwave radiation, an emerging heating method, presents advantages such as swift heating, convenient regulation, and uniform heat dispersion. Given their elevated microwave absorption capacity, carbon materials can be transformed under microwave heating, generating new carbons with tailored characteristics.[145] The rapid heating facilitated by microwave radiation may prompt the formation of new pores and modify the pore structures and surface functional groups in carbon materials. Studies suggested an increase in the number of functional groups on the molecular bonds of graphene materials after microwave treatment, providing additional adsorption sites for the adsorption process.[146]

Ultrasonic treatment has emerged as a novel method for altering carbon materials. By exploiting cavitation and microjet effects, ultrasonic treatment effectively eradicates the lumps formed during the pyrolysis of biomass, thus preventing pore blockage and facilitating the creation of additional microporous structures.[134] Typically, ultrasonic treatment is paired with chemical modification techniques to optimize its effectiveness. For example, in the study by Cao *et al.*, biochar was synthesized through ultrasonic treatment followed by amination at room temperature. Preceding amination, ultrasonic treatment of biochar induced the detachment of the graphite layer, resulting in the formation of new pores.[147] The resultant exfoliated biochar exhibited an abundance of functional groups such as –COOH, –OH, and –CH(O)CH–, which facilitated amine grafting. As a result, the biochar treated with ultrasound and amines exhibited a nine-times greater CO_2 adsorption capacity than that of the untreated biochar. Plasma, consisting of cations, particles, and free electrons, serves as a neutral substance for modifying the surface characteristics of materials, which is typically generated through corona, glow, or microwave discharge methods. During the modification process, interactions between plasma and the material surface facilitate the formation of new groups. In the study by Khan *et al.*, they utilized atmospheric pressure plasma to modify activated carbon, observing improvements in its surface area and pore volume together with the enrichment of surface oxygen-containing functional groups.[148]

4.1.3 Impact of activation temperature. The impact of activation temperature on the properties and efficacy of activated carbon cannot be overstated. This comprehensive review explores the intricate interplay between activation temperature and the resultant characteristics of activated carbon. A multitude of factors, including pore volume, pore size distribution, microporosity development, and surface area, are significantly influenced by the temperature regime employed during the carbonization and activation processes. Higher temperatures facilitate the removal of moisture and volatile matter from the precursor material, fostering the creation of pores, which are essential as adsorption sites. Consequently, an increase in temperature often results in the generation of a more extensive network of pores, enhancing the adsorption capacity of materials. However, this comes at the cost of the carbon content in the activated carbon, impacting its purity and suitability for specific applications.

Furthermore, the choice of chemical treatment is pivotal in determining the optimal activation temperature. Various activating agents interact differently with the carbonaceous components in biomass, leading to diverse outcomes in terms of pore structure and surface characteristics. Studies conducted by numerous researchers have underscored the significance of

selecting the appropriate chemical treatment based on the reactivity with the precursor material and its specific chemical properties.[149–151] Factors such as boiling and melting points, as well as the ability to mobilize metallic ions, further influence the effectiveness of the activation process. Understanding these intricate relationships among chemical treatment, activation temperature, and the resultant properties of activated carbon is essential for tailoring materials to meet the diverse needs of industrial, environmental, and technological applications.

4.1.3.1 Optimum KOH activation temperature. Determining the optimal activation temperature for KOH is paramount for the production of activated carbon, given that it profoundly influences the properties and performance of materials. This review summarizes a vast body of literature dedicated to pinpointing the ideal activation temperature using KOH as the activating agent. The activation temperature serves as a critical parameter in modulating the pore structure, surface area, and adsorption properties of the resulting activated carbon. By collating insights from various studies, this review endeavors to elucidate the multifaceted factors shaping the selection of the optimum activation temperature for KOH, considering variables such as precursor material, activation duration, and intended applications. Dewi asserted that the most effective activation temperature for KOH treatment is in the range of 700 °C to 800 °C.[152] Correspondingly, Williams *et al.* observed a significant enhancement in surface area and micropore volume with an increase in activation temperature from 700 °C to 800 °C.[153] The surface area experienced a remarkable 33% enhancement, increasing from 1955 $m^2 g^{-1}$ to 2600 $m^2 g^{-1}$, in contrast to the less than 10% improvement witnessed when the temperature was increased from 600 °C to 700 °C. This trend was corroborated by a group of researchers, further demonstrating that elevating the activation temperature from 700 °C to 800 °C led to a substantial increase in surface area, reaching up to 3228 $m^2 g^{-1}$, albeit at the expense of carbon yield and surface area when the temperature exceeded 850 °C.[154–156] Additionally, Ma *et al.* observed a progressive widening of the average pore width from 0.520 nm at 500 °C to 0.573 nm at 800 °C.[156] This exponential enhancement can be attributed to the formation and mobilization of metallic potassium at around 700 °C, facilitating pore development. Furthermore, the interaction among potassium, carbon and water yields potassium carbonate, which mitigates precursor burn-off, contributing to enhanced pore formation. Understanding these intricate temperature-dependent mechanisms is indispensable for optimizing KOH activation processes and tailoring activated carbon for diverse applications.

4.1.3.2 Optimum H_3PO_4 activation temperature. Determining the most effective activation temperature for H_3PO_4 is crucial in producing activated carbon, given its significant influence on the characteristics and performance of materials. This review presents an in-depth exploration of the extensive research dedicated to identifying the optimal activation temperature using phosphoric acid as the activating agent. The activation temperature plays a pivotal role in shaping the pore structure, surface area, and adsorption capabilities of the resulting activated carbon. By summarizing the insights from various studies, this review aims to highlight the factors influencing the selection of the best temperature for H_3PO_4 activation, considering variables such as precursor material, activation duration, and intended applications. Notably, empirical studies suggest that the most suitable activation temperature for H_3PO_4-treated precursors is typically 500 °C or lower, regardless of the impregnation ratio or precursor source.[152,157] For instance, researchers treated Paulownia wood with H_3PO_4 at a ratio of 4 and subjected it to carbonization in the temperature range of 300 °C to 600 °C.[158] The results indicated that higher temperatures were associated with a decrease in the activated carbon yield. Additionally, a notable trend emerged, wherein the micropore volume and BET surface area exhibited trend for activated carbon carbonized in the range of 300 °C to 400 °C, followed by a decline as the carbonization temperature increased from 400 °C to 600 °C.[152,157] This phenomenon was attributed to the contraction of the carbon structure on Paulownia wood at elevated temperatures, resulting in a diminished void space. Moreover, the activated carbon produced in these experiments demonstrated a dual-porosity nature, comprising micropores and mesopores, which is consistent with findings from prior studies utilizing alternative precursor materials such as date pits.

The observed trends in activation behavior can be elucidated by considering the chemical properties and organic chemistry of phosphoric acid. In the temperature range of 300 °C to 400 °C, phosphoric acid not only acts as a heat facilitator but also as a dehydrating agent, capturing minerals to inhibit ash formation, and thereby promoting pore development. Additionally, H_3PO_4 forms a protective layer on carbon in liquid materials and various chemical structures such as acetic acid, methanol, and polyphosphates, which reinforce the pore stability against temperature-induced collapse. However, at higher temperatures, these supporting structures, particularly acetic acid, encounter resistance limits. Beyond 440 °C, acetic acid decomposes into a mixture of carbon dioxide and methane or water and ketene, resulting in compromised pore stability and subsequent surface area reduction. Thus, understanding these intricate temperature-dependent mechanisms is vital for optimizing the H_3PO_4 activation processes and tailoring activated carbon for diverse applications in industries, environmental remediation, and emerging technologies.

4.1.3.3 Optimum $ZnCl_2$ activation temperature. Determining the optimal activation temperature for $ZnCl_2$ is a critical factor in the production of activated carbon, given its significant impact on the properties and performance of materials. This review aims to delve into the extensive research dedicated to identifying the ideal activation temperature using zinc chloride as the activating agent. The activation temperature plays a pivotal role in molding the pore structure, surface area, and adsorption properties of the resulting activated carbon. By summarizing the insights from various studies, this review endeavors to elucidate the factors influencing the selection of the optimum temperature for $ZnCl_2$ activation, considering variables such as precursor material, activation duration, and intended applications. According to the study conducted by a research group, the optimal activation temperature for $ZnCl_2$

treatment was suggested to be 500 °C, which is attributed to the higher surface area and micropore volume reported for activated carbon precursor cherry stones.[159] This finding was corroborated by other researchers, where an increase in temperature from 500 °C to 800 °C resulted in a decrease in surface area.[151] Additionally, Nurdin *et al.* reported the highest surface area of activated carbon precursor oil palm shell at 1429.71 $m^2 g^{-1}$ when activated at 500 °C, with a high micropore volume also observed.[149] However, an increase in activation temperature from 500 °C to 800 °C led to a decrease in specific surface area and micropore volume, coupled with an increase in average pore size distribution, as supported by similar research utilizing different precursors.[152] Furthermore, in the adsorption-based study by Njeh *et al.*, the highest iodine and methylene blue adsorption capacities were recorded for sawdust activated at 500 °C.[160] It was noted that $ZnCl_2$ can vaporize at temperatures above 400 °C, potentially leading to rapid carbon burnout due to the loss of protective carbon elements, according to Wei *et al.*[161] However, Huang disagreed these claims, suggesting that the optimum activation temperature for $ZnCl_2$ treatment is around 700 °C.[162] Though scarce, this assertion is reinforced by similar findings, where the highest micropore formation upon activation up to 800 °C is possibly linked to the physical properties of $ZnCl_2$, with a boiling point of 732 °C.[151,163] In summary, higher temperatures generally result in increased pore formation, but each activating agent exhibits a specific range of optimum temperatures, depending on their chemical and physical properties such as boiling point. According to the literature, the suggested activation temperatures for precursors incorporating KOH, H_3PO_4, and $ZnCl_2$ are 700–800 °C, 500 °C, and 500 °C, respectively.

4.1.4 Impact of impregnation ratio. The impregnation ratio stands as a pivotal factor shaping the quality and attributes of activated carbon manufacture, delineating the proportion of activating agent to precursor material employed throughout the process. This ratio has a profound influence on the ultimate pore structure, surface area, and adsorption capacity of the resulting activated carbon. Fine-tuning the impregnation ratio is paramount in customizing activated carbon for specific applications, demanding equilibrium among parameters such as porosity, yield, and cost-effectiveness. Additionally, another crucial element that greatly affects the characteristics of the final activated carbon is the impregnation ratio during chemical activation processes. This signifies the ratio between the activating agent weight and the raw material impregnated. Fundamentally, a higher impregnation ratio tends to induce more swelling, thereby facilitating the more vigorous release of volatile matter contents, consequently widening the pores. Conversely, lower concentrations of activating agent foster the steadier elimination of volatile matter content, while curbing tar deposition, resulting in the formation of more micropores.

In the case of biomass-derived materials, the impregnation ratio is particularly important, influencing their structural and functional characteristics. Several studies conducted by researchers underscore the significance of the impregnation ratio in shaping the pore structures.[151,164,165] The typical impregnation ratios for biomass are in the range of 1 : 1 to 3 : 1, depending on the type of biomass and the specific requirements of the end product.[166] Studies have highlighted the effect of the impregnation ratio on the structural properties of activated carbons. For example, increasing the impregnation ratio has been shown to improve the porosity and surface functionality of activated carbon from coconut shells, enhancing its adsorption capabilities.[167] Additionally, optimizing the impregnation ratio is crucial for achieving a well-balanced pore structure and thermal stability, as seen in biochar produced from rice husks. Research also indicates that an impregnation ratio of 1 : 1 can result in activated carbons with higher surface areas and larger pore volumes compared to lower ratios.[168] Increasing the ratio of phosphoric acid from 1 : 1 to 2 : 1 was found to significantly increase the micropore volume in activated carbons.[169] However, it is important to note that excessively high impregnation ratios can lead to the overactivation of carbon materials, compromising their structural integrity. Therefore, it is essential to carefully optimize the impregnation ratio to achieve the desired balance among surface area, pore structure, and mechanical stability, tailoring the properties of activated carbon to meet specific application needs.

In essence, the impregnation ratio plays a critical role in the production of activated carbon, shaping its pore structure and surface area, and consequently affecting its adsorption capacity and performance. The optimal adjustment of this ratio is indispensable for tailoring activated carbon to specific applications, harmonizing diverse factors such as porosity, yield, and cost-effectiveness. A profound comprehension of the intricate interplay between the impregnation ratio and properties of activated carbon is pivotal for refining production processes and devising activated carbon materials endowed with enhanced performance attributes.

4.1.5 Impact of inert gases on carbonization process. The application of inert gases during the carbonization process plays a crucial role in determining the structural characteristics of the resulting activated carbons. Inert gases create an oxygen-free environment, which prevents oxidation and undesirable side reactions that can compromise the quality of the carbon material. Carbonization involves the thermal breakdown of organic substances in this inert atmosphere, producing a carbon-rich material with unique textural properties.[170] The choice of inert gas, together with the specific conditions under which it is applied, has a significant impact on the development of the porosity, surface area, and adsorption capabilities of materials.

Research indicates that the temperature at which carbonization occurs and the flow rate of the inert gas, typically nitrogen are critical factors in determining the porous architecture of carbon materials. Studies have shown that the optimal conditions for achieving the maximum specific surface area, pore volume, and micropore content are carbonization temperature in the range of 800–850 °C with a nitrogen flow rate of 7.5–15 $dm^3 min^{-1}$. These parameters help in effectively removing volatile components from the precursor material, promoting the formation of a well-developed porous structure and increasing the surface area.[171]

Inert gases such as nitrogen play multiple roles during the carbonization process. Primarily, they prevent the oxidation of the carbon material by displacing oxygen and other reactive gases, thus maintaining the integrity of the carbon structure. Additionally, the flow rate of nitrogen influences how quickly volatile compounds are expelled from the carbon matrix. A higher nitrogen flow rate facilitates the faster removal of volatiles, enhancing the development of a more extensive pore network and higher surface areas. Alternatively, a lower flow rate can lead to a less porous structure due to the slower release of volatiles and potential re-deposition of carbonaceous residues within the pores.[96,171]

Furthermore, the interaction between the carbonization temperature and inert gas flow rate is vital in achieving the desired textural properties. Higher temperatures enhance the decomposition of the precursor material, and when combined with a controlled nitrogen flow, can result in a uniform and highly porous structure. However, if the temperature is too high or the nitrogen flow is inadequate, the pore structure may collapse or unwanted tar formation may occur, clogging the pores and reducing the overall effectiveness of the material.[172]

Overall, the use of inert gases such as nitrogen during carbonization is critical for regulating the textural characteristics of activated carbon. By optimizing the carbonization temperature and gas flow rate, it is possible to fine-tune the pore structure and surface area, thereby enhancing the adsorption capacity and overall performance of the material.

4.2 Utilizing waste-derived activated carbon for CO_2 capture

The widespread application of activated carbon spans multiple sectors, encompassing gas and water purification, gold processing, wastewater treatment, metal extraction, decaffeination, and pharmaceuticals. The rapid expansion of the AC market is underscored by the significant rise in its annual demand. According to Market Data Forecast, the global AC market is projected to grow from $9.17 billion in 2023 to $11.46 billion by 2029, indicating robust growth.[96] Thus, to meet escalating demands and address cost considerations, researchers are actively exploring alternative pathways for the production of AC, with a specific emphasis on low-cost or waste materials. The utilization of waste materials not only addresses environmental and waste management challenges but also unlocks lucrative opportunities for the business sector. In parallel, biomass can be broadly classified into two main categories, conventional waste and non-conventional waste. Conventional waste is comprised of biomasses sourced from the agricultural and wood industries, such as coconut shells, rice straws, sawdust, and wood, while non-conventional wastes include materials such as plastic, sugarcane bagasse, citrus peel, and tires, originating from municipal and industrial sources. Coconut shells, in particular, have attracted significant attention as a frequently studied precursor due to their elevated carbon content and robust mechanical properties, as evidenced by the compositional analysis in Fig. 9. Comparative studies conducted by several researchers have focused on determining the adsorption capacity and practical feasibility of coconut shell-derived AC precursors.[173–176] The literature underscores the importance of understanding the carbon content and compositions of potential raw materials, given that these factors profoundly influence the characteristics of the resulting AC. Crucially, parameters such as fixed carbon and volatile matter levels play pivotal roles in evaluating the effects of carbonization and pore formation processes, with carbonization notably enhancing pore development by augmenting the mobility and reducing the volatile matter content.

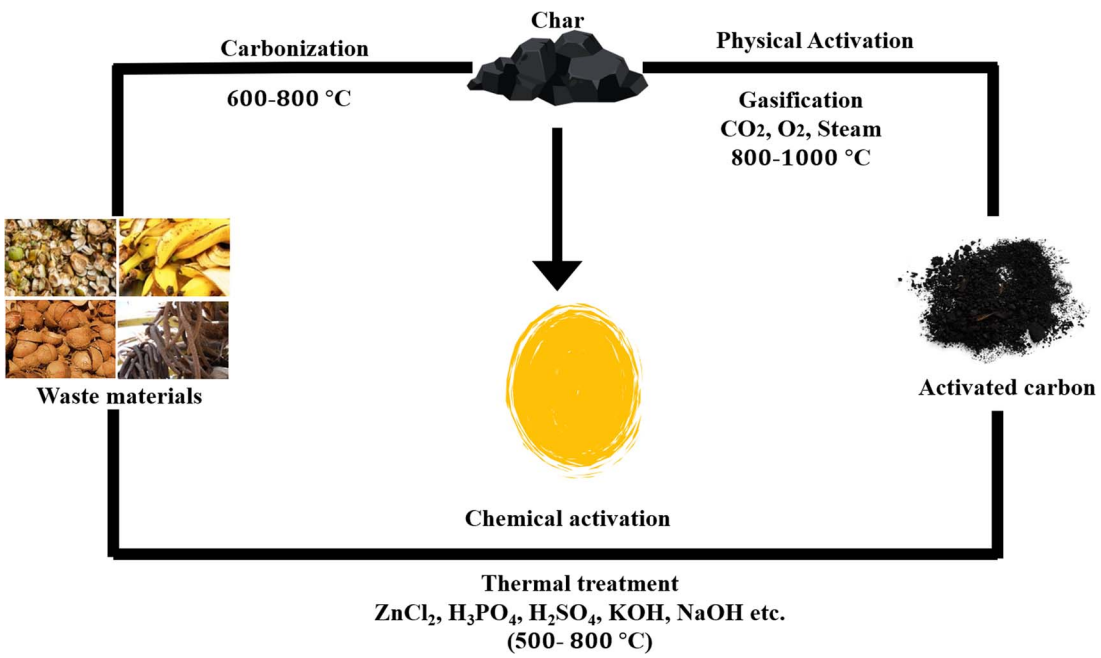

Fig. 9 Process for the synthesis of activated carbon.

Table 4 Variations in compositional elements linked to diverse precursors

	Elemental composition (weight%)					
Precursor materials	Carbon	Oxygen	Hydrogen	Nitrogen	Ash	Ref.
Corn stover	60.50	24.30	5.60	1.20	7.40	53
Miscanthus	74.60	17.42	3.38	0.45	3.41	147
Miscanthus	84.47	7.61	2.28	0.30	5.02	147
Switchgrass	78.64	4.88	1.46	0.79	13.94	147
Sugarcane bagasse	59.00	25.00	7.00	1.30	8.70	150
Walnut shell	84.86	13.63	1.16	0.34	—	177
Shrimp shell	42.07	—	5.74	24.81	—	178
Crab shell	10.23	—	2.82	3.94	—	179
Algae	50.20	35.00	6.80	7.20	6.70	180
Bituminous coal	85.09	5.05	3.13	1.50	5.23	181
Bituminous coal	83.26	12.20	3.44	0.77	—	182
Anthracite coal	90.02	3.15	3.50	1.25	2.08	181
Apple tree branches	80.01	6.59	2.72	1.28	9.40	183
Torrefied cornstalk	35.63	32.31	4.48	1.04	—	184
Raw cornstalk	39.57	40.05	5.61	0.52	—	184
Lignite coal	52.54	17.94	2.88	0.77	—	184
Palm kernel shell	45.40	41.92	6.10	0.70	5.00	185
Cotton stalk	38.96	56.47	3.56	1.01	6.03	186
Bamboo waste	65.00	20.01	6.99	0.90	7.10	187
Rambutan peel	76.36	19.22	2.90	1.35	—	188
Rambutan peel	83.38	14.71	0.90	0.77	—	188
Buckwheat husks	78.40	15.50	3.10	1.30	—	189
Sewage sludge	12.37	8.94	0.83	0.95	—	190
Olive stone	47.10	46.46	6.23	0.21	0.45	191
Microalgae	54.28	31.45	9.12	4.74	—	192
Apricot stone	48.45	45.08	6.03	0.44	1.68	193
Date stone	48.43	44.46	6.44	0.67	1.58	194
Cherry stone	49.90	44.15	6.37	0.24	0.24	195
Almond shell	51.40	41.60	6.10	0.30	1.30	196
Peanut shell	46.82	37.64	6.58	0.80	8.61	197
Macadamia nut shell	53.19	40.68	5.78	0.29	0.30	198
Pecan shell	47.53	45.97	5.53	0.33	—	199
Rice husk	36.52	41.10	4.82	0.86	16.70	200
Sugarcane bagasse	41.55	52.86	5.55	0.03	6.20	200
Coconut shell	49.62	42.75	7.31	0.22	0.80	201
Coconut shell	40.33	51.57	2.78	0.72	4.18	202
Hemp straw	48.40	44.90	6.40	0.30	1.80	203
Wheat straw	39.90	41.97	5.75	0.65	12.30	204
Soybean straw	41.50	41.39	5.52	0.28	8.87	205
Wheat straw	41.52	36.24	5.76	0.61	—	206
Rice straw	40.67	32.30	5.73	0.80	—	206
Waste tea	48.47	37.60	6.40	0.32	3.37	207
Douglas fir	47.90	45.57	6.55	0.08	0.21	208
Pinewood sawdust	49.09	44.53	6.05	0.33	—	209
Citrus peel	41.87	51.62	5.49	0.58	2.86	210
Cassava peel	47.21	43.70	7.74	1.35	1.92	211
Lemon peel	38.48	—	4.98	1.21	3.68	212
Cassava peel	38.34	38.55	6.13	2.08	4.32	213
Waste palm peel	51.00	39.00	7.00	3.00	4.00	214

The analysis presented in Table 4 highlights that nutshell, coconut shell, algae, and sea mango possess a carbon content exceeding the average of 44.95 wt%. Other studies suggest that utilizing a concentrated carbon precursor can potentially enhance the yield of AC by leveraging its higher carbon content, thereby facilitating the formation of microporous structures.[215] Moreover, gaining a thorough understanding of the structural intricacies of various waste materials, influenced by variations in lignocellulose compositions, is considered crucial. Comparative studies indicate that precursors abundant in lignin tend to yield activated carbon with spherical porous structures, while that rich in cellulose tends to produce cylindrical pore structures. These observations emphasize the pivotal role of precursor type in determining the texture of AC.[177,216] However, achieving the optimal activated carbon for CO_2 adsorption poses significant challenges due to the diverse composition properties of waste materials from different sources. Notably, it can be observed in Table 4 that algae, walnut

shell, and waste palm shell exhibit elevated nitrogen levels compared to other waste samples. With nitrogen levels of 7.20 wt%, 3.20 wt%, and 3.00 wt%, respectively, surpassing the average nitrogen content of 1.67 wt% among the samples. Despite the significance of the carbon content in precursor selection, this indicates that a higher nitrogen concentration in the precursor enhances both the carbon dioxide adsorption performance and CO_2 selectivity, irrespective of the carbon composition.[178,217] Treeweranuwat *et al.* emphasized that a low carbon content in the precursor leads to a reduction in the surface area of the resulting activated carbon. However, incorporating heteroatom-rich materials during the carbonization and activation of shrimp-derived AC not only increased its surface area but also boosted the carbon yield.[218] Furthermore, the addition of melamine, sodium thiosulfate, and KOH was shown to double the AC yield due to the enhanced thermal stability.

An essential criterion for an effective precursor in the production of adsorbents is a minimal ash content.[219] Douglas fir stands out with its notably low recorded ash content of 0.21 wt% (as indicated in Table 4), which is significantly lower than the average of 4.12 wt%. In contrast, algae and rice husk exhibit a higher ash content of 6.70 wt% and 16.70 wt%, respectively. The reduced ash content in Douglas fir suggests its potential as a superior adsorbent precursor. Although the ash content does not directly influence the development of porosity, it impacts the adsorption properties due to the formation of inert sites. Understanding the prevalent lignocellulose structure is crucial due to the diverse compositions of waste materials. Comparative analyses indicate that precursors rich in lignin tend to yield activated carbon with spherical porous structures, while that with a higher cellulose content tends to yield cylindrical pore structures.[177,180] The varying composition properties of waste materials pose challenges in achieving the optimal activated carbon for CO_2 adsorption. Agricultural residues, such as palm kernel shells, rice husks, coconut shells, and bagasse, are extensively utilized for producing activated carbon due to their abundance, high carbon content, and relatively low ash levels. Conducting a comprehensive precursor analysis is essential to facilitate the conversion of AC into a suitable CO_2 adsorbent. Besides possessing a substantial surface area and high microporosity concentration, waste-derived synthesized AC materials must be economically feasible, possess basic functionalities, exhibit low heat absorption, high CO_2 selectivity, and be suitable for industrial-scale production. Also, the composition of waste products plays a crucial role in determining the quality of the resulting activated carbon.

4.2.1 Utilizing agricultural waste for the synthesis of activated carbon. Utilizing agricultural waste for the synthesis of activated carbon presents a significant opportunity to address pressing environmental challenges, while simultaneously contributing to sustainable waste management practices and resource optimization. This comprehensive review critically examines a range of agricultural residues and elucidates their conversion methodologies, resulting properties, and myriad applications of the produced activated carbon. Through meticulous investigation, this review underscores the transformative potential of agricultural waste as a versatile and eco-friendly alternative across diverse industrial and environmental sectors. Recent research efforts have increasingly focused on harnessing agricultural waste as a valuable source of activated carbon precursors tailored for CO_2 adsorption applications. For instance, in the study by Hidayu and Muda, palm kernel shells and coconut shells were employed as primary raw materials for the synthesis of activated carbon.[219] These agricultural residues were subjected to carbonization at 800 °C after being ground to a uniform size, followed by physical and chemical activation using $ZnCl_2$ in a 1 : 1 ratio. This study revealed that coconut shells exhibited a higher yield of activated carbon precursors compared to palm kernel shells, positioning them as promising candidates for raw material utilization in carbon capture applications.

Similarly, another research group investigated the efficacy of utilizing bagasse and rice husk as precursor materials for the production of activated carbon.[200] Employing $ZnCl_2$ as an activator at a temperature of 500 °C for 60 min, this study demonstrated that bagasse-derived activated carbon displayed superior adsorption capabilities over its rice husk-derived counterpart across various adsorption temperatures. These findings underscore the potential of leveraging readily available agricultural waste streams for the scalable and economically viable production of activated carbon, thereby facilitating the transition towards a more sustainable waste management paradigm. However, despite the notable advancements in CO_2 adsorption performance observed in these studies, challenges persist in ensuring the thermal stability of the synthesized activated carbon for sustained CO_2 capture efficacy. Particularly, the decline in CO_2 adsorption performance at elevated temperatures underscores the need for targeted modifications to enhance the thermal stability of activated carbon materials tailored for CO_2 capture applications. According to the findings gleaned from extensive literature studies, coconut shell and palm kernel shells emerge as the most promising agricultural waste precursors for the production of activated carbon, owing to their high carbon content and low ash composition.[176,219] This ranking underscores the critical importance of selecting appropriate precursor materials to optimize the performance and sustainability of activated carbon production processes.

4.2.2 Utilizing industrial waste for the synthesis of activated carbon. The utilization of industrial waste for synthesizing activated carbon has emerged as a compelling strategy for promoting sustainable resource management and environmental remediation endeavors. This comprehensive review delves into the diverse array of industrial by-products and waste materials, assessing their potential as viable precursors for the synthesis of activated carbon, while elucidating the intricacies of various conversion techniques employed in their transformation. For instance, in a study, sewage sludge was investigated as a precursor for CO_2 adsorption, undergoing activation with KOH and NaOH at temperatures in the range of 600 °C to 800 °C.[220] Despite yielding activated carbon with a relatively modest surface area of 179 $m^2\ g^{-1}$, this material exhibited an enhanced CO_2 adsorption capacity, which was attributed to its high content of basic functional groups. Notably, optimal CO_2

adsorption was achieved when solid NaOH was utilized as the activating agent, facilitating enhanced interaction between hydroxide and the carbon elements within the sewage sludge matrix. Furthermore, Wang *et al.* explored alkaline activation (KOH) to develop activated carbon fibers, varying the KOH to fiber ratio and activating the samples at 700 °C.[221] The resulting activated carbon fibers demonstrated a high surface area and micropore concentration, with the incorporation of nitrogen contributing to expedited sorption kinetics, which is a desirable attribute for CO_2 adsorbents. Similarly, another research group investigated municipal solid waste compost as a precursor, activating the waste using H_2SO_4 in the temperature range of 400 °C to 800 °C.[222] Interestingly, the activated carbon impregnated with H_2SO_4 before pyrolysis exhibited superior properties such as enhanced surface area and micropore volume compared to the post-pyrolysis incorporation of the activating agent, with a notable CO_2 adsorption of 2.6 mmol g^{-1}. Through the repurposing of industrial waste streams, this approach not only tackles waste management challenges but also presents a cost-effective and environmentally friendly avenue for producing activated carbon with multifaceted applications in pollutant removal, energy storage, and beyond.

4.2.3 Utilizing food waste for the synthesis of activated carbon. Exploring the potential of food waste for the synthesis of activated carbon represents a pivotal step towards sustainable waste management practices and resource optimization. This review critically examines various types of food waste as promising precursors for activated carbon production, elucidating their respective conversion methodologies and the resulting properties of the synthesized activated carbon. For instance, researchers utilized chitin aerogel as a raw material, activating it with potassium hydroxide at a ratio of 3 : 1 activating agent to carbon, and subjecting it to activation at 850 °C for 4 h.[223] Similarly, Jia *et al.* investigated shrimp shells as activated carbon precursors, leveraging their high nitrogen content to enhance the formation of basic functional groups in the synthesized activated carbon.[217] In another study, coffee grounds were utilized as the raw material and activated with KOH at 400 °C, yielding activated carbon with an average CO_2 adsorption capacity of 0.27 cm^3 g^{-1} at 0 °C.[224] Moreover, Wen *et al.* demonstrated the potential of beer waste as an activated carbon precursor, employing hydrothermal carbonization followed by activation at 800 °C for 2 h, resulting in activated carbon with high CO_2 selectivity compared to other studied precursors.[225] Comprehending the structural and elemental makeup of waste materials is crucial for confirming their viability as precursors for activated carbon in CO_2 capture. Although agricultural residues are favored due to their abundance, high carbon content, and low ash content, food waste shows promise despite its lower average carbon content, which is attributed to its high nitrogen heteroatoms. Furthermore, industrial residues often possess elevated concentrations of functional groups, potentially enhancing the carbon capture capabilities. Consideration of factors such as volatile matter fraction, ash content, moisture content, and compositional complexity of biomass is crucial to ensure the uniform performance of the produced activated carbon, particularly for commercial applications where a high variation in carbon dioxide adsorption capacity is intolerable. Agricultural wastes are favored due to their abundance, ease of management, and the ability to categorize the raw materials based on species, age, and origin. By repurposing food waste streams, this approach not only mitigates food waste disposal challenges but also offers an environmentally friendly solution for producing activated carbon with diverse applications in water treatment, air purification, and energy storage.

5. Application

5.1 CO_2 capture with carbon materials

Carbon materials are increasingly recognized for their potential in industrial applications, particularly due to their cost-effectiveness, efficient regeneration, and exceptional ability to capture substantial amounts of CO_2. These materials play a crucial role in addressing the growing need for CO_2 capture from various emission sources, leveraging their high surface area and adaptable pore structures to serve as effective adsorbents for CO_2 molecules. The versatility of carbon materials extends beyond CO_2 capture, where they are also employed in pollutant adsorption, catalysis, and energy storage, making them vital in confronting environmental challenges and promoting sustainable technologies. Recent research has focused on the use of carbon materials for CO_2 capture, largely driven by the increasing release of carbon dioxide from industrial activities, which exacerbates the global warming crisis. In this case, biomass, rich in carbon content, is emerging as a valuable resource for producing biochar or hydrochar, contributing to efforts in reducing CO_2 emissions. However, pristine carbon materials face limitations in their textural structure and chemical composition, which restricts their effectiveness in CO_2 capture. Thus, to overcome these challenges, pre-capture modifications are necessary to enhance the properties of carbon materials and improve their CO_2 capture efficiency. This review critically examines the reported studies on biomass-derived carbon materials for CO_2 capture, exploring the underlying adsorption mechanisms and identifying promising avenues for future research and practical application. By understanding these mechanisms and advancing the development of modified carbon materials, it is possible to optimize the CO_2 capture processes, thereby contributing to the global effort to mitigate the impacts of climate change and move towards a more sustainable future.

5.1.1 The process of CO_2 capture. Capturing CO_2 using carbon materials is a process in which carbon dioxide molecules adhere to the surface of these materials, aided by their large surface area and specialized pore structures, which enhance adsorption.[226] This process involves a variety of interactions, including van der Waals forces, π–π interactions, and electrostatic forces, which draw CO_2 molecules to the surface of carbon materials. The effectiveness of carbon materials in CO_2 capture stems from their high porosity, extensive surface area, and well-optimized pore size distribution, which enhance their interaction with CO_2. The CO_2 capture mechanism in biomass-derived carbon materials occurs through two primary

processes, *i.e.*, physical adsorption and chemical adsorption. Physical adsorption, or physisorption, is an exothermic process dependent on temperature and pressure, where CO_2 molecules adhere to the surface *via* van der Waals forces and other non-covalent interactions.[227] This process is energy-efficient for regenerating the adsorbent, especially under higher pressure conditions.[228] Alternatively, chemical adsorption, or chemisorption, involves the formation of covalent or ionic bonds between CO_2 molecules and the functional sites on the adsorbent, driven by acid–base neutralization reactions.[229] Although chemisorption is energetically favorable during the adsorption phase, desorption and adsorbent regeneration require more energy. By incorporating basic organic groups or inorganic metal oxides, such as amines and alkali metals, respectively, the efficiency of chemisorption can be significantly enhanced. For example, polyethyleneimine-functionalized mesoporous silica and nitrogen-doped activated carbon have shown increased CO_2 capture performances through these mechanisms.[230] These findings underscore the importance of both adsorption processes in optimizing the CO_2 capture efficiency, making carbon materials derived from biomass crucial for advancing sustainable carbon capture technologies. When captured, CO_2 molecules are temporarily held on the carbon surface, effectively extracting them from the gaseous phase. The continual release of anthropogenic CO_2 into the atmosphere has led to the significant and escalating issues of global warming and climate change.[231,232] Between 1970 and 2004, the annual global CO_2 emissions substantially increased by 80%, contributing to the current CO_2 concentration in the air exceeding the maximum permissible limit for climate safety and forecasted to reach 700 ppm by the end of the century. As a result, a temperature rise of 1.8 °C to 4 °C is expected due to global warming, posing significant risks to the ecosystem and causing irreparable harm to the environment.[233] This surpassed climate safety threshold underscores the urgent need for remedial measures to mitigate anthropogenic greenhouse gas emissions. CO_2 capture methods can be applied directly from the atmosphere or from industrial processes flue gas streams, employing suitable techniques.[234] Subsequently, the captured CO_2 can be utilized in various strategies, including the production of clean energy fuels for the future or as a carbon source for the synthesis of industrially important chemicals.

Numerous adsorbents have been proposed for CO_2 capture, each possessing unique characteristics that contribute to their effectiveness in this application. As shown in Fig. 10, an optimal CO_2 adsorbent should exhibit high adsorptive capacity, selectivity for CO_2 in gaseous mixtures, rapid sorption kinetics, a microporous structure, and morphological and chemical stability, while also offering a low heat of adsorption, high regeneration rate, and cost-effectiveness.[235] The following table presents a comprehensive overview of various AC and carbon materials derived from different precursors, including details on their synthesis and activation methods. It includes information on the precursor materials, synthesis techniques,

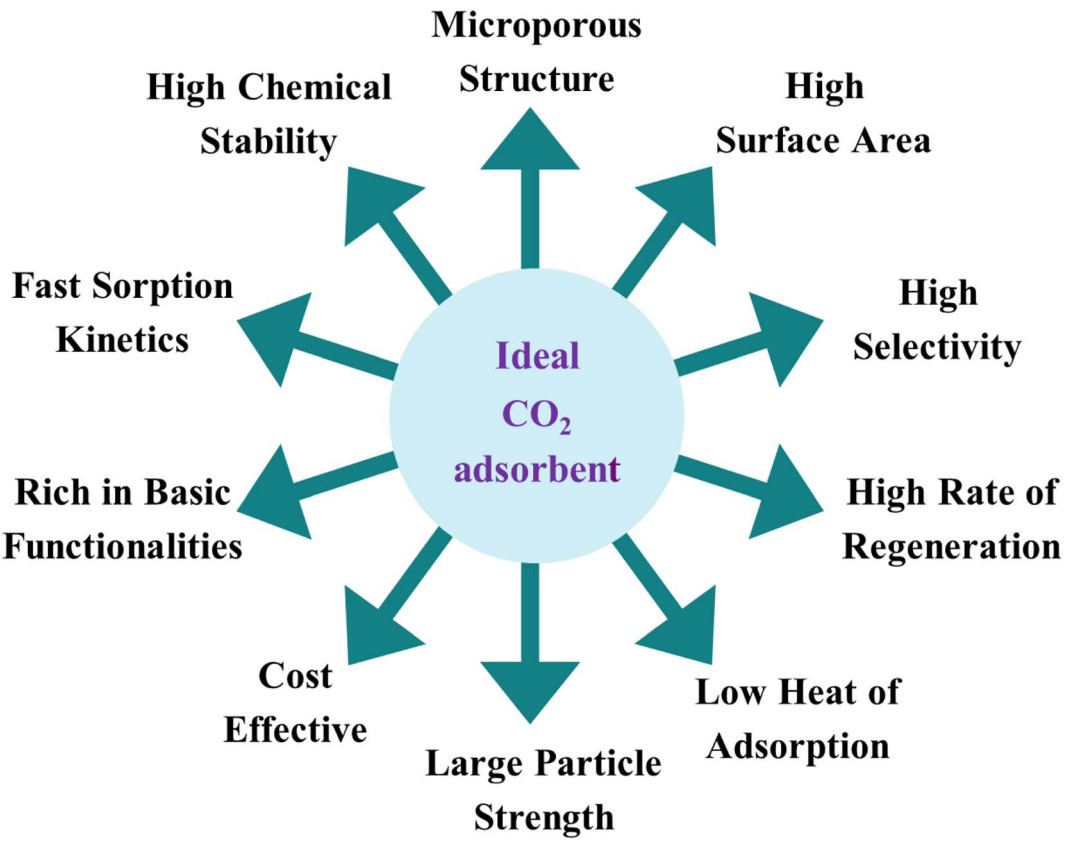

Fig. 10 Characteristic properties required for an ideal adsorbent for CO_2 capture.

Table 5 Properties of activated carbons from various precursors and activation methods

Precursor	Synthesis method	Activation method/agent	Ratio (precursor)	Surface area ($m^2\ g^{-1}$)	Pore size (nm)	Pore volume ($cm^3\ g^{-1}$)	Surface functionalities	Ref.
Olive stones	Hydrothermal carbonization	KOH solution	1 : 1	969	—	0.443	Functional groups: –OH, C=O	191
Olive stones	Hydrothermal carbonization	Bioorganic solution	1 : 1	915	—	0.444	Functional groups: –OH, C=O	191
Olive stones	Hydrothermal carbonization	H_3PO_4	1 : 1	849	—	0.339	Functional groups: –OH, C=O	191
Rice husk	Carbonization	Potassium acetate	1 : 1.5	80	3.0	0.58	Carboxylic and –OH	236
Rice husk	Carbonization	H_3PO_4	1 : 1	1500	2.5	0.8	High oxygen content	237
Coconut shell	Physical activation (steam)	CO_2/KOH	1 : 2	2300	2.8	1.12	High carbon content, OH, C=O	238
Coconut shell	Pyrolysis	Potassium citrate	1 : 2	1050	2.5	0.62	High oxygen content, acetic groups	239
Citric acid residue	Hydrothermal carbonization	H_3PO_4	1 : 4	1100	2.0	0.7	Carboxylic and phenolic groups	240
Corncob	Pyrolysis	Bioorganic K_2CO_3	1 : 2	1500	1.8	0.758	High oxygen content, carboxyl, hydroxyl, and lactone groups	241
Cashew nut shell	Hydrothermal carbonization	K_2CO_3	1 : 1	1693	1.63	0.839	Functional groups: –OH, C=O, COOH	242
Sugarcane bagasse	Sol–gel method	Potassium oxalate	1 : 2	1250	2.7	0.78	Carboxyl, phosphate, lactone group	216
Guhanshan coal	Direct carbonization	KOH	1 : 2	1300	1.5	1.0	Nitrogen-doped groups	7
Gulfweed	Chemical activation	KOH	1 : 1	2500	2.8	1.2	High surface oxygen groups	243
Rambutan peel	Hydrothermal carbonization	KOH	1 : 1	2500	2.8	0.313	High oxygen content	52
Pine cone	Hydrothermal carbonization	KOH	1 : 3	2100	2.3	0.87	Functional groups: –OH, C=O	244
Pineapple peel	Wet impregnation	K_2CO_3	1 : 1.25	1006	0.59	0.28	Functional groups: –OH, C=O	245
Lotus leaf	Hydrothermal carbonization	KOH	1 : 4	2020	3.4	0.92	Functional groups: –OH, C=O, COOH	246
N-doped carbon	Carbonization	KOH	1 : 3	1800	3.5	1.0	Pyridinic-N, OH, C=O	247
Sunflower seed hull	Wet impregnation	$ZnCl_2$	1 : 4	1956	1.12	0.28	Functional groups: –OH, C=O	248
Sawdust	N & C doping carbonization	KOH	1 : 4	1600	3.2	1.1	Functional groups: –OH, C=O, SO_x	156
N-rich organic compound	One-pot synthesis	KOH or $ZnCl_2$	1 : 3	2000	3.0	0.8	Pyridinic-N, OH, C=O	249
Bamboo shoot shell	Carbonization	KOH (heteroatom doping)	1 : 3	1850	1.2	0.75	Pyridinic-N, OH, C=O	250
Agricultural residue	Hydrothermal carbonization	KOH	1 : 3	1800	3.0	1.2	Functional groups: –OH, C=O	251
Oak wood	Wet impregnation	H_3PO_4	1 : 1	2553	1.61	0.94	Functional groups: –OH, C=O	96
Organic polymer-rich biomass	Carbonization	KOH	1 : 3	1900	3.5	1.1	Functional groups: thiols, sulfides, –OH, C=O	252
Lignin	Carbonization	KOH (N, S-doping)	1 : 4	2200	3.0	1.2	Pyridinic-N, thiols, OH, C=O	253
Argan paste cake waste	Carbonization	KOH	1 : 4	1500	3.0	1.0	High carbon content, OH, C=O	254
PET bottles	Carbonization	KOH + urea	1 : 2:1	1165	0.47	0.47	Pyridinic-N, OH, C=O	255
Chestnut	Soft-templating method	KOH	1 : 2	747	4.0	0.8	High carbon content, OH, C=O	256
Fox nut shell	Chemical activation	H_3PO_4	1 : 3	2000	1.2	1.1	Functional groups: –OH, C=O	257
Crustacean shell	Carbonization	KOH	1 : 4	2000	4.0	1.2	High carbon content, OH, C=O	178
Hazelnut shell	Chemical activation	KOH	1 : 1	1696	3.5	0.7	Pyridinic-N, OH, C=O	258
Celtuce leaves	Carbonization	KOH	1 : 4	3404	3.5	1.2	High carbon content	259

activation agents, and the ratio of precursor to activation agent used. Additionally, this table summarizes key textural properties such as surface area, pore size or volume, and pore size distribution (PSD), as well as the surface functionalities of each material. This comparative analysis provides valuable insights into the performance and characteristics of different carbon materials for applications such as CO_2 capture (Table 5).

Recent studies on CO_2 capture, both pre- and post-combustion, have investigated various techniques, including adsorption on functionalized porous materials, absorption in liquid amine solutions, membrane separation, and cryogenic separation at ultra-low temperatures.[260] However, each method has its strengths and limitations, such as the use of harsh chemicals, equipment wear and tear, disposal challenges, performance inconsistencies, and high associated costs. In contrast, activated porous carbons derived from biomass have emerged as promising and economically viable options for addressing the elevated CO_2 levels in the atmosphere. These carbons produced *via* biomass pyrolysis offer a sustainable approach by converting unwanted biomass materials into efficient adsorbents suitable for large-scale CO_2 capture.[261] Porous carbon materials offer a triple advantage in CO_2 emission reduction, as follows: firstly, by mitigating CO_2 emissions from decomposing biomass; secondly, by amending soils with porous carbon to diminish CO_2 generation; and thirdly, by utilizing porous carbons for CO_2 capture in flue gas streams during both pre- and post-combustion processes. This section delves into the potential applications of biochar and activated porous carbons derived from various biomass precursors for CO_2 capture. Although pristine biochar may possess limited porosity and efficacy for CO_2 capture, activation procedures can enhance its surface area and porosity, making it suitable for this purpose. Researchers have explored diverse biomass sources and experimental parameters to develop various types of activated porous carbons, aiming to optimize their CO_2 capture efficiency.

5.1.2 Optimizing carbon for CO_2 capture. Carbon materials are widely employed for CO_2 capture due to their expansive surface area and customizable pore structures, making them effective adsorbents for CO_2 molecules. These materials play a vital role in addressing the urgent challenge of reducing CO_2 emissions from diverse sources, spanning industrial processes to atmospheric sources. By harnessing their inherent attributes, such as high adsorption capacity and selectivity, carbon materials offer a promising avenue for capturing CO_2 and mitigating its atmospheric concentration. Various strategies have been explored to enhance the CO_2 capture capabilities of carbon materials. Table 6 offers an overview of carbon materials prepared through different modification methods, together with a comparison of their CO_2 capture efficiencies. Pristine carbon materials often exhibit limited pore structures and surface chemistry, constraining their CO_2 capture effectiveness. For example, the pristine biochar derived from coffee grounds displayed a modest CO_2 capture capacity of 0.14 mmol g^{-1}, whereas KOH activation (500 °C, 1 h) significantly increased it to 4.76 mmol g^{-1}.[269] Thus, modifications such as acid or alkaline activation, heteroatom doping, and metal impregnation are indispensable for achieving heightened CO_2 capture capacities. The efficacy of these modifications relies heavily on the choice of modifier, treatment temperature, and duration. One research group explored the synthesis of porous carbon from tobacco stems *via* KOH activation at varying temperatures, observing that higher temperatures yielded an augmented surface area and micropore volume, initially enhancing the CO_2 capture capacity before reaching a saturation point.[262] This phenomenon was ascribed to the reduction in oxygen content in the

Table 6 An overview of CO_2 adsorption capabilities exhibited by various carbon materials

Precursor	Modification	Sample name	Adsorption condition	S_{BET} (m^2 g^{-1})	CO_2 capture (mmol g^{-1})	Ref.
Tobacco stem	KOH (500 °C 1 h)	OC500	0 °C, 1 bar	786	4.76	262
	KOH (600 °C 1 h)	OC600		1086	6.32	
	KOH (700 °C 1 h)	OC700		1922	7.98	
	KOH (800 °C 1 h)	OC800		2399	6.60	
Coconut shell	500 °C 2 h	C-500	0 °C, 1 bar	21	2.0	263
	$(NH_2)_2CO$ (600 °C 2 h)	C-600		1023	5.6	
	KOH (650 °C 1 h)	A-650		1535	7.0	
Olive stones	H_3PO_4	AC-H_3PO_4	30 °C, 1 bar	1178	10.9	264
	CO_2	AC-CO_2		757	5.89	
	H_2O (g)	AC-H_2O		754	7.97	
Black locust	—	AC	0 °C, 1 bar	1175	2.79	265
	KOH	AC-KOH		2064	5.86	
	NH_3	AC-KOH-N		2511	7.19	
Walnut shells	Urea/carbon 1 : 3	KNWS-13	25 °C, 10 bar	1047	5.72	266
	Urea/carbon 2 : 3	KNWS-23		2707	10.06	
	Urea/carbon 3 : 3	KNWS-33		2461	11.02	
Persian ironwood	H_3PO_4	HP5	30 °C, 1 bar	1802	3.02	267
	NiO	HP5/Ni3-1		1945	6.48	
	CuO	HP5/Cu3-1		1954	6.78	
Coffee grounds	—	HC	35 °C, 1 bar	34	0.14	268
	Melamine	MHC		402	0.85	
	Melamine, KOH	KMHC		990	2.67	

carbon framework at elevated temperatures, typically enhancing the adsorption of CO_2. Additionally, activated carbon was produced from corn stover and activated using H_3PO_4, CO_2, and H_2O, with the H_3PO_4-activated carbon exhibiting the highest CO_2 capture capacity of 10.9 mmol g^{-1}, owing to its elevated specific surface area and microporous volume resulting from chemical activation.[264] Moreover, urea-doped nanoporous carbon synthesized from walnut shells showed an increase in CO_2 capture capacity with higher urea doping levels.[266] Furthermore, the CO_2 uptake of activated carbon was enhanced by modification with NiO and CuO, respectively, resulting in notable improvements in CO_2 capture capacity.[267] Subsequent sections of this review will explore the application of various types of carbon materials in CO_2 capture, including pristine carbon, activated carbon, heteroatom-doped carbon, metal-loaded carbon, and carbon-based nanomaterials, examining their individual advantages and challenges in CO_2 capture.

5.1.2.1 Pristine carbon materials. Pristine carbon materials, in their natural state, serve as the fundamental building blocks for various applications, including the capture of CO_2. However, despite possessing inherent carbonaceous properties such as surface area and porosity, pristine carbon materials often have limited CO_2 adsorption capabilities due to their underdeveloped pore structures and surface chemistry. These materials are directly derived from the thermochemical conversion of biomass, such as biochar or hydrochar, well-known for their environmentally friendly characteristics and wide availability from diverse biomass sources. Despite their initial limitations, pristine carbon materials provide the foundation for subsequent modifications aimed at enhancing their CO_2 capture efficiency. Through the implementation of various activation methods and doping techniques, pristine carbon materials can be customized to meet specific requirements for CO_2 capture, making them a versatile platform for developing effective CO_2 adsorbents to counteract the rising atmospheric CO_2 levels. Numerous studies have highlighted the CO_2 adsorption potential of biochar, which is attributed to its polarity, high specific surface area, and functional groups.[270] For instance, composite biochar synthesized from sewage sludge and *Leucaena* wood in different proportions showed superior CO_2 uptake compared to pure sewage sludge biochar. Increasing the *Leucaena* wood biochar content resulted in a higher carbon content, and subsequently enhanced CO_2 adsorption capacity.[271] Similarly, date palm leaf biochar produced at varying temperatures exhibited a corresponding increase in CO_2 adsorption capacity with higher preparation temperatures, owing to the increased carbon content of the biochar.[272] These findings underscore the potential of pristine carbon materials, particularly biochar, as effective CO_2 adsorbents and emphasize the significance of optimizing preparation conditions to maximize their CO_2 capture efficiency.

5.1.2.2 Activated porous carbon. Activated porous carbon (APC) has emerged as a pivotal material for CO_2 capture due to its unique properties, including highly porous structure and large surface area, which enhance its adsorption capabilities. Traditionally, APC has been extensively utilized in various applications such as pollutant removal, industrial purification, and air filtration. Its versatility is attributed to its ability to be tailored through different activation methods, both physical and chemical, to achieve the desired porosity and surface characteristics. Biomass provides a distinctive opportunity for creating activated porous carbons with beneficial structural characteristics. This approach is considered more advantageous than using traditional fossil fuel-based precursors for the production of activated carbons due to low cost and abundant availability of biomass and the environmentally friendly nature of the pyrolysis process used. The process of converting biomass into APC involves pyrolysis, followed by activation using agents such as steam, CO_2, and chemical reagents such as KOH or $ZnCl_2$. This process results in a material with a high surface area and tunable pore size distribution, making it highly effective for capturing CO_2.[273]

Physical activation, such as CO_2 or steam activation, plays a crucial role in enhancing the microporosity of the carbon structure, thereby increasing its specific surface area and improving CO_2 adsorption. The choice of biomass precursor and the conditions of the pyrolysis process, including temperature and residence time, significantly influence the final properties of the APC. For instance, CO_2 activation is known to produce microporous carbons with uniform pore structures, which are ideal for gas adsorption, while steam activation can introduce mesopores and macropores, potentially enhancing the diffusion of CO_2 molecules into the carbon matrix.[274] Alternatively, chemical activation can further enhance the porosity and surface functionality of APCs, making them even more effective for CO_2 capture. Activating agents such as KOH and $ZnCl_2$ facilitate the development of a hierarchical pore structure and the introduction of functional groups that can interact with CO_2 molecules, improving the adsorption efficiency.[226,275] The ability to engineer APCs with specific surface properties through controlled activation processes makes them highly promising materials for addressing the growing challenge of CO_2 emissions and climate change.

Fig. 11 illustrates the process of CO_2 capture using activated porous carbon derived from biomass, which was chemically activated with potassium hydroxide (KOH). The process begins with the raw biomass of Jujun grass, which undergoes KOH activation to create a highly porous carbon material. Subsequently, this activated porous carbon is used for CO_2 adsorption, effectively capturing CO_2 molecules at 25 °C as a function of pressure.[276] This highlights the potential of KOH-activated porous carbon as a highly efficient material for CO_2 capture, which is crucial for mitigating the impact of greenhouse gases on the environment.

5.1.2.3 Non-functionalized activated carbon. Non-functionalized activated carbon derived from various precursor materials undergoes activation processes without additional chemical modifications to its surface, preserving its inherent physical and chemical attributes. In contrast to functionalized activated carbon, which incorporates specific functional groups to target adsorption, non-functionalized activated carbon relies solely on its porous structure and high surface area for adsorption. Generally, activated carbons demonstrate

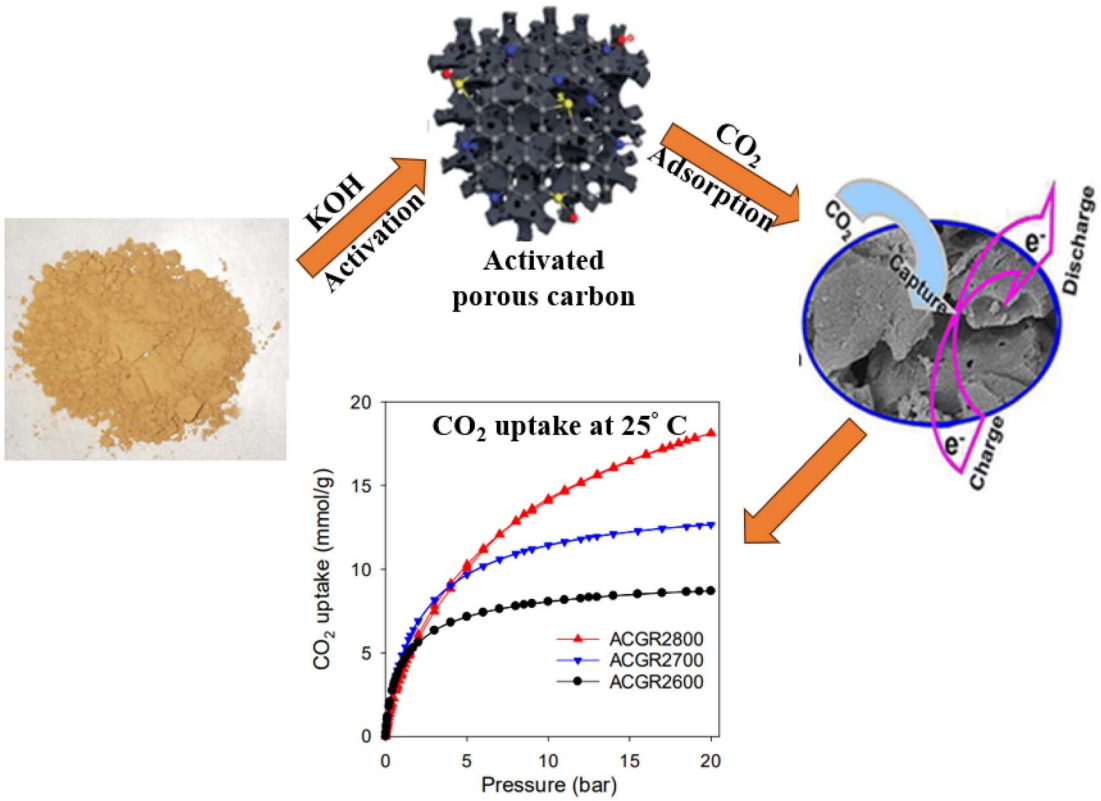

Fig. 11 CO_2 adsorption performance of KOH-activated biomass-derived porous carbon.[276]

superior CO_2 adsorption capacities compared to biochar due to their improved textural properties and surface chemistry resulting from activation treatments. CO_2 capture mechanisms involve both physical and chemical processes. Physical adsorption arises from van der Waals forces between CO_2 molecules and the carbon surface, with surface area and pore size playing critical roles in the adsorption efficiency. Conversely, chemical adsorption is attributed to the alkali functional groups on the carbon surface, enhancing the interaction and uptake of CO_2. Activation significantly enhances the textural properties of carbon materials, thereby boosting their CO_2 adsorption performance.

Highly microporous KOH-activated carbons derived from Jujun grass (JG) and *Camellia japonica* (CJ) biomass exhibited significant CO_2 capture capabilities in both pre- and post-combustion scenarios.[277] The activated carbons produced at 700 °C with a KOH impregnation ratio of 2 demonstrated the highest CO_2 adsorption at 1 bar (4.9–5.0 mmol g^{-1}) under room temperature conditions. Conversely, that prepared at 800 °C with a higher KOH impregnation ratio of 4 showed the highest CO_2 adsorption at 20 bar (21.1 mmol g^{-1}). Mesquite wood, when transformed into carbon-rich material through single-step KOH activation at 800 °C, achieved a high surface area of 3167 m^2 g^{-1} and CO_2 adsorption of 26.0 mmol g^{-1} at 23 °C and 30 bar.[261] Similarly, microporous activated carbons synthesized from *Arundo donax* at 600 °C displayed an excellent CO_2 adsorption capacity of 15.4 mmol g^{-1} at 30 bar, with a surface area of 1122 m^2 g^{-1}. $ZnCl_2$ activation of *Arundo donax* resulted in an even higher surface area of 3298 m^2 g^{-1} and CO_2 adsorption of 30.2 mmol g^{-1} at 30 bar.[278] These results emphasize the critical role of surface area and porosity in enhancing the CO_2 adsorption by activated porous carbons.

The microporous content of activated carbon significantly influences CO_2 adsorption, with a higher micropore content correlated with increased CO_2 adsorption.[279] Research on KOH-activated rice husk char showed that lower activation temperatures (640–710 °C), reduced KOH impregnation ratios (1 : 1), and elevated nitrogen content resulted in the high CO_2 uptake of 2.11 mmol g^{-1} at 0.1 bar. A narrow pore size distribution and micropores less than 0.7 nm were identified as crucial for the enhanced CO_2 adsorption at sub atmospheric pressures. These activated carbons also exhibited high selectivity (19.9) for CO_2 over N_2. Another study highlighted the importance of ultra-micropores in CO_2 capture using KOH-activated bamboo porous carbons, reporting a notable CO_2 adsorption value of 7.0 mmol g^{-1} at 0 °C and 1 bar, which was attributed to the micropores of 0.55 nm.[280] However, wider pores resulting from increased KOH impregnation amounts led to reduced CO_2 adsorption due to the limited pore diffusion.

Likewise, Patel *et al.* highlighted the importance of narrow micropores (<1 nm) in CO_2 capture by activated porous carbons produced through the KOH activation of sawdust.[281] Mild KOH treatment resulted in narrow micropores with lower surface areas compared to severe treatment, yielding high CO_2 uptake

(4.8 mmol g^{-1}) at room temperature. The presence of a microporous structure, hydroxyl groups, and heteroatoms such as nitrogen and oxygen collectively regulated the CO_2 adsorption on activated porous carbons derived from KOH activation of gelatin and starch biomasses, resulting in substantial CO_2 adsorption (7.49 mmol g^{-1}) at 1 bar and 0 °C, with favorable selectivity for CO_2 over N_2 (52–98%).[282] The isosteric heats of adsorption values (21.7–62.9 kJ mol^{-1}) suggest the involvement of both chemical and physical adsorption mechanisms. Additionally, wood ash-based activated porous carbon has been proposed for CO_2 capture, primarily *via* chemical sorption.[283] Analysis pre- and post-CO_2 adsorption revealed the participation of alkali and alkaline earth metals in wood ash, facilitating chemical reactions with CO_2 and H_2O and resulting in the formation of diverse carbonate products.

5.1.2.4 Heteroatom-doped activated porous carbon. Doping activated porous carbon with heteroatoms such as nitrogen, oxygen, and sulfur during activation modifies its electronic properties and surface chemistry, enhancing its adsorption capabilities and selectivity, particularly for CO_2. Although micropores are crucial for CO_2 capture, they also promote the adsorption of other gases such as CH_4 and N_2, leading to reduced CO_2 adsorption capacity due to competitive adsorption. However, heteroatom doping addresses this issue by introducing functional groups that exclusively interact with CO_2, boosting the CO_2 selectivity. Incorporating basic or electron-rich heteroatoms such as nitrogen into the carbon framework further enhances the CO_2 absorption capacity, given that the abundant basic sites on the surface act as anchors for capturing the weakly acidic CO_2 molecules. For example, Nazir *et al.* added nitrogen-containing functional groups to activated porous carbons for CO_2 extraction during carbonization using an NH_3 solution.[265] This three-step process resulted in a final carbon material with a high nitrogen content (7.21%) incorporated as functional groups, exhibiting a higher surface area (2511 m^2 g^{-1}) compared to the carbon prepared using KOH activation alone (2064 m^2 g^{-1}). The enhanced surface area and basic sites facilitated significant CO_2 adsorption at both 0 °C (7.19 mmol g^{-1}) and 25 °C (5.5 mmol g^{-1}), with high ultra-microporosity aiding in physical and chemical CO_2 adsorption.[284] Additionally, the sample demonstrated high selectivity for CO_2 over N_2 (30.75%), rapid kinetics, and efficient regeneration, presenting a promising approach for CO_2 capture using biomass-based materials.

In a study conducted by a research group, activated carbon was produced from husk using carbonization and KOH activation, with chitosan introduced during its activation.[200] The resultant doped activated carbon displayed an enhanced CO_2 adsorption capacity, reaching 5.83 mmol g^{-1} at 0 °C. The XPS analysis detected pyridine-N and pyrrole-N on the surface of the doped activated carbon, enhancing its surface alkalinity and facilitating CO_2 uptake. Similarly, another research team enhanced the CO_2 capture performance of activated carbon by modifying it with ammonium sulfate.[285] The presence of sulfur functional groups enabled interaction with CO_2 molecules, thereby improving their adsorption. Nitrogen doping plays a vital role in heteroatom doping to boost the CO_2 capture efficiency. Nazir and Wang *et al.* employed various amines (TEPA, MEA, DEA, PEI, and DETA) to modify waste wood ashes for CO_2 capture. Among them, the TEPA-sorbent exhibited a superior CO_2 capture performance, with a capacity of 1.76 mmol g^{-1} and an impressive regeneration rate of 92.6% (Fig. 12).[265,286] Despite the DEA-sorbents having the highest actual nitrogen loading, their adsorption capacity was lower than that of TEPA, highlighting the multifaceted nature of CO_2 adsorption, where the nitrogen content alone does not determine the capacity. The significance of micropores in CO_2 adsorption was demonstrated by the optimized loading of TEPA (45 wt%), which yielded a superior CO_2 capture performance (2.02 mmol g^{-1}). Furthermore, the type of nitrogen-containing functional groups significantly impacts the CO_2 capture efficiency. Wang *et al.* investigated the roles of various nitrogen functional groups in the CO_2 adsorption process, with pyridine-N showing the highest CO_2 adsorption energy (−21.4 kJ mol^{-1}) due to its robust dipole–dipole interactions with CO_2, similar to H^+ and O^{2-}.[269,287] Thus, understanding these mechanisms is crucial for tailoring adsorbents for the optimal CO_2 capture performance.

5.1.2.5 Metal/metal oxide-embedded activated porous carbon. Metal or metal oxide-embedded activated porous carbons stand out as a versatile and highly effective class of carbon-based materials, which are characterized by the integration of metal or metal oxide nanoparticles into their porous structure. These materials are synthesized using a variety of methods, such as impregnation, co-precipitation, and *in situ* growth, resulting in enhanced adsorption properties and catalytic activity owing to the incorporation of metal or metal oxide nanoparticles into the carbon matrix. Another strategy to boost the CO_2 adsorption capacity involves functionalizing activated porous carbons with metal atoms to create additional surface-active sites. Numerous studies have explored the impact of metal functionalization on CO_2 uptake, with alkaline metals proving particularly effective in adsorbing acidic carbon dioxide. In the adsorption process, CO_2 serves as an electron acceptor, capable of receiving electrons from metal oxides possessing basic characteristics.

The adsorption mechanism of CO_2 onto metal-impregnated AC is depicted in the Fig. 13. Metal oxides are typically incorporated in the surface of AC using the wet impregnation method. This involves mixing the carbon precursor with metal oxide solutions before subjecting it to a high-temperature carbonization process, or alternatively, mixing the already prepared AC with metal oxide solutions followed by calcination at elevated temperatures.[13] For instance, Botomé *et al.* produced AC from wood treated with chromated copper arsenate (CCA), which was pyrolyzed at 700 °C, and the resulting material demonstrated an adsorption capacity of 1.88 mmol g^{-1} for CO_2.[288] The metal oxide impregnation on AC significantly impacts both the structural characteristics and CO_2 adsorption capacity, depending on the metal loading. A low metal loading may not enhance the adsorption capacity, while an excessively high metal loading can cause pore clogging, which reduces the surface area and pore volume, thereby diminishing the adsorption performance.

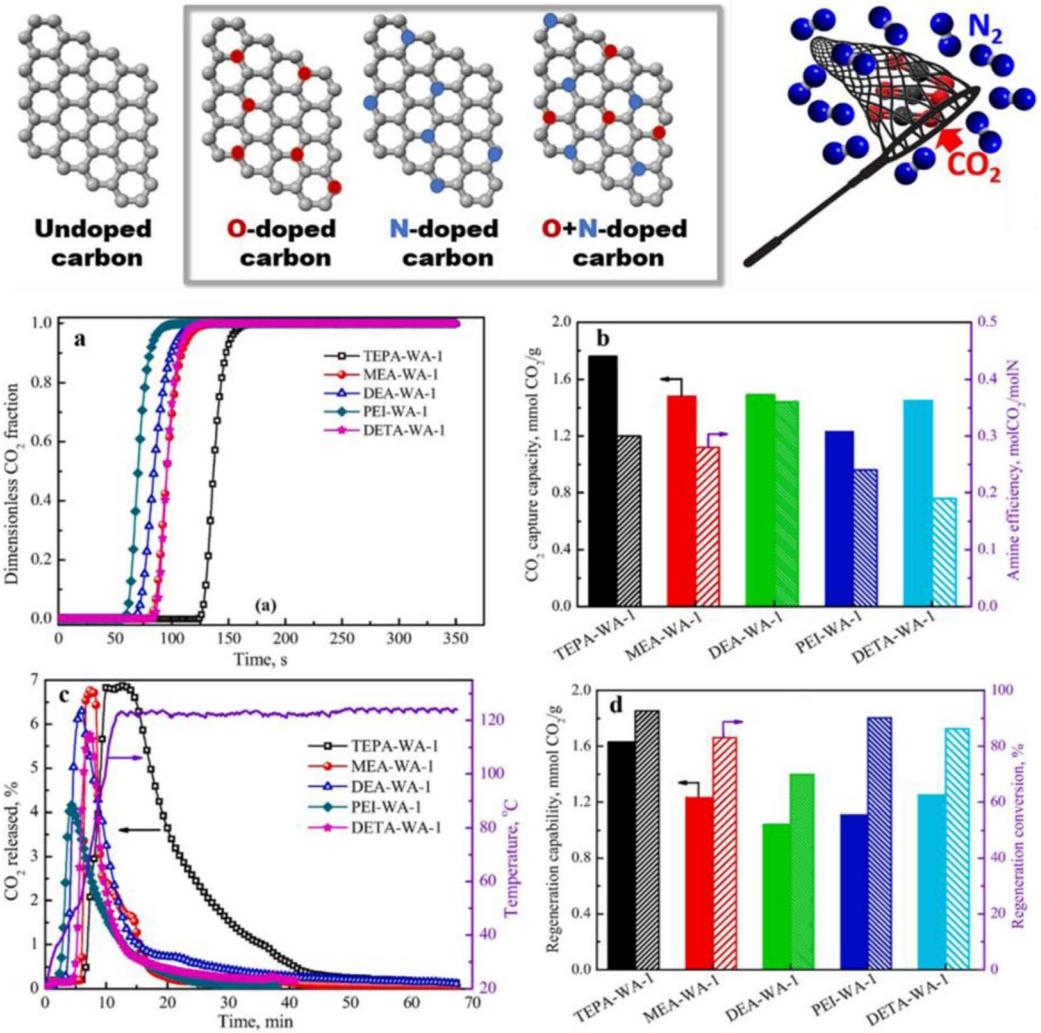

Fig. 12 Heteroatom-doped carbons for CO_2 capture and CO_2 adsorption performance of wood ash (WA-1) activated with various polyamines, showing (a) CO_2 adsorption breakthrough profiles, and (b) adsorption capacity along with amine efficiency. Regeneration performance of WA-1 activated with different polyamines: (c) CO_2 desorption curves, and (d) adsorbent regeneration potential and conversion efficiency. Reprinted with the permission.[265,286]

Recent studies have focused on enhancing CO_2 capture using carbon composites derived from walnut shells and doped with metals such as Mg and Mg–Al. Although metal loading led to reduced specific surface areas due to pore clogging, the CO_2 capture performance of these composites improved significantly.[289] Notably, the composites with 10% Mg and 5% Al achieved a CO_2 uptake of 4.5 mmol g^{-1}. Scanning electron microscopy (SEM) and energy-dispersive X-ray spectroscopy (EDX) confirmed the effective distribution of Mg and Al on the carbon surface, while Fourier-transform infrared spectroscopy (FTIR) and X-ray diffraction (XRD) revealed weakened metal oxide peaks after CO_2 adsorption, indicating enhanced chemisorption. This improved performance is attributed to the combined effects of physical and chemical adsorption mechanisms in the metal-doped carbon materials.[290]

In parallel, biochar modified with $AlCl_3$ demonstrated superior CO_2 uptake compared to unmodified biochar. This was due to the primary role of surface adsorption facilitated by the metallic oxides present. Additionally, activated porous carbons derived from pine cones and treated with KOH, incorporating nitrogen and metals, showed high CO_2 adsorption capacities.[291] For instance, the samples prepared at 700 °C with a KOH ratio of two, containing 0.5% nitrogen and calcium, achieved a CO_2 uptake of 4.7 mmol g^{-1}.[292] These materials also exhibited an excellent performance in the oxygen reduction reaction (ORR), suggesting their potential in various applications beyond CO_2 capture. Table 7 provides a comparative overview of various types of sorbents, highlighting their physical and chemical properties together with their CO_2 adsorption capacities.

Furthermore, the incorporation of metal oxides such as MgO, BaO, and Fe_2O_3 into activated carbon has been shown to enhance its CO_2 adsorption capacity. Basic oxides, in particular, are more effective than acidic or neutral oxides. For example, MgO significantly improved the CO_2 capture at higher temperatures, and BaO provided the greatest enhancement due to its high electronegativity.[294] These findings underscore the

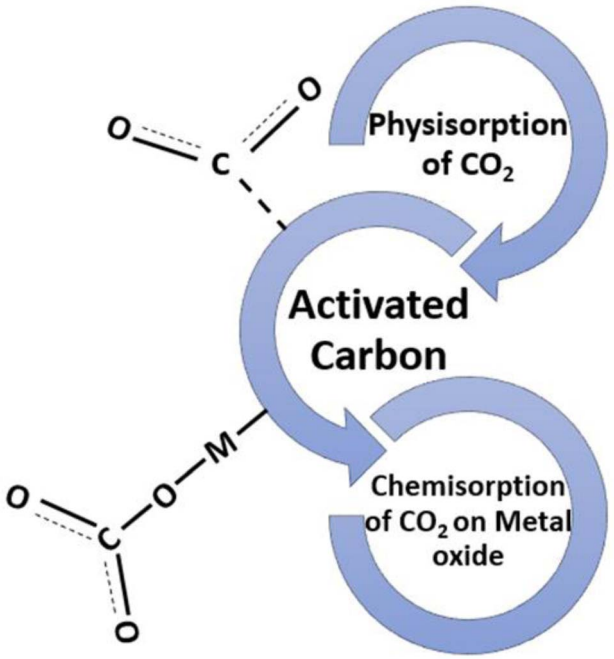

Fig. 13 Mechanism of impregnating activated carbon with metal oxides.

potential of metal-functionalized activated carbons in optimizing CO_2 capture and other environmental applications.

5.1.3 Processes involved in CO_2 capture. Here, the potential mechanisms for CO_2 uptake by carbon materials are depicted, distinguishing between physical adsorption and chemical adsorption based on the surface interactions between CO_2 molecules and carbon materials (Fig. 14).[269,295] Physical adsorption primarily relies on van der Waals forces and pore filling, with the adsorption temperature exerting a significant influence. In contrast, chemical adsorption involves the formation of chemical bonds between CO_2 and the adsorbents, predominantly facilitated by Lewis acid–Lewis base interactions and hydrogen bonding. Micropores, oxygen functional groups, N functional groups, and aromaticity emerge as critical factors influencing CO_2 capture.

Physisorption, a reversible process driven by van der Waals forces and electrostatic forces, is primarily governed by the textual properties of carbon materials, including pore structure and surface area. Although the large specific surface area and porosity of carbon materials enhance CO_2 capture, their pore size is more crucial than specific surface area and total pore volume for CO_2 adsorption. Micropores significantly contribute to CO_2 adsorption, particularly at low adsorption pressures. Notably, studies have identified narrow micropores with sizes in the range of 0.5 to 0.7 nm as critical for enhancing the CO_2 adsorption capacity.[295] Under higher adsorption pressures, adsorption occurs through surface coverage, where the specific surface area plays a pivotal role. Adsorption temperature also influences physical adsorption, with higher temperatures promoting CO_2 diffusion and weakening CO_2–carbon material interactions. Chemisorption, an irreversible chemical reaction process, involves the formation of new chemical bonds between adsorbents and adsorbates, facilitated by surface functional groups and alkali ions. Hydrogen bonds and Lewis acid–base interactions play crucial roles in chemisorption. Studies have highlighted the significance of hydroxyl groups in enhancing CO_2 capture, given that CO_2 molecules can form hydrogen bonds with –OH, promoting CO_2 adsorption. Nitrogen-containing polymers have been employed to modify carbon materials, enhancing their alkalinity and electron density to strengthen the Lewis acid–base interaction. Moreover, the covalent coordination bonds formed between CO_2 and the adsorbent surface contribute to chemisorption. Researchers have developed novel N, P co-doped porous carbon materials with high specific surface areas and rich mesopores, micro pores, and N, P, resulting in enhanced CO_2 uptake capacity.[296] The presence of N groups in porous carbon derived from lotus stalks has been linked to excellent CO_2 adsorption capacity, with the N groups playing a dominant role in CO_2 adsorption at higher temperatures and lower pressures. However, the excessive loading of modifying agents such as melamine can clog the pores and reduce the specific surface area of carbon materials, thus impacting their CO_2 capture performance. Thus, achieving a balance between loading amount and porosity changes is essential to realize the optimal CO_2 capture efficiency. Studies have demonstrated an enhancement in surface area through heat treatment after melamine impregnation, highlighting the

Table 7 Overview of sorbent types, properties, and CO_2 adsorption capacities

Sorbent type	Physical properties	Chemical properties	CO_2 adsorption capacity	Ref.
Non-modified carbon	High surface area, microporous structure	Primarily carbon, with surface oxides	30.2 mmol g^{-1} at 25 °C, 30 bar	278
Nitrogen-doped carbon	Moderately high surface area, mesoporous	Nitrogen groups improve basicity	5.83 mmol g^{-1} at 0 °C, 1 bar	285
Sulfur-doped carbon	Microporous and mesoporous structure	Sulfur groups increase binding sites	~2.8–3.8 mmol g^{-1} at 25 °C, 1 bar	293
Metal-modified carbon	Surface area depends on metal type, porosity varies	Enhanced by metal oxides (*e.g.*, Al, Cu, Fe)	4.5 mmol g^{-1} at 25 °C, 1 bar	290
Metal oxide-embedded AC	High surface area (~600–1200 m^2 g^{-1}), microporous/mesoporous	Embedded metal oxides (*e.g.*, Fe_3O_4), surface oxygen groups	4.7 mmol g^{-1} at 25 °C, 1 bar	292

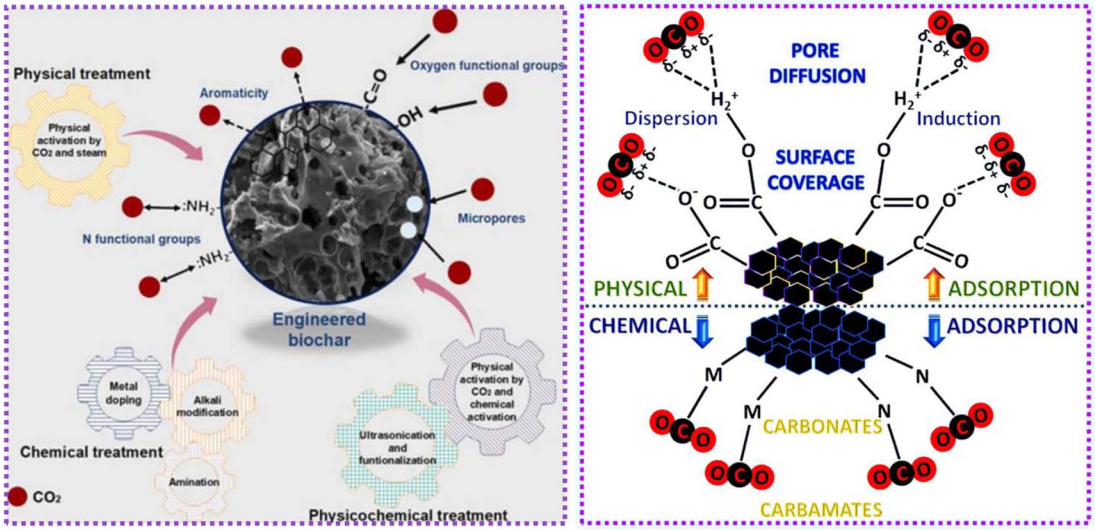

Fig. 14 Processes involved in CO_2 capture by carbon materials. Reprinted with permission.[269,295]

importance of carefully managing the loading amounts to maximize the capture performance. These findings underscore the multifaceted mechanisms underlying CO_2 capture by carbon materials and emphasize the need for tailored material design to optimize the efficiency in various applications.

5.1.4 Traditional and alternative CO_2 adsorbents. Activated carbons, zeolites, and molecular sieves are among the traditional CO_2 adsorbents that have received extensive scrutiny for CO_2 capture applications due to their well-established traits and commercial accessibility. These materials frequently demonstrate impressive adsorption capacities and selectivity, but they may face challenges such as limited thermal stability and difficult regeneration. Table 8 provides an overview of the advantages and disadvantages associated with both

Table 8 Advantages and drawbacks of CO_2 adsorbents

Sorbent	Characteristics/processes/advantages	Drawbacks/disadvantages	Ref.
Metal oxides	Both low toxicity and abundant availability	High energy needs for regeneration	297 and 298
Waste products	Renewable sources, low cost and abundant	CO_2 adsorption capacity varies significantly based on the chemical, physical, and structural properties of the raw material, as well as its preparation history and treatment conditions	299–301
Commercial activated carbon	The best adsorbent available	Initial cost of the carbon and non-renewable resources	302
Activated alumina	Relatively well-known and commercially available	High cost of adsorbent	303–305
Zeolites	Large surface area, stable temperature, and less heat needed for regeneration	Performance decrease in the presence of moisture and impurities in gas feed	306
MOF	High surface area and physiochemical stability	Costly and difficult to produce for industrial scale	307–309
Silica	Large surface area, strong thermal and mechanical stability	High regeneration energy requirements	310 and 311
Agricultural wastes	Low cost and abundant	Performance varies depending on the precursor	312
Industrial by products	Highly available and low-cost precursor	Varies adsorption strength depending on the precursor	313
Shrimp shells/chitosan	Plentiful, renewable, biodegradable, and environmentally friendly resource	Low surface area	314 and 315
Peat	A cheap, plentiful, and easily accessible biosorbent	Low mechanical strength	316
Biomass	Plenty resources with high adsorption capacity, low cost and effective technology	In study/experimental stage	222 and 225
Biochar	Many resources with a large capacity for adsorption, inexpensive costs, and efficient technology	Low CO_2 uptake compared to AC	317

conventional and non-conventional CO_2 adsorbents. Identifying the optimal CO_2 adsorbent is intricate due to the complex interplay among the synthesis parameters for activated carbons and adsorption conditions. Discrepancies in research data hinder the unbiased assessment of the potential of waste products as CO_2 adsorbents given that their effectiveness cannot be solely gauged by comparing the CO_2 uptake under standardized conditions. The characteristics of activated carbons are heavily influenced by the synthesis process, which varies across different studies. Furthermore, many investigations fail to present a comprehensive view of the adsorption system, often overlooking potential competitive adsorbates such as CO, N_2, and CH_4, while focusing solely on CO_2 removal efficiency. Besides cost considerations, factors such as operational intricacy, regeneration feasibility, source availability, and environmental impact must be carefully weighed when selecting appropriate adsorbents.

5.1.5 Mechanism of CO_2 adsorption on acrylic carbon. The application of acrylic carbon for CO_2 adsorption is increasingly recognized due to its promising potential with unique structural properties and customizable surface chemistry. Derived from the polymerization of acrylonitrile or its copolymers, acrylic carbon undergoes carbonization to form a material with a highly tunable porous structure and substantial surface area, both of which are essential for effective CO_2 capture. The adsorption process primarily involves physisorption and chemisorption mechanisms. In physisorption, CO_2 molecules are adsorbed on the acrylic carbon surface *via* van der Waals forces, allowing reversible adsorption without altering the chemical structure of CO_2. This characteristic is particularly beneficial for cyclic adsorption–desorption processes, given that it enables low-energy regeneration, making it an energy-efficient option for repeated use.[318] The porous structure of materials is instrumental in enhancing CO_2 capture by providing numerous adsorption sites and promoting efficient gas diffusion. Moreover, the performance of acrylic carbon can be significantly enhanced by modifying its surface chemistry to introduce functional groups that facilitate chemisorption. Chemisorption involves the formation of strong chemical bonds between CO_2 molecules and surface groups such as amine, hydroxyl, and carboxyl, which can be introduced either during the synthesis of the polymer precursor or through post-synthesis modifications. For example, incorporating nitrogen-containing groups *via* ammonia treatment or co-polymerizing with nitrogen-rich monomers increases the CO_2 uptake due to the formation of carbamate species during chemisorption. This dual mechanism approach, leveraging both physisorption and chemisorption, positions acrylic carbon as a highly effective material for CO_2 capture applications.[319]

Activated carbon fibers (ACFs) were developed from mechanically recycled acrylic (PAN), cotton (CO), and their blends (PAN/CO) to enhance CO_2 capture.[320] The production process involved stabilization, carbonization, and chemical activation. However, although PAN is effective for ACF production, it is costly and has significant environmental impacts due to its energy-intensive production. Thus, to address these issues, recycled or renewable materials were utilized to reduce both costs and environmental footprint. PAN fibers were stabilized using oxidation and phosphoric acid treatment, followed by carbonization at a temperature of 800 °C or 900 °C under nitrogen, and activation with various KOH ratios at 700 °C. The stabilization process preserved the fiber structure and improved the heat resistance.[321] Generally, the PAN fibers maintained their integrity after carbonization and activation, although some samples showed rough surfaces due to the incomplete KOH removal.

The CO_2 adsorption capacity of ACFs made from recycled fibers was notably high, with higher KOH ratios enhancing their surface area and pore volume, which in turn improved their CO_2 capture performance. These recycled ACFs showed comparable or superior CO_2 adsorption capacities to commercial ACFs, highlighting their potential for sustainable CO_2 capture. Additionally, this study evaluated the mass yield and elemental composition of PAN and PAN/cellulose (PAN/cell) nanofibers in producing activated carbon nanofibers (ACnFs). Oxidative stabilization reduced the mass of PAN/cell fibers more than PAN fibers. Carbonization and activation caused significant mass loss in the PAN/cell nanofibers due to their lower carbon content and thermal stability, although the PAN/cell fibers had a higher nitrogen content. The SEM and FTIR analyses confirmed the changes in the fiber diameter and chemical structure. Fig. 15a shows SEM images of biomass fibers before and after grafting with poly(acrylic acid) (PAAc), highlighting the increase in surface roughness.[322] Fig. 15b presents the SEM images of the PAN fibers at various stages, showing changes in surface texture and porosity with treatment. Fig. 15c shows a comparison of the untreated PAN fibers with that carbonized at different temperatures, revealing significant structural transformations. The PAN-based ACnFs carbonized at 800 °C exhibited higher CO_2 adsorption compared to that processed at 900 °C, emphasizing the impact of the production conditions on CO_2 capture efficiency.[324] Recent evaluations of the CO_2 adsorption capacities for various the carbon-based adsorbents at 1 bar and 25 °C highlight their effectiveness in CO_2 capture. This study shows that recycled ACFs derived from acrylic carbon show a comparable performance or surpass that of many commercial carbon adsorbents.[323]

Furthermore, doping acrylic carbon with metal nanoparticles, such as alkali and alkaline earth metals, has shown to boost the CO_2 adsorption significantly. Metals such as sodium, calcium, and magnesium interact synergistically with CO_2, combining the benefits of both physisorption and chemisorption. Metal-doped acrylic carbon adsorbents exhibit higher CO_2 capture capacities and improved selectivity, given that the metal sites provide additional reactive centers for CO_2 binding.[265] These modifications not only enhance the CO_2 capture performance but also improve the stability and recyclability of the adsorbent, making them viable for long-term industrial applications.

The application of acrylic carbon for CO_2 adsorption holds promise across various sectors, including flue gas treatment, air purification, and carbon capture and storage technologies. The versatility in its synthesis and the ability to finely tune its structural and chemical properties make acrylic carbon a highly

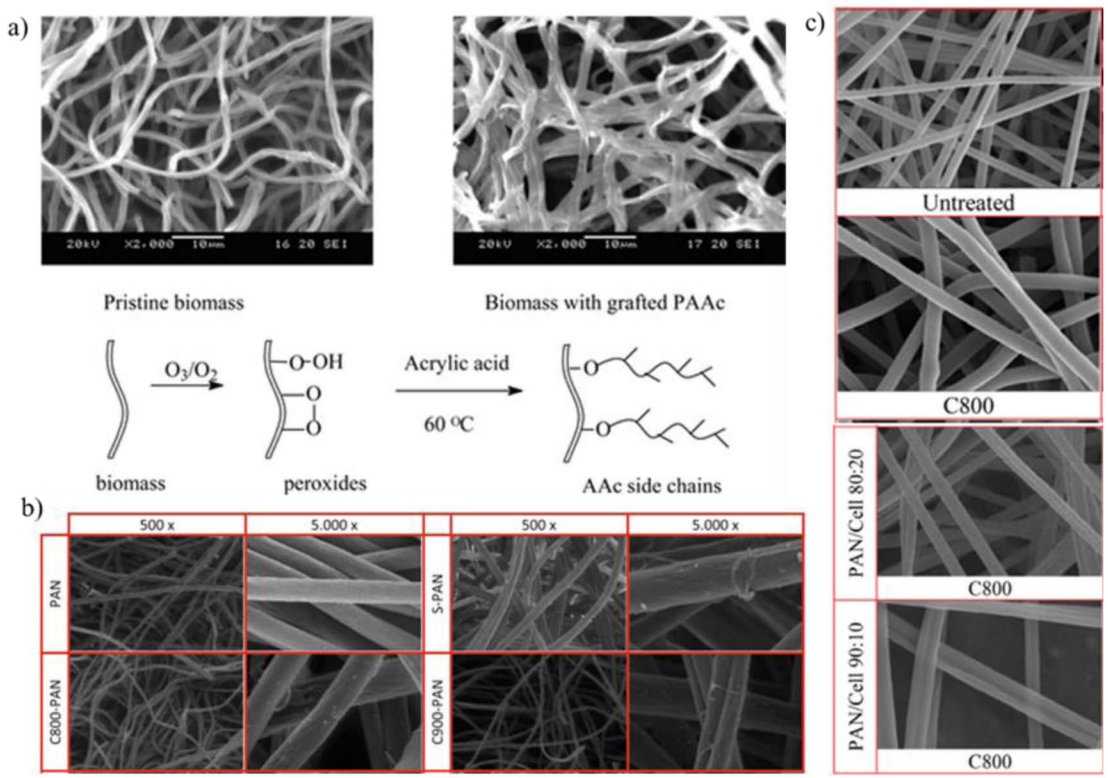

Fig. 15 Surface morphology of biomass and polyacrylonitrile (PAN)-based nanofibers for enhanced CO_2 capture: (a) pristine *vs.* PAAc-grafted biomass, (b) SEM comparison of untreated PAN, C800, and PANC/cell composites, and (c) PAN nanofiber morphology under varying treatments and magnifications. Reproduced from ref. 322 and 323.

adaptable material for CO_2 capture. Recent advancements focus on optimizing the synthesis routes to improve its pore structure and surface functionality, thereby maximizing its adsorption efficiency under different operational conditions.[325] Continued research is essential to fully understand the adsorption mechanisms at the molecular level, which will aid in designing more efficient and cost-effective acrylic carbon-based adsorbents. Moreover, scaling up the production of these materials, while maintaining their performance and stability is crucial for practical applications. As global efforts to mitigate climate change intensify, the development of advanced materials such as acrylic carbon for CO_2 capture is becoming increasingly critical. The integration of these materials into existing CO_2 capture frameworks can significantly enhance their efficiency and contribute to reducing atmospheric CO_2 levels.[326]

5.2 Prospects for commercialization

The potential for commercializing a product or technology relies on diverse factors such as market demand, technological feasibility, scalability, regulatory compliance, and economic viability. In the domain of CO_2 adsorbents, the prospects for their commercialization depend on their capacity to meet or exceed industry-defined performance standards, while remaining cost-effective and environmentally sustainable. Additionally, considerations such as the availability of raw materials, manufacturing simplicity, and compatibility with existing infrastructure play pivotal roles in determining the feasibility of their large-scale production and deployment. With various synthesis strategies for biomass-derived porous carbon materials, the transition from laboratory-scale or pilot plant development to industrial-scale production capacity becomes crucial. Achieving this transition requires integrating chemistry and chemical engineering technologies. Nonetheless, several challenges need to be addressed. Firstly, scaling up synthesis protocols from gram to kilo batch sizes poses a significant hurdle, compounded by uncertainties in biomass supply and associated logistical costs. Establishing local biomass resources, enhancing annual yields, and devising new logistics routes can offer sustainable supply chains from field to processing plant. Subsequently, for improved qualities, micro and mesoporous carbon powder materials must be transformed into granules, pellets, beads, or extrudates with or without binders. Granulation techniques sometimes result in the loss of specific surface area, despite the fact that granular materials offer higher mechanical strength, decreased attrition, and lower resistance in the adsorbent bed. However, studies suggest that incorporating biomass-based pore-forming materials can enhance the sorption properties.[327] Once the characteristics of materials are understood, finalizing the design of CO_2 capture plants becomes essential. Strategies may involve temperature swing adsorption (TSA), pressure swing adsorption (PSA), vacuum swing adsorption (VSA), or combinations thereof.

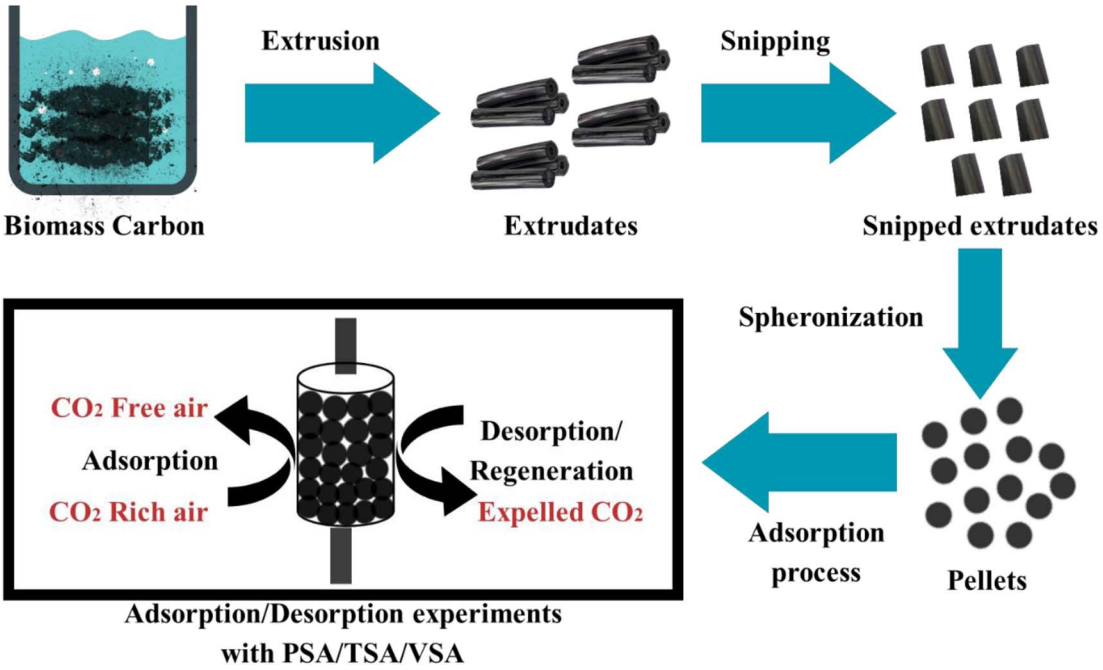

Fig. 16 Diagram illustrating the complete CO_2 capture process, starting from powder form to palletization, and depicting the sorption cycle for real-world application.

These next-generation carbon materials outperform traditional sorbents such as zeolites due to their inherent hydrophobic properties, low isosteric heat of adsorption, high CO_2 adsorption capacities, and long-term stability across multiple cycles. Fig. 16 schematically illustrates the transition from porous carbon powder to plant-level deployment. Further material and design considerations should be made based on the specific CO_2 removal application, whether for pre- or post-combustion scenarios requiring high CO_2 concentration removal or for confined environments such as cockpits and underground spaces with lower CO_2 concentrations. In these cases, high-performance materials such as carbon with strong interactions at low surface coverage, requiring minimal heat for regeneration, are essential. Additionally, anticipating the adsorption of CO_2 under humid conditions underscores the need for porous carbons capable of efficient operation in these circumstances.

5.3 Cost assessment framework

Cost assessment frameworks for producing activated porous carbons, especially for CO_2 capture, play a pivotal role in determining the economic feasibility of transitioning from laboratory-scale experiments to full-scale industrial production. Producing activated carbons from biomass encompasses various cost components, which can be broadly categorized into fixed and variable costs. Typically, fixed costs involve capital investments in infrastructure, equipment, and facilities necessary for the initial setup of the production plant. Alternatively, variable costs include raw materials, energy consumption, labor, maintenance, and other operational expenses. The interplay among these costs significantly impacts the overall financial outlook of producing activated carbon on an industrial scale.

Establishing a production plant to meet industrial demand involves substantial capital investments, which are proportional to the plant size and the scale of equipment required for different production stages, from raw material preparation to the final collection of activated carbon. For instance, producing around 450 tonnes of physically activated carbon from biomass annually necessitates an initial capital investment of approximately $2.12 million, coupled with annual operational costs of about $1.22 million. In contrast, using a chemical activation method, such as with H_3PO_4, for similar production volumes requires a total cost investment of approximately $4.25 million, with market prices ranging from $2.7 kg^{-1} to $2.9 kg^{-1}. These figures underscore the significant financial commitment required for large-scale production, emphasizing the importance of precise cost assessment frameworks.[328] The cost dynamics of producing activated carbon from biomass are complex and multifaceted, as shown by recent studies. Skoczko *et al.* estimated that physical activation processes generally cost between $1.5 and $2.0 per kilogram, with variations influenced by factors such as the scale of operation and the type of biomass feedstock used.[329] Chemical activation, particularly with H_3PO_4, incurs significantly higher costs, with Raja *et al.* reporting costs ranging from $3.0 to $3.5 per kilogram.[330] This difference underscores the importance of selecting the appropriate activation method, given that it plays a crucial role in the overall production costs.

The feedstock choice is another critical factor affecting the cost structure. Agricultural residues and forestry by-products are often more affordable options, but chemical activation

methods tend to drive up costs due to the expensive reagents required. For instance, Ng *et al.* found that producing activated carbon from pecan shells costs between $2.60 and $2.76 per kilogram, depending on the activation method.[331] Similarly, Lima *et al.* achieved a competitive cost of $1.38 per kilogram for activated carbon derived from organic waste using physical activation, assuming no raw material expenses.[332] In contrast, Stavropoulos *et al.* provided a comparative analysis of the production costs for activated carbon from various materials, revealing significantly higher costs for non-biomass sources such as used tires ($10.88 kg^{-1}), wood ($6.09 kg^{-1}), and lignite ($5.13 kg^{-1}).[333] Serafin *et al.* further illustrated the variability in production costs by estimating that producing 50 000 kg of activated carbon from fern leaves will cost approximately $2.72 per kilogram based on an annual production cost of $135.690.[334,335] Additionally, energy consumption remains a key cost component due to the energy-intensive nature of the carbonization process, with market prices for activated carbon ranging from $2.7 to $3.3 per kilogram, depending on its quality and application.[336]

According to the comparison of these market prices with the estimated production costs, biomass-derived activated carbons show a competitive edge, particularly when considering the environmental benefits of using renewable resources and minimizing waste. Looking at the commercial landscape, the global production of activated carbon reached USD 7.2 billion in 2023 and is projected to grow by 12.42%, reaching USD 14.50 billion by 2031. This surge in demand for activated carbon can be attributed to various factors, including population growth, extensive consumption across industries, and stringent environmental regulations governing air and water purification systems. Currently, the commercial-scale production of activated carbon predominantly relies on coconut shell and coal-based precursors. However, these raw materials alone may not be sufficient to meet the escalating demand across diverse sectors. Therefore, exploring alternative precursors, particularly biomass, can offer a cost-effective solution to meet the projected demands. Globally, approximately 105 billion metric tonnes of biomass, sourced from both land and oceans, is available annually.[337]

Refining the cost assessment frameworks involves a comprehensive analysis of the production costs, market trends, and operational efficiencies. As technological advancements and process optimizations continue to lower production costs, the economic feasibility of large-scale biomass-based activated carbon production is improving, making it an increasingly attractive option for applications such as CO_2 capture. Ongoing research and development will be crucial in further reducing costs and enhancing the viability of this sustainable production pathway.

6. Research gap

Despite the considerable volume of research conducted on the potential of waste products as precursors for AC, a significant research gap exists concerning the cost-effectiveness and scalability of the process. Many studies lack detailed procedures during the synthesis stage, resulting in inconsistent characteristics and adsorption properties of the manufactured product. To commercialize this type of activated carbon, there is a need for a thorough investigation into the continuity of waste supply for precursors, given that abundant resources are essential. Although the average biochar yield is around 20 wt% compared to the raw materials, detailed statistics on precursor availability are necessary to ensure long-term sustainability. Additionally, more research effort is required to explore regeneration methods for activated carbon, given that current technologies often necessitate high heat, which may not be feasible in the long run. Furthermore, there is a lack of studies on the synthesis of hybrid activated carbons incorporating heteroatoms and metal oxides. These hybrid materials have the potential to exhibit enhanced adsorption properties and stability. Moreover, there is a dearth of research focusing on the detailed understanding of CO_2 adsorption at the quantum level. These insights are crucial for predicting the behavior and performance of activated carbons under various operating conditions accurately. Comprehensive studies in this area will significantly contribute to advancing the understanding of the CO_2 capture mechanisms and optimizing the performance of activated carbon-based adsorbents for practical applications.

7. Summary and prospects for future investigations

This review article provided a comprehensive examination of the synthesis and modification techniques for biomass-derived carbon materials intended for CO_2 capture. It delved into the fundamental methodologies for converting biomass into carbon materials and the critical factors influencing their properties. The importance of selecting appropriate biomass sources and processing parameters to tailor the structure and chemical composition of carbon materials was emphasized. Various modification approaches, both physical and chemical, were outlined, highlighting their role in modifying pore structures or introducing functional groups or metals to enhance the CO_2 capture efficiency. However, despite the advancements, challenges and research opportunities persist, particularly in understanding the relationship between pore structure and factors such as biomass characteristics, pyrolytic conditions, and activation methods. Optimizing the pore structure of activated carbons, especially that activated with agents such as KOH and $ZnCl_2$, is crucial. Additionally, synthesizing hybrid activated carbons using multiple activating agents holds promise for improving the CO_2 capture performance through hybrid porous features.

Moreover, although renewable biomass serves as a cost-effective precursor for carbon capture materials, pristine carbon materials have inherent limitations in terms of pore structure and surface chemistry, constraining their adsorption capacities. Although various modification methods have emerged to address these limitations, some processes are complex and costly, hindering their scalability for industrial applications. Template carbonization offers a viable alternative,

providing control of the material pore diameter and structure without additional modification treatments. However, much of the research on CO_2 adsorption by carbon materials remains confined to laboratory settings, overlooking real-world challenges such as moisture and corrosion. Future research should focus on enhancing the mechanical properties of carbon materials to withstand harsh environments and assessing their suitability for industrial applications. Furthermore, it is necessary to explore competitive adsorption mechanisms among different gases and simulate the carbon material adsorption performance in complex gas compositions. Additionally, research efforts should extend beyond CO_2 capture to encompass CO_2 conversion, leveraging the catalytic properties of biomass-based carbon materials. The *in situ* conversion of adsorbed CO_2 presents an intriguing avenue for sustainable CO_2 recovery. However, challenges related to regenerating CO_2-saturated carbon materials and mitigating the effects of contaminants require further investigation. Understanding the impact of contaminants on carbon materials and developing strategies to enhance their resistance can enhance their longevity and performance in CO_2 capture applications.

Transitioning from laboratory-scale studies to pilot-scale investigations is crucial to evaluate material performance under realistic industrial conditions. Furthermore, gaining deeper insights into the underlying mechanisms for the formation of activated porous carbons from biomass and their regeneration processes can facilitate the design of advanced carbon materials for various applications. Addressing these research gaps and challenges is essential to harness the full potential of biomass-derived activated porous carbons for CO_2 capture, water decontamination, and energy storage, thereby advancing carbon capture technologies and promoting environmental sustainability.

Data availability

The data supporting the findings of this review can be obtained from the corresponding author upon request. Due to privacy concerns and other restrictions, the data are not publicly accessible.

Author contributions

Shreyase Kundu, Tasmina Khandaker & Md Al-Amin Mia Anik: writing – original draft, review and editing; Md. Kamrul Hasan, Palash Kumar Dhar, Sagar Kumar Dutta & M. Abdul Latif: proof reading and editing; Muhammad Sarwar Hossain: formal analysis, methodology, resources, validation, writing and editing, supervision and project administration.

Conflicts of interest

The authors declare that they have no known financial or personal conflicts of interest that could have influenced the work reported in this paper.

Acknowledgements

The authors express their deep gratitude to the Chemistry Discipline at Khulna University for offering a conducive research environment and necessary facilities. This project was funded by the faculty budget and research grant of Khulna University, Bangladesh.

References

1 B. Dziejarski, J. Serafin, K. Andersson and R. Krzyżyńska, *Mater. Today Sustain.*, 2023, 100483.
2 G. Polya, WMO Warning: 1.5 Degree C Warming Breach Very Soon & With Increasing Frequency. Act Now!, *Climate Change*, 2023.
3 T. Khandaker, M. S. Hossain, P. K. Dhar, M. S. Rahman, M. A. Hossain and M. B. Ahmed, *Processes*, 2020, **8**, 654.
4 V. Ntouros, I. Kousis, A. L. Pisello and M. N. Assimakopoulos, *Energies*, 2022, **15**, 1489.
5 J. Serafin, B. Dziejarski, X. Vendrell, K. Kiełbasa and B. Michalkiewicz, *Biomass Bioenergy*, 2023, **175**, 106880.
6 Y. Liu, Z. Weng, B. Han, Z. Guo, H. Tian, Y. Tang, Y. Cai and Z. Yang, *J. Cleaner Prod.*, 2023, 138495.
7 Y. Zhang, J. Jia, Y. Sun, B. Xu, Z. Jiang, X. Qu and C. Zhang, *Nanomaterials*, 2023, **13**, 2909.
8 G. Singh, A. M. Ruban, X. Geng and A. Vinu, *Chem. Eng. J.*, 2023, **451**, 139045.
9 K. H. H. Aziz, F. S. Mustafa, K. M. Omer, S. Hama, R. F. Hamarawf and K. O. Rahman, *RSC Adv.*, 2023, **13**, 17595–17610.
10 J. O. Ighalo, J. Conradie, C. R. Ohoro, J. F. Amaku, K. O. Oyedotun, N. W. Maxakato, K. G. Akpomie, E. S. Okeke, C. Olisah and A. Malloum, *Ind. Crops Prod.*, 2023, **204**, 117300.
11 G. Singh, K. S. Lakhi, S. Sil, S. V. Bhosale, I. Kim, K. Albahily and A. Vinu, *Carbon*, 2019, **148**, 164–186.
12 S. Ha, S. G. Jeong, S. Myeong and Y.-S. Lee, *J. CO_2 Util.*, 2023, **76**, 102589.
13 K. Malini, D. Selvakumar and N. Kumar, *J. CO_2 Util.*, 2023, **67**, 102318.
14 C. Deng, L. Xu, K. Hu, X. Chen, R. Gao, L. Zhang, L. Wang and C. Zhang, *Atmosphere*, 2023, **14**, 1510.
15 Z. Nezafat, M. Nasrollahzadeh, S. Javanshir, T. Baran and Y. Dong, *Green Chem.*, 2023, **25**, 9603–9643.
16 J. Gopalan, A. Buthiyappan and A. A. A. Raman, *J. Ind. Eng. Chem.*, 2022, **113**, 72–95.
17 W. A. Rasaq, C. O. R. Okpala, C. A. Igwegbe and A. Białowiec, *Materials*, 2024, **17**, 725.
18 A. Devi, S. Bajar, H. Kour, R. Kothari, D. Pant and A. Singh, *BioEnergy Res.*, 2022, **15**, 1820–1841.
19 K. S. Khoo, I. Ahmad, K. W. Chew, K. Iwamoto, A. Bhatnagar and P. L. Show, *Prog. Energy Combust. Sci.*, 2023, **96**, 101071.
20 T. Sharma, I. G. Hakeem, A. B. Gupta, J. Joshi, K. Shah, A. K. Vuppaladadiyam and A. Sharma, *J. Energy Inst.*, 2024, 101559.
21 A. K. Vuppaladadiyam, S. S. V. Vuppaladadiyam, A. Awasthi, A. Sahoo, S. Rehman, K. K. Pant, S. Murugavelh, Q. Huang,

E. Anthony and P. Fennel, *Bioresour. Technol.*, 2022, **364**, 128087.
22 X. Peng, Y. Jiang, Z. Chen, A. I. Osman, M. Farghali, D. W. Rooney and P.-S. Yap, *Environ. Chem. Lett.*, 2023, **21**, 765–801.
23 P. Manasa, S. Sambasivam and F. Ran, *J. Energy Storage*, 2022, **54**, 105290.
24 K. Yogalakshmi, P. Sivashanmugam, S. Kavitha, Y. Kannah, S. Varjani, S. AdishKumar and G. Kumar, *Chemosphere*, 2022, **286**, 131824.
25 M. Xu, Z. Shi, X. Zhu, Y. Lai, A. Xia, Y. Huang, X. Jiang, J. He, M. Zhou and X. Zhu, *Int. J. Hydrogen Energy*, 2024, **52**, 83–96.
26 R. D. L. C. Iturbides, L. Ubiera, U. J. Haza and I. Polaert, *React. Chem. Eng.*, 2024, **9**, 1235–1250.
27 N. A. Binti Mohd, Conventional and microwave pyrolysis of empty fruit bunch and rice husk pellets, PhD thesis, University of Sheffield, 2017.
28 W. Song, Y. Zhang, C. H. Tran, H. K. Choi, D.-G. Yu and I. Kim, *Prog. Polym. Sci.*, 2023, **142**, 101691.
29 N. Vasiraja, R. S. S. Prabhahar and A. Joshua, *J. Cleaner Prod.*, 2023, **397**, 136579.
30 A. Ali and R. Idris, *Adv. Mater. Lett.*, 2017, **8**, 70–76.
31 A. A. Adeleke, P. P. Ikubanni, S. S. Emmanuel, M. O. Fajobi, P. Nwachukwu, A. A. Adesibikan, J. K. Odusote, E. O. Adeyemi, O. M. Abioye and J. A. Okolie, *Renewable Sustainable Energy Rev.*, 2024, **199**, 114502.
32 M. N. Romanias, M. M. Coggon, F. Al Ali, J. B. Burkholder, P. Dagaut, Z. Decker, C. Warneke, C. E. Stockwell, J. M. Roberts and A. Tomas, *ACS Earth Space Chem.*, 2024, **8**, 857–899.
33 S. P. S. Yadav, S. Bhandari, D. Bhatta, A. Poudel, S. Bhattarai, P. Yadav, N. Ghimire, P. Paudel, P. Paudel and J. Shrestha, *J. Agric. Food Res.*, 2023, **11**, 100498.
34 M. Fan, C. Li, Y. Shao, S. Zhang, M. Gholizadeh and X. Hu, *Sci. Total Environ.*, 2022, **825**, 153959.
35 N. I. W. Azelee, H. I. Mahdi, Y.-S. Cheng, N. Nordin, R. M. Illias, R. A. Rahman, S. M. Shaarani, P. Bhatt, S. Yadav and S. W. Chang, *Fuel*, 2023, **339**, 126982.
36 J. Liu, X. Chen, W. Chen, M. Xia, Y. Chen, H. Chen, K. Zeng and H. Yang, *Proc. Combust. Inst.*, 2023, **39**, 3157–3181.
37 A. Shafizadeh, H. Rastegari, H. Shahbeik, H. Mobli, J. Pan, W. Peng, G. Li, M. Tabatabaei and M. Aghbashlo, *J. Cleaner Prod.*, 2023, **400**, 136705.
38 W.-l. Xie, B. Hu, Y. Liu, H. Fu, J. Liu, B. Zhang and Q. Lu, *Proc. Combust. Inst.*, 2023, **39**, 3303–3311.
39 Y. Fan, Z. Zhang, Z. Wang, H. Yu, X. Kong, P. Li, M. Li, R. Xiao and C. Liu, *Bioresour. Technol.*, 2022, **360**, 127648.
40 A. L. Pauline and K. Joseph, *J. Hazard., Toxic Radioact. Waste*, 2024, **28**, 04024025.
41 R. H. Teoh, A. S. Mahajan, S. R. Moharir, N. A. Manaf, S. Shi and S. Thangalazhy-Gopakumar, *Energy Nexus*, 2024, 100301.
42 X. Zhuang, J. Liu, Q. Zhang, C. Wang, H. Zhan and L. Ma, *Renewable Sustainable Energy Rev.*, 2022, **154**, 111877.
43 T.-D. Hoang, L. Yan and T. M. Le, *Sustainability*, 2024, **16**, 5495.
44 C. Goel, S. Mohan, P. Dinesha and M. A. Rosen, *Chem. Pap.*, 2024, **78**, 3845–3856.
45 M. Cavali, N. L. Junior, J. D. de Sena, A. L. Woiciechowski, C. R. Soccol, P. Belli Filho, R. Bayard, H. Benbelkacem and A. B. de Castilhos Junior, *Sci. Total Environ.*, 2023, **857**, 159627.
46 T. Bi, H. Chen, J. Li, X. Zhang and Q. Lin, *Electrochim. Acta*, 2022, **433**, 141266.
47 P. Baghel, A. K. Sakhiya and P. Kaushal, *Renewable energy*, 2022, **185**, 538–551.
48 J. J. Alvear-Daza, A. Sosa, D. M. Ruiz, G. A. Pasquale, J. A. Rengifo-Herrera, G. P. Romanelli and L. R. Pizzio, *Catalysts*, 2024, **14**, 522.
49 Y. Liu, J. Pan, J. Wang, X. Yang, W. Zhang, K. H. D. Tang, H. Wang, X. Zhang, R. Gao and G. Yang, *Environ. Sci. Pollut. Res.*, 2024, 1–12.
50 J. O. Ighalo and A. G. Adeniyi, *Environ. Processes*, 2021, **8**, 267–285.
51 M. Pahnila, A. Koskela, P. Sulasalmi and T. Fabritius, *Energies*, 2023, **16**, 6936.
52 N. A. Zubbri, A. R. Mohamed, P. Lahijani and M. Mohammadi, *J. Environ. Chem. Eng.*, 2021, **9**, 105074.
53 A. Soomro, S. Chen, M. H. Mallah, I. A. Samo, A. A. Siyal, B. Ali, K. A. Samo, S. Ma, K. C. Mukwana and W. Xiang, *BioEnergy Res.*, 2024, 1–12.
54 D. Aboelela, H. Saleh, A. M. Attia, Y. Elhenawy, T. Majozi and M. Bassyouni, *Sustainability*, 2023, **15**, 11238.
55 W. Chen, X. Tao, X. Shi, W. Guo, Y. Wang, B. Liu and H. Yang, *npj Mater. Sustain.*, 2024, **2**, 25.
56 A. A. Ahmad, A. Alwahbi, L. A. Al Khatib and H. Dammag, in *From Biomass to Biobased Products*, IntechOpen, 2024.
57 S. Pathak, A. K. Sakhiya and P. Kaushal, in *Thermochemical and Catalytic Conversion Technologies for Future Biorefineries*, Springer, 2022, vol. 1, pp. 205–239.
58 R. Blanchard and T. H. Mekonnen, *RSC appl. polym.*, 2024, **2**, 557–582.
59 Q. Ma, W. Chen, Z. Jin, L. Chen, Q. Zhou and X. Jiang, *Fuel*, 2021, **289**, 119932.
60 R. Muzyka, E. Misztal, J. Hrabak, S. W. Banks and M. Sajdak, *Energy*, 2023, **263**, 126128.
61 Q. Wu, S. Yu, N. Hao, T. Wells Jr, X. Meng, M. Li, Y. Pu, S. Liu and A. J. Ragauskas, *Bioresour. Technol.*, 2017, **244**, 78–83.
62 M. J. Ahmed and B. H. Hameed, *Environ. Res.*, 2024, 118203.
63 A. N. Amenaghawon, C. L. Anyalewechi, C. O. Okieimen and H. S. Kusuma, *Environ. Dev. Sustain.*, 2021, 1–55.
64 Z.-H. Chen, X.-L. Du, J.-B. He, F. Li, Y. Wang, Y.-L. Li, B. Li and S. Xin, *ACS Appl. Mater. Interfaces*, 2017, **9**, 33855–33862.
65 X. Chen, X. Ma, X. Peng, Y. Lin and Z. Yao, *Bioresour. Technol.*, 2018, **249**, 900–907.
66 H. Su, X. Zhou, R. Zheng, Z. Zhou, Y. Zhang, G. Zhu, C. Yu, D. Hantoko and M. Yan, *Sci. Total Environ.*, 2021, **754**, 142192.
67 F. Liu, R. Yu, X. Ji and M. Guo, *Bioresour. Technol.*, 2018, **263**, 508–516.

68 W. Sangchoom and R. Mokaya, *ACS Sustain. Chem. Eng.*, 2015, **3**, 1658–1667.
69 L. Rao, R. Ma, S. Liu, L. Wang, Z. Wu, J. Yang and X. Hu, *Chem. Eng. J.*, 2019, **362**, 794–801.
70 N. U. Saqib, S. Baroutian and A. K. Sarmah, *Bioresour. Technol.*, 2018, **266**, 357–363.
71 L. Wang, G. Yin, Y. Chang and S. Qiao, *Waste Manage.*, 2024, **177**, 182–195.
72 Q. Wang, S. Wu, D. Cui, H. Zhou, D. Wu, S. Pan, F. Xu and Z. Wang, *Sci. Total Environ.*, 2022, **850**, 158034.
73 S. Ullah, S. S. A. Shah, M. Altaf, I. Hossain, M. E. El Sayed, M. Kallel, Z. M. El-Bahy, A. ur Rehman, T. Najam and M. A. Nazir, *J. Anal. Appl. Pyrolysis*, 2024, 106480.
74 N. Rathnayake, S. Patel, I. G. Hakeem, J. Pazferreiro, A. Sharma, R. Gupta, C. Rees, D. Bergmann, J. Blackbeard and A. Surapaneni, *Process Saf. Environ. Prot.*, 2023, **173**, 75–87.
75 W.-H. Chen, B.-J. Lin, Y.-Y. Lin, Y.-S. Chu, A. T. Ubando, P. L. Show, H. C. Ong, J.-S. Chang, S.-H. Ho and A. B. Culaba, *Prog. Energy Combust. Sci.*, 2021, **82**, 100887.
76 K. Van der Cruijsen, M. Al Hassan, G. van Erven, O. Dolstra and L. M. Trindade, *Molecules*, 2021, **26**, 254.
77 H. Sun, D. Feng, S. Sun, Y. Zhao, L. Zhang, G. Chang, Q. Guo, J. Wu and Y. Qin, *J. Anal. Appl. Pyrolysis*, 2021, **156**, 105128.
78 F. Narciso-Romero and F. Rodriguez-Reinoso, *J. Mater. Sci.*, 1996, **31**, 779–784.
79 Y. X. Seow, Y. H. Tan, N. Mubarak, J. Kansedo, M. Khalid, M. L. Ibrahim and M. Ghasemi, *J. Environ. Chem. Eng.*, 2022, **10**, 107017.
80 M. Rasul, M. Hazrat, M. Sattar, M. Jahirul and M. Shearer, *Energy Convers. Manage.*, 2022, **272**, 116326.
81 P. Lahijani, M. Mohammadi and A. R. Mohamed, *J. CO_2 Util.*, 2018, **26**, 281–293.
82 M. Ahmed and B. Hameed, *J. Cleaner Prod.*, 2020, **265**, 121762.
83 M. Siddique, S. Akram, Z. Liaqat and M. Mushtaq, *Sewage and Biomass from Wastewater to Energy*, 2024, pp. 1–41.
84 D. Lachos-Perez, P. C. Torres-Mayanga, E. R. Abaide, G. L. Zabot and F. De Castilhos, *Bioresour. Technol.*, 2022, **343**, 126084.
85 X. Li, K. Cen, L. Wang, D. Jia, X. Zhu and D. Chen, *Ind. Crops Prod.*, 2024, **219**, 119071.
86 Y. Li, H. Yu, L. Liu and H. Yu, *J. Hazard. Mater.*, 2021, **420**, 126655.
87 C. Li, J.-i. Hayashi, Y. Sun, L. Zhang, S. Zhang, S. Wang and X. Hu, *J. Anal. Appl. Pyrolysis*, 2021, **155**, 105031.
88 Q. Hu, W. Cheng, Q. Mao, J. Hu, H. Yang and H. Chen, *Fuel*, 2022, **314**, 122789.
89 K. Rasouli, J. Rasouli, M. S. Mohtaram, S. Sabbaghi, H. Kamyab, H. Moradi and S. Chelliapan, *J. Cleaner Prod.*, 2023, 138181.
90 M. Gayathiri, T. Pulingam, K. Lee and K. Sudesh, *Chemosphere*, 2022, **294**, 133764.
91 P. B. n. Ramos, A. Mamaní, M. Erans, F. Jerez, M. F. Ponce, M. F. Sardella, A. Arencibia, M. A. Bavio, E. S. Sanz-Pérez and R. l. Sanz, *Energy Fuels*, 2024, **38**, 6102–6115.
92 M. Mujtaba, L. F. Fraceto, M. Fazeli, S. Mukherjee, S. M. Savassa, G. A. de Medeiros, A. d. E. Santo Pereira, S. D. Mancini, J. Lipponen and F. Vilaplana, *J. Cleaner Prod.*, 2023, **402**, 136815.
93 S. Purayil, M. O. Hamdan, S. Al-Omari, M. Selim and E. Elnajjar, *Energy Rep.*, 2023, **9**, 4547–4573.
94 Q. Pu, J. Zou, J. Wang, S. Lu, P. Ning, L. Huang and Q. Wang, *J. Alloys Compd.*, 2021, **887**, 161406.
95 Y. Li, L. Lu, S. Lyu, H. Xu, X. Ren and Y. A. Levendis, *J. Anal. Appl. Pyrolysis*, 2021, **156**, 105137.
96 J. Serafin and B. Dziejarski, *Environ. Sci. Pollut. Res.*, 2024, **31**, 40008–40062.
97 J. Fu, J. Zhang, C. Jin, Z. Wang, T. Wang, X. Cheng and C. Ma, *Bioresour. Technol.*, 2020, **310**, 123413.
98 Y. Xie, L. Wang, H. Li, L. J. Westholm, L. Carvalho, E. Thorin, Z. Yu, X. Yu and Ø. Skreiberg, *J. Anal. Appl. Pyrolysis*, 2022, **161**, 105405.
99 A. Rehman, G. Nazir, K. Y. Rhee and S.-J. Park, *Chem. Eng. J.*, 2021, **420**, 130421.
100 W. Suliman, J. B. Harsh, N. I. Abu-Lail, A.-M. Fortuna, I. Dallmeyer and M. Garcia-Perez, *Biomass Bioenergy*, 2016, **85**, 1–11.
101 L. Chen, W. Fang, J. Liang, M. Nabi, Y. Cai, Q. Wang, P. Zhang and G. Zhang, *Resour., Conserv. Recycl.*, 2023, **188**, 106720.
102 B. Petrovic, M. Gorbounov and S. M. Soltani, *Microporous Mesoporous Mater.*, 2021, **312**, 110751.
103 D. Kim and S. Hadigheh, *Renewable Energy*, 2024, **224**, 120106.
104 Q. Qin, F. Zhong, T. Song, Z. Yang, P. Zhang, H. Cao, W. Niu and Z. Yao, *Chem. Eng. J.*, 2023, **477**, 146763.
105 J. H. Lee, S. J. Sim, J. H. Kang and S. S. Choi, *Chem. Phys. Lett.*, 2021, **780**, 138962.
106 O. Tomin, R. Vahala and M. R. Yazdani, *Heliyon*, 2024, **10**, e24722.
107 W. K. Tong, C. Dai, C. Jia, J. Hu, M.-t. Gao, J. Li, J. B. Zhang, H. Tang, Y. Liang and W. Teng, *Chem. Eng. J.*, 2024, **481**, 148422.
108 J. Ma, L. Zheng and F. Yu, *Desalination*, 2024, 117597.
109 F. Yang, Z. He, F. Yu, S. Zhou and X. Zhu, *Sci. Total Environ.*, 2023, **867**, 161425.
110 L. Cao, X. Zhang, Y. Xu, W. Xiang, R. Wang, F. Ding, P. Hong and B. Gao, *Sep. Purif. Technol.*, 2022, **287**, 120592.
111 M. Lillo-Ródenas, D. Cazorla-Amorós and A. Linares-Solano, *Carbon*, 2003, **41**, 267–275.
112 A. El Hadrami, S. Ojala and R. Brahmi, *Surf. Interfaces*, 2022, **30**, 101849.
113 J. Shin, J. Kwak, Y.-G. Lee, S. Kim, M. Choi, S. Bae, S.-H. Lee, Y. Park and K. Chon, *Environ. Pollut.*, 2021, **270**, 116244.
114 F. Ma, H. Zhao, X. Zheng, B. Zhao, J. Diao and Y. Jiang, *J. Environ. Chem. Eng.*, 2023, **11**, 109747.
115 J. Li, L. Zheng, S.-L. Wang, Z. Wu, W. Wu, N. K. Niazi, S. M. Shaheen, J. Rinklebe, N. Bolan and Y. S. Ok, *Sci. Total Environ.*, 2019, **672**, 572–582.
116 B. Liu, R. Shi, X. Ma, R. Chen, K. Zhou, X. Xu, P. Sheng, Z. Zeng and L. Li, *Carbon*, 2021, **181**, 270–279.

117 M. Olivares-Marín, C. Fernández-González, A. Macías-García and V. Gómez-Serrano, *Carbon*, 2006, **44**, 2347–2350.
118 K. Chen, D. Ma, H. Yu, S. Zhang, B. C. Seyler, Z. Chai and S. Peng, *Chemosphere*, 2022, **291**, 132721.
119 C. Bonga, L. Y. Lima, C. T. Leea, P. Y. Ongb, J. Jaromír, C. L. Klemešc and Y. Gaod, *Chem. Eng.*, 2020, **81**, 427–432.
120 X. Ma, C. Su, B. Liu, Q. Wu, K. Zhou, Z. Zeng and L. Li, *Sep. Purif. Technol.*, 2021, **259**, 118065.
121 M. Olivares-Marín, C. Fernández-González, A. Macías-García and V. Gómez-Serrano, *J. Anal. Appl. Pyrolysis*, 2012, **94**, 131–137.
122 D. Li, W. Li, J. Shi and F. Xin, *RSC Adv.*, 2016, **6**, 50138–50143.
123 C. Cheng, H. Liu, P. Dai, X. Shen, J. Zhang, T. Zhao and Z. Zhu, *J. Taiwan Inst. Chem. Eng.*, 2016, **67**, 532–537.
124 E. Wolak and A. Orzechowska-Zięba, *Adsorption*, 2024, **30**, 121–128.
125 J. M. Illingworth, B. Rand and P. T. Williams, *Fuel Process. Technol.*, 2022, **235**, 107348.
126 Z. Liu, W. Fan and Y. Xu, *Environ. Sci. Pollut. Res.*, 2024, 1–12.
127 A. Komaei, M. Yadollah-Roudbari and S. M. Fattahi, *Cleaner Mater.*, 2024, 100264.
128 J. O. Velasco, Biomass to chemicals and fuels using advanced thermochemical concepts, PhD thesis, University of Groningen, 2024.
129 W. Shi, J. Yu, H. Liu, D. Gao, A. Yuan and B. Chang, *ACS Appl. Nano Mater.*, 2023, **6**, 7887–7900.
130 M. S. Khosrowshahi, H. Mashhadimoslem, H. Shayesteh, G. Singh, E. Khakpour, X. Guan, M. Rahimi, F. Maleki, P. Kumar and A. Vinu, *Advanced Science*, 2023, **10**, 2304289.
131 A. M. Elewa, A. A. Amer, M. F. Attallah, H. A. Gad, Z. A. M. Al-Ahmed and I. A. Ahmed, *Materials*, 2023, **16**, 1251.
132 D. Hong, J. Zhou, C. Hu, Q. Zhou, J. Mao and Q. Qin, *Fuel*, 2019, **235**, 326–335.
133 M. Kwiatkowski, C. Belver and J. Bedia, *Sci. Rep.*, 2024, **14**, 2266.
134 N. M. Amer, P. Lahijani, M. Mohammadi and A. R. Mohamed, *Biomass Convers. Biorefin.*, 2024, **14**, 7401–7448.
135 X. Duan, G. Song, G. Lu, Y. Wang, J. Sun, A. Chen and X. Xie, *Mater. Today Sustain.*, 2023, **23**, 100453.
136 A. U. Khan, O. Samuel, M. H. D. Othman, M. Younas, R. Kamaludin, M. H. Puteh, T. A. Kurniawan, K. Y. Wong, F. Kadirkhan and N. Yoshida, *Sep. Purif. Technol.*, 2024, **347**, 127511.
137 Y. Guo, G. Wang, J. Yu, P. Huang, J. Sun, R. Wang, T. Wang and C. Zhao, *Sep. Purif. Technol.*, 2023, **305**, 122455.
138 S. Park, J. Kim and K. Kwon, *Chem. Eng. J.*, 2022, **446**, 137116.
139 X. Ma, X. Li, H. Cui, W. Zhang, Z. Cheng and Z. Zhou, *AIChE J.*, 2023, **69**, e17520.
140 L. Shao, L. Wang, J. Wang, Z. Liu, Z. Wu, P. Zhan, L. Zhang, X. Ma and J. Huang, *Sep. Purif. Technol.*, 2023, **313**, 123440.
141 W. Tian, H. Zhang, X. Duan, H. Sun, G. Shao and S. Wang, *Adv. Funct. Mater.*, 2020, **30**, 1909265.
142 X. Guo, G. Zhang, C. Wu, J. Liu, G. Li, Y. Zhao, Y. Wang and Y. Xu, *J. Environ. Chem. Eng.*, 2021, **9**, 105165.
143 D. Zhang, Q. He, X. Hu, K. Zhang, C. Chen and Y. Xue, *Colloids Surf., A*, 2021, **615**, 126254.
144 Y. Qiao and C. Wu, *Carbon Capture Sci. Technol.*, 2022, **2**, 100018.
145 A. D. Kute, R. P. Gaikwad, I. R. Warkad and M. B. Gawande, *Green Chem.*, 2022, **24**, 3502–3573.
146 P. Pareek, H. Dave and L. Ledwani, *Mater. Today: Proc.*, 2021, **43**, 3277–3285.
147 W. Cao, H. Xu, X. Zhang, W. Xiang, G. Qi, L. Wan and B. Gao, *Chem. Eng. J.*, 2023, **471**, 144523.
148 A. A. Khan, Y. S. Ling and Z. Z. Chowdhury, *Eur. Phys. J. Plus*, 2024, **139**, 1–11.
149 A. Nurdin, I. Iriani, H. Harahap and A. Fahmi, *Indones. J. Chem. Res.*, 2022, **10**, 8–13.
150 A. El Nemr, R. M. Aboughaly, A. El Sikaily, M. S. Masoud, M. S. Ramadan and S. Ragab, *Carbon Lett.*, 2022, **32**, 229–249.
151 M. N. Islam, J. Sarker, A. Khatton, S. M. Hossain, H. A. Sikder, R. Ahmed and A. S. Chowdhury, *Sch. Int. J. Chem. Mater. Sci.*, 2022, **5**, 33–39.
152 R. Dewi, A. Azhari and I. Nofriadi, *J. Teknol. Kim. Unimal*, 2021, **9**, 12–22.
153 N. E. Williams, O. A. Oba and N. P. Aydinlik, *ChemBioEng Rev.*, 2022, **9**, 164–189.
154 S. Li, K. Han, J. Li, M. Li and C. Lu, *Microporous Mesoporous Mater.*, 2017, **243**, 291–300.
155 Z. Gu, X. Wang, P. Huang, Y. Huang, X. He, X. Wei, J. Yue, J. Jiang and C. Zhao, *Process Saf. Environ. Prot.*, 2022, **160**, 573–583.
156 C. Ma, T. Lu, J. Shao, J. Huang, X. Hu and L. Wang, *Sep. Purif. Technol.*, 2022, **281**, 119899.
157 Y. Cao, L. Yang, F. Liu and Q. Yu, *Biomass Bioenergy*, 2024, **182**, 107074.
158 Y. Chen, C. Zhou, X. Xing, L. Chen, B. Yao, L. Chao, Y. Zhang, J. Wang, J. Dong and C. Liu, *Chem. Eng. J.*, 2024, **495**, 153579.
159 S. Sangon, K. Kotebantao, T. Suyala, Y. Ngernyen, A. J. Hunt and N. Supanchaiyamat, *Environ. Sci.: Water Res. Technol.*, 2024, **10**, 1389–1405.
160 F. Njeh, M. Hamza, I. Bouaziz, R. Abdelhedi and M. Abdelmouleh, *Korean J. Chem. Eng.*, 2022, 1–15.
161 S. Wei, Q. Qin and Z. Liu, *J. Anal. Appl. Pyrolysis*, 2024, **179**, 106500.
162 B. Huang, W. Li, Z. Shi, L. Yang, Z. Wen, G. Zi and L. Luo, *Clean: Soil, Air, Water*, 2024, **52**, 2300148.
163 W. Li and J. Shi, *Front. Bioeng. Biotechnol.*, 2023, **11**, 1121027.
164 P. M. Yeletsky, M. V. Lebedeva and V. A. Yakovlev, *J. Energy Storage*, 2022, **50**, 104225.
165 P. Ozpinar, C. Dogan, H. Demiral, U. Morali, S. Erol, C. Samdan, D. Yildiz and I. Demiral, *Renewable Energy*, 2022, **189**, 535–548.
166 B. S. Rathi and R. V, *Environ. Qual. Manag.*, 2024, **33**, 907–928.

167 A. A. Chan, A. A. A. Raman, W. L. Chong and A. Buthiyappan, *J. Cleaner Prod.*, 2024, **437**, 140655.
168 Z. Baassou, F. Benmahdi, A. Reffas and A. Benhaya, *Biomass Convers. Biorefin.*, 2024, 1–14.
169 J. Liang, C. Li, S. Zhang, S. Wang and X. Hu, *Ind. Crops Prod.*, 2024, **221**, 119387.
170 A. Martusevich, A. Surovegina, A. Popovicheva, N. Didenko, M. Artamonov and V. Nazarov, *BioMed Res. Int.*, 2022, **2022**, 5857979.
171 J. Serafin, K. Kiełbasa and B. Michalkiewicz, *Chem. Eng. J.*, 2022, **429**, 131751.
172 X. Wang, H. Cheng, G. Ye, J. Fan, F. Yao, Y. Wang, Y. Jiao, W. Zhu, H. Huang and D. Ye, *Chemosphere*, 2022, **287**, 131995.
173 N. Karić, A. S. Maia, A. Teodorović, N. Atanasova, G. Langergraber, G. Crini, A. R. Ribeiro and M. Đolić, *Chem. Eng. J. Adv.*, 2022, **9**, 100239.
174 S. Das, *Microbial Biodegradation and Bioremediation*, Elsevier, 2014.
175 İ. Kılınçer, L. Khanyile, K. Gürcan, Ö. Şimşek, A. Uzun and A. Nikbakht-Dehkordi, *Genet. Resour. Crop Evol.*, 2024, **71**, 2229–2246.
176 P. Chaudhary, S. Bansal, B. B. Sharma, S. Saini and A. Joshi, *J. Energy Storage*, 2024, **78**, 109996.
177 H. Ma, W. Xu, P. Wang, Y. Ding and S. Zhou, *Environ. Geochem. Health*, 2024, **46**, 1–20.
178 S. Shao, Y. Wang, L. Ma, Z. Huang and X. Li, *Fuel*, 2024, **355**, 129287.
179 D. Pereira, M. Ilkaeva, F. Vicente, R. Vieira, M. Sardo, M. A. Lourenço, A. Silvestre, I. Marin-Montesinos and L. Mafra, *ACS Omega*, 2024, **9**, 17956–17965.
180 S. Amreen, S. K. Dash, B. Naik, A. K. Dash, A. K. Verma and A. Pradhan, *Environ. Qual. Manag.*, 2024, **34**, e22213.
181 R. Ganjoo, S. Sharma, A. Kumar and M. Daouda, *Royal Society of Chemistry Books*, 2023, p. 450.
182 M. An, T. Guo and Q. Guo, *Carbon Resour. Convers.*, 2024, **7**, 100205.
183 S.-X. Zhao, N. Ta and X.-D. Wang, *Energies*, 2017, **10**, 1293.
184 Y. Liu, W. Tan, S. Liang, X. Bi, R. Sun and X. Pan, *Biomass Convers. Biorefin.*, 2024, **14**, 781–793.
185 U. Onochie, A. Obanor, S. Aliu and O. Igbodaro, *Niger. J. Technol.*, 2017, **36**, 987–990.
186 P. Pramanik, H. Patel, S. Charola, S. Neogi and S. Maiti, *J. CO_2 Util.*, 2021, **45**, 101450.
187 Z. Wu, Y. Liu, Y. Xu, W. Zhan, Y. Liu, D. Zhang and Y. Xu, *Biomass Convers. Biorefin.*, 2024, 1–13.
188 H. Li, M. Tang, X. Huang, L. Wang, Q. Liu and S. Lu, *Chem. Eng. J.*, 2023, **466**, 143095.
189 J. Kawalerczyk, J. Walkiewicz, J. Sedliačik, D. Dukarska, M. Woźniak and R. Mirski, *Polymers*, 2024, **16**, 1350.
190 Y.-j. Wang, Y. Yu, H.-j. Huang, C.-l. Yu, H.-s. Fang, C.-h. Zhou, X. Yin, W.-h. Chen and X.-c. Guo, *Sci. Total Environ.*, 2022, **803**, 149874.
191 J. Serafin, B. Dziejarski and J. Sreńscek-Nazzal, *Sustainable Mater. Technol.*, 2023, **38**, e00717.
192 J. de Siqueira Castro, P. P. Assemany, A. C. de Oliveira Carneiro, J. Ferreira, M. M. de Jesus Júnior, F. de Ávila Rodrigues and M. L. Calijuri, *Sci. Total Environ.*, 2021, **768**, 144480.
193 M. Farnane, A. Machrouhi, M. Abdennouri, H. Tounsadi, Z. Rais, S. Qourzal and N. Barka, *Biointerface Res. Appl. Chem.*, 2021, **12**, 5941–5952.
194 A. B. Fadhil and B. A. Kareem, *J. Anal. Appl. Pyrolysis*, 2021, **158**, 105249.
195 J. M. González-Domínguez, C. Fernández-González, M. Alexandre-Franco and V. Gómez-Serrano, *Processes*, 2024, **12**, 149.
196 P. Riquelme-García, J. Chaparro-Garnica, M. Navlani-García and D. Cazorla-Amorós, *ChemCatChem*, 2024, e202400160.
197 X. Li, H. Tian, S. Yan, H. Shi, J. Wu, Y. Sun, Y. Xing, H. Bai and H. Zhang, *Int. J. Hydrogen Energy*, 2024, **50**, 324–336.
198 K. Suwannahong, S. Wongcharee, T. Kreetachart, C. Sirilamduan, J. Rioyo and A. Wongphat, *Appl. Sci.*, 2021, **11**, 7432.
199 M. Hamid, S. A. Amaturrahim, I. B. Dalimunthe and A. Daulay, *Mater. Sci. Energy Technol.*, 2023, **6**, 429–436.
200 S. He, G. Chen, H. Xiao, G. Shi, C. Ruan, Y. Ma, H. Dai, B. Yuan, X. Chen and X. Yang, *J. Colloid Interface Sci.*, 2021, **582**, 90–101.
201 S. Omokafe, A. Adeniyi, E. Igbafen, S. Oke and P. Olubambi, *Int. J. Electrochem. Sci.*, 2020, **15**, 10854–10865.
202 J. Liu, X. Yang, H. Liu, X. Jia and Y. Bao, *Chemosphere*, 2021, **282**, 131116.
203 L. Manjakkal, A. Jain, S. Nandy, S. Goswami, J. T. Carvalho, L. Pereira, C. H. See, S. C. Pillai and R. A. Hogg, *Chem. Eng. J.*, 2023, **465**, 142845.
204 M. V. Penzik, A. N. Kozlov, S. Zhang, V. V. Badenko, I. K. Sosnovsky and V. A. Shamansky, *Thermochim. Acta*, 2022, **711**, 179209.
205 S. Leng, W. Li, C. Han, L. Chen, J. Chen, L. Fan, Q. Lu, J. Li, L. Leng and W. Zhou, *Bioresour. Technol.*, 2020, **298**, 122502.
206 H. Wang, H. Teng, X. Wang, J. Xu and L. Sheng, *J. Environ. Manage.*, 2022, **310**, 114758.
207 M. A. A. Mariah, K. Rovina, J. M. Vonnie and K. H. Erna, *S. Afr. J. Chem. Eng.*, 2023, **44**, 113–122.
208 E. Huo, D. Duan, H. Lei, C. Liu, Y. Zhang, J. Wu, Y. Zhao, Z. Huang, M. Qian and Q. Zhang, *Energy*, 2020, **199**, 117459.
209 C. H. Pimentel, M. S. Freire, D. Gómez-Díaz and J. González-Álvarez, *Appl. Sci.*, 2024, **14**, 841.
210 J. Weng, M.-M. Wei, S.-J. Wu, Y.-Q. Liu, S.-R. Li, Y.-Y. Ye, M. Wang and D. Wang, *BioResources*, 2019, **14**, 3899–3913.
211 V. T. W. Thuppahige, L. Moghaddam, Z. G. Welsh, T. Wang, H.-W. Xiao and A. Karim, *LWT-Food Sci. Technol.*, 2023, **182**, 114787.
212 A. Herrera-Barros, N. Bitar-Castro, Á. Villabona-Ortíz, C. Tejada-Tovar and Á. D. González-Delgado, *Sustainable Chem. Pharm.*, 2020, **17**, 100299.
213 G. Cruz, A. d. L. P. Rodrigues, D. F. da Silva and W. C. Gomes, *J. Therm. Anal. Calorim.*, 2021, **143**, 3611–3622.
214 M. L. Yeboah, *Int. J. Environ. Anal. Chem.*, 2023, **103**, 4411–4429.

215 R. I. Ismail, K. C. Yee, A. R. Shaari, A. R. Mohamed, M. H. B. A. Halim, A. A. A. Rahman, L. Y. Leng, N. L. Makhtar and N. A. Razak, *AIP Conf. Proc.*, 2023, **2703**, 130001.
216 I. K. Tetteh, I. Issahaku and A. Y. Tetteh, *Carbon Trends*, 2024, 100328.
217 W. Jia, S. Li, J. Wang, J. T. Lee, C. S. K. Lin, O. Mašek, H. Zhang and X. Yuan, *Green Chem.*, 2024, **26**, 1790–1805.
218 P. Treeweranuwat, P. Boonyoung, M. Chareonpanich and K. Nueangnoraj, *ACS Omega*, 2020, **5**, 1911–1918.
219 A. Hidayu and N. Muda, *Procedia Eng.*, 2016, **148**, 106–113.
220 C. Wu, Q. Huang, Z. Xu, A. T. Sipra, N. Gao, L. P. de Souza Vandenberghe, S. Vieira, C. R. Soccol, R. Zhao and S. Deng, *Carbon Capture Sci. Technol.*, 2024, **11**, 100178.
221 C. Ma, J. Bai, X. Hu, Z. Jiang and L. Wang, *J. Environ. Sci.*, 2023, **125**, 533–543.
222 S. Song, Z. Liu, G. Liu, X. Cui and J. Sun, *Constr. Build. Mater.*, 2023, **405**, 133373.
223 A. Zaker, S. ben Hammouda, J. Sun, X. Wang, X. Li and Z. Chen, *J. Environ. Chem. Eng.*, 2023, **11**, 109741.
224 X. Xiong, Recycling food waste into value-added chemicals over carbon-based catalysts, PhD thesis, Hong Kong Polytechnic University, 2021.
225 C. Wen, T. Liu, D. Wang, Y. Wang, H. Chen, G. Luo, Z. Zhou, C. Li and M. Xu, *Prog. Energy Combust. Sci.*, 2023, **99**, 101098.
226 O. H. Gunawardene, C. A. Gunathilake, K. Vikrant and S. M. Amaraweera, *Atmosphere*, 2022, **13**, 397.
227 A. Mukhtar, S. Ullah, A. Inayat, S. Saqib, N. B. Mellon, M. A. Assiri, A. G. Al-Sehemi, M. B. K. Niazi, Z. Jahan and M. A. Bustam, *Energy*, 2021, **216**, 119230.
228 S. Kamalakannan, K. R. Maiyelvaganan, K. Palanisamy, A. Thomas, R. B. Said, M. Prakash and M. Hochlaf, *Chemosphere*, 2022, **286**, 131612.
229 N. Abuelnoor, A. AlHajaj, M. Khaleel, L. F. Vega and M. R. Abu-Zahra, *Chemosphere*, 2021, **282**, 131111.
230 Y. Han, G. Bai, J. Yang, J. Huang, Z. Fei, Q. Liu, Z. Zhang, X. Chen, J. Tang and M. Cui, *J. Solid State Chem.*, 2020, **290**, 121531.
231 V. Patel, A. Baskar, S. Tiburcius, B. Morrison, B. Mod, P. S. Tanwar, P. Kumar, A. Karakoti, G. Singh and A. Vinu, *Adv. Sens. Res.*, 2023, **2**, 2300024.
232 Y. Ye, Y. Qu and J. Sun, *Catal. Rev.*, 2023, 1–56.
233 C. Zhou, L. Xu, H. Song, J. Feng, Z. Hu, M.-J. Yang, P. Shi, Y.-R. Li, Y.-J. Guo and H.-Z. Li, *Aquaculture*, 2023, **563**, 738916.
234 Z. Chen, S. Deng, H. Wei, B. Wang, J. Huang and G. Yu, *Front. Environ. Sci. Eng.*, 2013, **7**, 326–340.
235 H. Liu, H. Lu and H. Hu, *Renewable Sustainable Energy Rev.*, 2024, **189**, 113908.
236 M. M. Alam, M. A. Hossain, M. D. Hossain, M. Johir, J. Hossen, M. S. Rahman, J. L. Zhou, A. K. Hasan, A. K. Karmakar and M. B. Ahmed, *Processes*, 2020, **8**, 203.
237 N. A. Rashidi, Y. H. Chai, I. S. Ismail, M. F. H. Othman and S. Yusup, *Biomass Convers. Biorefin.*, 2022, 1–15.
238 J. Bai, J. Huang, Q. Yu, M. Demir, E. Akgul, B. N. Altay, X. Hu and L. Wang, *Front. Chem. Sci. Eng.*, 2023, **17**, 1122–1130.
239 X. Gao, S. Yang, L. Hu, S. Cai, L. Wu and S. Kawi, *Carbon Capture Sci. Technol.*, 2022, **3**, 100039.
240 M. P. Maniscalco, M. Volpe and A. Messineo, *Energies*, 2020, **13**, 4098.
241 L. Zhu, N. Zhao, L. Tong and Y. Lv, *RSC Adv.*, 2018, **8**, 21012–21019.
242 Ó. J. Fonseca-Bermúdez, L. Giraldo, R. Sierra-Ramírez, J. Serafin, B. Dziejarski, M. G. Bonillo, G. Farid and J. C. Moreno-Pirajᾶn, *J. CO_2 Util.*, 2024, **83**, 102799.
243 V. Thithai, X. Jin, M. Ajaz Ahmed and J.-W. Choi, *Energies*, 2021, **14**, 3002.
244 N. Kaya and Z. Y. Uzun, *Biomass Convers. Biorefin.*, 2021, **11**, 1067–1083.
245 K. Foo and B. Hameed, *Microporous Mesoporous Mater.*, 2012, **148**, 191–195.
246 Q. Li, S. Liu, L. Wang, F. Chen, J. Shao and X. Hu, *J. Environ. Sci.*, 2021, **103**, 268–278.
247 J. Shao, J. Wang, Q. Yu, F. Yang, M. Demir, O. C. Altinci, A. Umay, L. Wang and X. Hu, *Sep. Purif. Technol.*, 2024, **333**, 125891.
248 M. M. Hassan and C. M. Carr, *Chemosphere*, 2021, **265**, 129087.
249 Q. Yu, J. Bai, J. Huang, M. Demir, B. N. Altay, X. Hu and L. Wang, *Molecules*, 2022, **27**, 6816.
250 W. Wu, C. Wu, J. Liu, H. Yan, G. Li, Y. Zhao, K. Bei and G. Zhang, *Sep. Purif. Technol.*, 2024, **339**, 126690.
251 M. Vega, E. Díaz-Faes and C. Barriocanal, *J. CO_2 Util.*, 2024, **81**, 102716.
252 C. Liu, Y. Zhi, Q. Yu, L. Tian, M. Demir, S. G. Colak, A. A. Farghaly, L. Wang and X. Hu, *ACS Appl. Nano Mater.*, 2024, **7**, 5434–5441.
253 Y. Bai, Y. Li, M. Li, X. Lin, C. Cai, H. He and S. Liu, *Ind. Crops Prod.*, 2024, **220**, 119183.
254 J. Serafin, M. C. Román-Martínez, M. Saidi, A. R. Gallego, S. Atlas and M. Ouzzine, *J. Anal. Appl. Pyrolysis*, 2024, **181**, 106637.
255 X. Yuan, S. Li, S. Jeon, S. Deng, L. Zhao and K. B. Lee, *J. Hazard. Mater.*, 2020, **399**, 123010.
256 K. M. Nelson, S. M. Mahurin, R. T. Mayes, B. Williamson, C. M. Teague, A. J. Binder, L. Baggetto, G. M. Veith and S. Dai, *Microporous Mesoporous Mater.*, 2016, **222**, 94–103.
257 A. Kumar and H. M. Jena, *Results Phys.*, 2016, **6**, 651–658.
258 R. Pang, T. Lu, J. Shao, L. Wang, X. Wu, X. Qian and X. Hu, *Energy Fuels*, 2020, **35**, 1620–1628.
259 R. Wang, P. Wang, X. Yan, J. Lang, C. Peng and Q. Xue, *ACS Appl. Mater. Interfaces*, 2012, **4**, 5800–5806.
260 Y.-Y. Hao, M.-X. Xiao, G.-C. Mao, J.-P. Wang, Z.-K. Guo, B.-X. Dong and Y.-L. Teng, *J. Environ. Manage.*, 2024, **359**, 120782.
261 M. S. Ribeiro, M. Zanatta and M. C. Corvo, *Fuel*, 2022, **327**, 125164.
262 M. S. Khosrowshahi, M. A. Abdol, H. Mashhadimoslem, E. Khakpour, H. B. M. Emrooz, S. Sadeghzadeh and A. Ghaemi, *Sci. Rep.*, 2022, **12**, 8917.
263 J. Chen, J. Yang, G. Hu, X. Hu, Z. Li, S. Shen, M. Radosz and M. Fan, *ACS Sustain. Chem. Eng.*, 2016, **4**, 1439–1445.

264 B. N. Ho, D. Pino-Perez, C. M. Ghimbeu, J. Diaz, D. Peredo-Mancilla, C. Hort and D. Bessieres, *J. Nat. Gas Sci. Eng.*, 2021, **95**, 104124.
265 G. Nazir, A. Rehman, S. Hussain, Q. Mahmood, M. Fteiti, K. Heo, M. Ikram and M. A. U. Din, *Green Chem.*, 2023, **25**, 4941–4980.
266 O. Hakami, *Surf. Interfaces*, 2023, **37**, 102668.
267 A. Ghaemi, H. Mashhadimoslem and P. Zohourian Izadpanah, *Int. J. Environ. Sci. Technol.*, 2022, **19**, 727–746.
268 A. Mukherjee, Generation of Activated Carbon from Spent Coffee Grounds: Process Optimization, Kinetics and CO_2 Capture, PhD thesis, University of Saskatchewan, 2022.
269 C. Quan, Y. Zhou, J. Wang, C. Wu and N. Gao, *J. CO_2 Util.*, 2023, **68**, 102373.
270 X.-F. Tan, S.-S. Zhu, R.-P. Wang, Y.-D. Chen, P.-L. Show, F.-F. Zhang and S.-H. Ho, *Chin. Chem. Lett.*, 2021, **32**, 2939–2946.
271 Y.-F. Huang, P.-T. Chiueh and S.-L. Lo, *Environ. Sci. Pollut. Res.*, 2023, **30**, 22211–22221.
272 C. Zhang, S. Sun, S. Xu and C. Wu, *Biomass Bioenergy*, 2022, **166**, 106608.
273 S. K. Guchhait, S. Khatana, R. K. Saini, A. D. Singh and A. K. Sarma, *Appl. Catal. O*, 2024, 206924.
274 M. Vafaeinia, M. S. Khosrowshahi, H. Mashhadimoslem, H. B. M. Emrooz and A. Ghaemi, *RSC Adv.*, 2022, **12**, 546–560.
275 H. Zhang, Z. Wei, D. Xiong, Y. Wu, M. Tong, H. Su, Z. Zhang and J. Liao, *Materials*, 2024, **17**, 942.
276 H. M. Coromina, D. A. Walsh and R. Mokaya, *J. Mater. Chem. A*, 2016, **4**, 280–289.
277 M. T. Islam, A. I. Sultana, C. Chambers, S. Saha, N. Saha, K. Kirtania and M. T. Reza, *Energies*, 2022, **15**, 9340.
278 N. F. Attia, S. E. Elashery, A. A. Galhoum, H. Oh and I. E. T. El Sayed, *Sustainable Solutions for Environmental Pollution: Air, Water and Soil Reclamation*, 2022, pp. 503–531.
279 J. Serafin, B. Dziejarski, O. F. C. Junior and J. Sreńscek-Nazzal, *Carbon*, 2023, **201**, 633–647.
280 S. Heo, W. Kim, Y. Jo and A. A. Adelodun, *Sustainability*, 2024, **16**, 1634.
281 H. Patel, H. Weldekidan, A. Mohanty and M. Misra, *Carbon Capture Sci. Technol.*, 2023, **8**, 100128.
282 M. Karimi, L. F. Zafanelli, J. P. Almeida, G. R. Ströher, A. E. Rodrigues and J. A. Silva, *J. Environ. Chem. Eng.*, 2020, **8**, 104069.
283 W. Y. Wu, M. Zhang, C. Wang, L. Tao, J. Bu and Q. Zhu, *Chem.–Asian J.*, 2024, **19**, e202400180.
284 B. Petrovic, M. Gorbounov and S. M. Soltani, *Carbon Capture Sci. Technol.*, 2022, **3**, 100045.
285 S. Biti, A. J. McCue, D. Dionisi, I. Graça and C. F. Martín, *Fuel*, 2024, **358**, 130246.
286 P. Wang, Y. Guo, C. Zhao, J. Yan and P. Lu, *Appl. Energy*, 2017, **201**, 34–44.
287 G. A. R. Bari, H.-J. Kang, T.-G. Lee, H. J. Hwang, B.-H. An, H.-W. Seo, C. H. Ko, W. H. Hong and Y.-S. Jun, *Carbon Lett.*, 2023, **33**, 811–822.
288 M. L. Botomé, P. Poletto, J. Junges, D. Perondi, A. Dettmer and M. Godinho, *Chem. Eng. J.*, 2017, **321**, 614–621.
289 Q. Pu, Y. Wang, X. Wang, Z. Shao, S. Wen, J. Wang, P. Ning, S. Lu, L. Huang and Q. Wang, *J. CO_2 Util.*, 2021, **54**, 101756.
290 L. Zhao, Z.-F. Sun, X.-W. Pan, J.-Y. Tan, S.-S. Yang, J.-T. Wu, C. Chen, Y. Yuan and N.-Q. Ren, *Water Res.: X*, 2023, **18**, 100167.
291 Y. Shen, *Fuel Process. Technol.*, 2022, **236**, 107437.
292 B. Igliński, W. Kujawski and U. Kiełkowska, *Energies*, 2023, **16**, 1829.
293 A. Allangawi, E. F. Alzaimoor, H. H. Shanaah, H. A. Mohammed, H. Saqer, A. A. El-Fattah and A. H. Kamel, *C*, 2023, **9**, 17.
294 F. Nawaz, M. Ali, S. Ahmad, Y. Yong, S. Rahman, M. Naseem, S. Hussain, A. Razzaq, A. Khan and F. Ali, *Chemosphere*, 2024, 143014.
295 A. N. Shafawi, A. R. Mohamed, P. Lahijani and M. Mohammadi, *J. Environ. Chem. Eng.*, 2021, **9**, 106869.
296 J. Serafin and O. F. Cruz Jr, *J. Environ. Chem. Eng.*, 2022, **10**, 107642.
297 L. Fu, Z. Ren, W. Si, Q. Ma, W. Huang, K. Liao, Z. Huang, Y. Wang, J. Li and P. Xu, *J. CO_2 Util.*, 2022, **66**, 102260.
298 M. T. Dunstan, F. Donat, A. H. Bork, C. P. Grey and C. R. Müller, *Chem. Rev.*, 2021, **121**, 12681–12745.
299 K. Azam, N. Shezad, I. Shafiq, P. Akhter, F. Akhtar, F. Jamil, S. Shafique, Y.-K. Park and M. Hussain, *Chemosphere*, 2022, **306**, 135566.
300 S. K. Jena, *Min. Metall. Explor.*, 2021, **38**, 47–68.
301 M. H. Khan, N. M. Akash, S. Akter, M. Rukh, C. Nzediegwu and M. S. Islam, *J. Environ. Manage.*, 2023, **338**, 117825.
302 G. Ramalingam, A. Priya, L. Gnanasekaran, S. Rajendran and T. K. Hoang, *Fuel*, 2024, **355**, 129490.
303 C. Gao, J. Feng, W. Mo, W. Guo, S. Ma, X. Su, J. Yang, D. Wang, W. Sun and H. Jia, *Sep. Purif. Technol.*, 2024, **348**, 127756.
304 A. Shokri and A. Ghaemi, *Case Stud. Chem. Environ. Eng.*, 2024, **9**, 100725.
305 F. Bahmanzadegan, M. A. Pordsari and A. Ghaemi, *Sci. Rep.*, 2023, **13**, 12533.
306 E. Pérez-Botella, S. Valencia and F. Rey, *Chem. Rev.*, 2022, **122**, 17647–17695.
307 L. Santamaría, S. Korili and A. Gil, *Chem. Eng. J.*, 2023, **455**, 140551.
308 V. C. Nguyen, H. T. Nguyen, H. D. Tran, T. N. Tu, W.-S. Kim and J. Kim, *Microporous Mesoporous Mater.*, 2023, **360**, 112716.
309 R. Li, Z. Wang, Z. Yuan, C. Van Horne, V. Freger, M. Lin, R. Cai and J. Chen, *Crit. Rev. Environ. Sci. Technol.*, 2022, **52**, 4038–4071.
310 F. Bai, X. Liu, S. Sani, Y. Liu, W. Guo and C. Sun, *Sep. Purif. Technol.*, 2022, **299**, 121539.
311 H. Wang, Y. Huang, S. Liu, C. Meng, X. Cheng and Y. Gao, *Eur. Polym. J.*, 2024, 113367.
312 J. Zhang, C. Duan, X. Huang, M. Meng, Y. Li, H. Huang, H. Wang, M. Yan and X. Tang, *J. Mater. Sci.*, 2024, **59**, 5271–5292.

313 C. Han, J. Yang, S. Dong, L. Ma, Q. Dai and J. Guo, *Sep. Purif. Technol.*, 2024, 128957.
314 E. Priya, S. Kumar, C. Verma, S. Sarkar and P. K. Maji, *J. Water Proc. Eng.*, 2022, **49**, 103159.
315 M. M. Rahman and M. Maniruzzaman, *S. Afr. J. Chem. Eng.*, 2024, **47**, 300–311.
316 A. Singh and J. G. Vijayan, in *Application of Nanotechnology for Resource Recovery from Wastewater*, CRC Press, 2024, pp. 254–294.
317 M. H. Ali and A. H. Fahmi, *IOP Conf. Ser.: Earth Environ. Sci.*, 2024, **1371**, 082029.
318 R. Singh, L. Wang, K. Ostrikov and J. Huang, *Adv. Mater. Interfaces*, 2024, **11**, 2202290.
319 T.-D. Hoang, S. A. Bandh, F. A. Malla, I. Qayoom, S. Bashir, S. B. Peer and A. Halog, *Recycling*, 2023, **8**, 53.
320 A. C. Pina, N. Tancredi, C. O. Ania and A. Amaya, *J. Mater. Sci. Eng. B*, 2021, **268**, 115115.
321 S. Dubal, S. Chavan and P. Jadhav, *J. Inst. Eng. (India): C*, 2022, **103**, 1415–1422.
322 S. Deng and Y. P. Ting, *Langmuir*, 2005, **21**, 5940–5948.
323 S. Kocak, C. Akduman, J. Yanik, E. P. A. Kumbasar and A. Cay, *Polym. Eng. Sci.*, 2024, **64**, 1355–1364.
324 T. Töngüç Yalçınkaya, A. Çay, Ç. Akduman, E. P. Akçakoca Kumbasar and J. Yanık, *J. Appl. Polym. Sci.*, 2024, **141**, e55475.
325 Y. Fei and Y. H. Hu, *J. Mater. Chem. A*, 2022, **10**, 1047–1085.
326 F. Raganati and P. Ammendola, *Energy Fuels*, 2024, **38**, 13858–13905.
327 L. Jiang, Y. Zhang, P. Kong, L. Cheng, G. Liu and J. Sun, *Carbon Capture Sci. Technol.*, 2024, **10**, 100155.
328 J. He, Z. Jin, F. Gan, L. Xie, J. Guo, S. Zhang, C. Q. Jia, D. Ma, Z. Dai and X. Jiang, *Green Chem.*, 2022, **24**, 3376–3415.
329 I. Skoczko and R. Guminski, *J. Ecol. Eng.*, 2024, **25**(1), 285–302.
330 V. Raja, S. Dutta, P. Murugesan, J. Moses and C. Anandharamakrishnan, *Environ. Chem. Lett.*, 2023, **21**, 839–864.
331 C. Ng, W. E. Marshall, R. M. Rao, R. R. Bansode and J. N. Losso, *Ind. Crop. Prod.*, 2003, **17**, 209–217.
332 I. M. Lima, A. McAloon and A. A. Boateng, *Biomass Bioenergy*, 2008, **32**, 568–572.
333 G. Stavropoulos and A. Zabaniotou, *Fuel Process. Technol.*, 2009, **90**, 952–957.
334 J. Serafin, B. Dziejarski, P. Rodríguez-Estupiñán, V. B. Fernández, L. Giraldo, J. Sreńscek-Nazzal, B. Michalkiewicz and J. C. Moreno-Piraján, *Fuel*, 2024, **374**, 132462.
335 J. Serafin, J. Sreńscek-Nazzal, A. Kamińska, O. Paszkiewicz and B. Michalkiewicz, *J. CO_2 Util.*, 2022, **59**, 101970.
336 C. A. Toles, W. E. Marshall, M. M. Johns, L. H. Wartelle and A. McAloon, *Bioresour. Technol.*, 2000, **71**, 87–92.
337 T. Kalak, *Energies*, 2023, **16**, 1783.